ÉCOLE DE TECHNOLOGIE SUPÉRIEURE
UNIVERSITÉ DU QUÉBEC

MANUSCRIPT-BASED THESIS PRESENTED TO
ÉCOLE DE TECHNOLOGIE SUPÉRIEURE

IN PARTIAL FULFILLMENT OF THE REQUIREMENTS FOR
THE DEGREE OF DOCTOR OF PHILOSOPHY
PH.D.

BY
Seyedbehzad GHAFARIZADEH

# EXPERIMENTAL INVESTIGATION AND MODELING OF SURFACE MACHINING OF HIGH PERFORMANCE CFRP FOR THE AEROSPACE INDUSTRY

MONTREAL, DECEMBER 21, 2015

**BOARD OF EXAMINERS**

THIS THESIS HAS BEEN EVALUATED

BY THE FOLLOWING BOARD OF EXAMINERS


Prof. Jean-François Chatelain, Thesis Supervisor
Department of Mechanical Engineering at École de Technologie Supérieure

Prof. Gilbert Lebrun, Thesis Co-supervisor
Department of Mechanical Engineering at Université du Québec à Trois-Rivières

Prof. Claudiane Ouellet-Plamondon, Chair, Board of Examiners
Department of Construction Engineering at École de Technologie Supérieure

Prof. Vincent Demers, Member of the jury
Department of Mechanical Engineering at École de Technologie Supérieure

Prof. Marek Balazinski, Member of the jury
Department of Mechanical Engineering at École Polytechnique de Montréal


THIS THESIS WAS PRENSENTED AND DEFENDED

IN THE PRESENCE OF A BOARD OF EXAMINERS AND THE PUBLIC

DECEMBER 14, 2015

AT ÉCOLE DE TECHNOLOGIE SUPERIEURE

## ACKNOWLEDGMENTS

First of all, I would like to express my sincere gratitude and appreciation for my supervisor professor Jean-Francois Chatelain and my co-supervisor Professor Gilbert Lebrun whose guidance were indispensable for my doctoral research. I am grateful to them for their constant encouragement, guidance and support for my research as well as my professional development.

I would like to acknowledge Prof. Claudiane Ouellet-Plamondon, Prof. Marek Balazinski and Prof. Vincent Demers for serving on my thesis committee. I greatly appreciate for taking the time to critically review this doctoral dissertation.

I sincerely thank Mr. Eric Marcoux at ÉTS machining laboratory, and Mr. Serge St-Martin at Centre Technologique en Aerospatiale (CTA) for their technical assistance related to machining experiments.

I also would like to appreciate the financial support of Consortium for Research and Innovation in Aerospace in Quebec (CRIAQ) and its partners, the Natural Sciences and Engineering Research Council of Canada (NSERC), MITACS, Bombardier Aerospace, Avior Integrated Products, Delastek and AV&R Vision & Robotics.

Last but not least; I would like to thank my parents, Mohammad and Marzieh, for the support they provided me through my entire life. I thank my wife and best friend, Sheida, without whose love, encouragement and editing assistance, I would not have finished this thesis.

**ÉTUDE EXPÉRIMENTALE ET MODÉLISATION DE L'USINAGE DE SURFACE DE CFRP HAUTE PERFORMANCE POUR L'INDUSTRIE AÉRONAUTIQUE**

Seyedbehzad GHAFARIZADEH

## RÉSUMÉ

Les matériaux composites à fibres de carbone (CFRP) sont largement utilisés dans les structures d'avions en raison de leur faible poids, leur résistance spécifique élevée, leur bonne résistance en fatigue et corrosion ainsi que pour leur flexibilité pour la conception de pièces. Bien que les composantes CFRP soient généralement produites à la forme quasi-finale, l'usinage est souvent nécessaire et pourrait s'avérer plus économique pour éliminer certaines matières excédentaires et amener les pièces à leur taille et forme finales. Cependant, leur usinage est toujours un défi en raison de leur inhérente hétérogénéité et anisotropie, à la source de plusieurs types de dommages, tels que le délaminage, le déchaussement et la fragmentation des fibres. Afin d'améliorer la qualité des pièces produites, une meilleure compréhension de la coupe pendant le processus d''usinage est nécessaire. Le fraisage de surface est parmi les procédés de parachèvement des composites les moins étudiés pour la finition des pièces. Ainsi, le but de cette étude est de combiner des méthodes numériques et expérimentales afin de réduire les problèmes causés par l'usinage de surfaces de matériaux CFRP et d'acquérir une meilleure compréhension du processus de coupe associé à ce procédé.

Tout d'abord, l'effet des conditions de coupe, telles que la vitesse de coupe, la vitesse d'avance, de même que l'angle d'inclinaison de l'outil, sur les forces et la qualité des surfaces usinées a été étudié. Les résultats expérimentaux ont montré que la meilleure qualité de surface a été produite en utilisant une vitesse d'avance faible, une vitesse de coupe modérée, et un angle d'inclinaison nul de l'axe de l'outil relativement à la surface usinée. Dans la deuxième partie, l'effet des conditions de coupe et de l'orientation des fibres sur la température et les forces engendrées ont été étudiées. Il a été observé que la température de coupe augmentait de manière linéaire avec la vitesse de coupe. Les forces de coupe et températures, maximales et minimales, ont été atteintes pour les orientations des fibres de 90 et de 0 degrés, respectivement.

Finalement, un modèle par éléments finis est proposé afin de prédire les forces de coupe, les mécanismes de formation des copeaux et les dommages d'usinage induits dans un matériau CFRP unidirectionnel. Les résultats de la modélisation ont été validés par des données expérimentales, comprenant entre autres les forces de coupe et des images prises au microscope électronique à balayage (SEM). La comparaison du modèle avec les résultats expérimentaux indique que le modèle proposé est capable de raisonnablement prédire les forces de coupe et les dommages issus de l'usinage. Le modèle développé montre que les dommages d'usinage, la formation des copeaux, et le profil des forces de coupe dépendent fortement de l'orientation des fibres dans le processus de fraisage de surfaces de CFRP.

**Mots-clés:** usinage de surface, composites à fibres de carbone, plastiques renforcés de fibres de carbone (CFRP), température de coupe, forces de coupe, rugosité de surface, modélisation par éléments finis

# EXPERIMENTAL INVESTIGATION AND MODELING OF SURFACE MACHINING OF HIGH PERFORMANCE CFRP FOR THE AEROSPACE INDUSTRY

Seyedbehzad GHAFARIZADEH

## ABSTRACT

Carbon fiber reinforced plastics (CFRP) have been widely used in many aircraft structures due to their light weight, high specific strength, good resistance to fatigue/corrosion and flexibility in design. Although CFRP components are produced to near-net shape, machining is often needed to remove excess materials and bring the parts to the final size and shape. However, their machining still is a big challenge due to their inherent anisotropy and inhomogeneity, which are the source of several types of damage, such as delamination, fibers pullout, and fiber-fragmentation. In order to improve machining quality and decrease the damages, a better understanding of their machining is required. Surface milling is one of the most practical processes for finishing operations but very few studies have been dedicated to its use for composite components. Thus, the purpose of this study is to use numerical and experimental methods to minimize the machining problems of CFRP materials and to gain a better understanding of CFRP surface milling process.

First, the effects of different cutting conditions such as cutting speed, feed rate, and lead angle on cutting forces and surface quality were studied and the optimum cutting condition was determined. The experimental results showed that the best surface quality was achieved by using lower cutting feed rate, moderate cutting speeds, and zero degree tool lead angle. In the second part, the effects of cutting conditions and fiber orientation on cutting temperature were investigated. It was found that the cutting temperature increases linearly with the cutting speed. The maximum and minimum cutting forces and temperatures were achieved for fiber orientations of 90 and 0 degrees, respectively.

Then, a finite element model was developed to predict cutting forces, chip formation mechanism and machining damages obtained during milling of unidirectional CFRP. The modeling results were validated by experimental data, including cutting forces and SEM images. A comparison of modeling and experimental results indicated that the proposed model is able to successfully predict the cutting forces and machining damages. The developed model showed that the machining damages, the chip formation, and the cutting force profile strongly depend on fiber orientation in CFRP milling process.

**Keywords:** Surface machining, carbon fiber reinforced plastics (CFRP), cutting temperature, cutting forces, surface roughness, finite element method, machining damage

## TABLE OF CONTENTS

Page

## LIST OF TABLES

Page

## LIST OF FIGURES

Page

## LIST OF ABREVIATIONS

| | |
|---|---|
| *CFRP* | Carbon fiber reinforced plastic |
| *GFRP* | Glass fiber reinforced plastic |
| *ALE* | Arbitrary Lagrangian-Eulerian |
| *EHM* | Equivalent homogeneous material |
| *PCD* | Polycrystalline diamond |
| *WC* | Tungsten carbide |
| *FEM* | Finite element method |
| SEM | Scanning electron microscopy |
| 2D | Two dimensional |
| 3D | Three dimensional |

## LIST OF SYMBOLS AND UNITS OF MEASUREMENTS

| **Symbol** | **Unit** | **Description** |
|---|---|---|
| $v_C$ | m/min | Cutting speed |
| $a_f$ | mm | Feed per tooth |
| $N$ | rev/min | Spindle speed |
| $v_f$ | mm/min | Feed rate |
| $z$ | - | Number of edges |
| $D$ | mm | Cutter diameter |
| $a_p$ | mm | Axial depth of cut |
| $a_e$ | mm | Radial depth of cut |
| $R_a$ | µm | Arithmetic mean value of the roughness |
| $R_t$ | µm | Roughness - maximum peak to valley height |
| $R_p$ | µm | Roughness- maximum peak to mean height |
| $R_v$ | µm | Roughness - mean to valley height |
| $R_z$ | µm | Roughness - ten point average height |
| $S_a$ | µm | Arithmetic average of the 3D roughness |
| $S_t$ | µm | Maximum profile height of the 3D roughness |
| $B_{ij}$ | - | In-plane/flexure coupling stiffnesses |
| $A_{is}$ | - | In-plane shear coupling stiffnesses |
| $D_{is}$ | - | Bending/twisting coupling stiffnesses |
| $f_n$ | kHz | Natural frequency |
| $F_c$ | N | Resultant cutting force |
| $V_f$ | % | Fiber volume content |
| $W_f$ | % | Fiber weight content |
| $\theta_c$ | °C | Cutting temperature |
| $\mu$ | - | Friction coefficient |
| $T_g$ | °C | Glass transition temperature |
| $E_1$ | GPa | Longitudinal modulus |
| $E_2$ | GPa | Transverse modulus |
| $G_{12}$ | GPa | In-plane shear modulus |

| | | |
|---|---|---|
| $v_{12}$ | | Major Poisson's ratio |
| $X^T$ | MPa | Longitudinal tensile strength |
| $X^C$ | MPa | Longitudinal compressive strength |
| $Y^T$ | MPa | Transverse tensile strength |
| $Y^C$ | MPa | Transverse compressive strength |
| $S^L$ | MPa | Longitudinal shear strength |
| $S^T$ | MPa | Transverse shear strength |
| $G_{ft}^c$ | $KJ/m^2$ | Fracture energy - fiber tension |
| $G_{fc}^c$ | $KJ/m^2$ | Fracture energy - fiber compression |
| $G_{mt}^c$ | $KJ/m^2$ | Fracture energy - matrix cracking |
| $G_{fc}^c$ | $KJ/m^2$ | Fracture energy - matrix crushing |
| $\rho$ | $g/cm^3$ | Specific gravity |
| $\tau_n$ | MPa | Frictional stress |
| $\sigma_n$ | MPa | Normal stress |
| $\sigma_{11}$ | MPa | Normal stresses in fiber direction |
| $\sigma_{22}$ | MPa | Normal stresses in transverse direction |
| $\sigma_{12}$ | MPa | In-plane shear stress |

# INTRODUCTION

Carbon fiber reinforced plastics (CFRPs) are an important class of composite materials that are widely used in many industrial sectors such as aerospace, construction, and transportation. CFRPs are increasingly used for different aircraft parts, such as wing boxes, fuselage, ailerons, wings, spoilers, vertical stabilizers, cowlings, traps and struts (Daniel et Ishai, 2006; Girot et al., 2009). This group of composite materials have various advantages such as high strength and stiffness properties, long fatigue lifespan, low density, and high corrosion/wear resistance. Because carbon fibers have a negative coefficient of thermal expansion along their axis, CFRPs have very low in-plane expansions over a wide range of temperatures, and this is very important for aerospace structures (Sheikh-Ahmad, 2008). The first composite aircraft component was made in 1968 and since then, tendency for using composite materials in aerospace industry was unceasingly increased since late of 1970s (Daniel et Ishai, 2006). Currently, 52% of the weight of Airbus A350, 50% of the weight of the Boeing 787, and 46% of the weight of the Bombardier CSeries are made of composite materials such as CFRPs. As shown in (Figure 1-1), advanced composite materials (46% of the weight) including CFRPs are utilized in wings, torque box and wing skins in Bombardier CSeries (Marsh, 2011).


Figure 1-1 The application of composite materials in different parts of the Bombardier CSeries (Kafyeke, 2010)

CFRP parts are usually produced in near net-shape but machining operations are often required to remove excess of materials, to bring the parts to their final size and shape, and to produce high quality surfaces. The machining of CFRP has many challenges due to their heterogeneous and anisotropic nature causing some damages such as delamination, fiber pull out, fiber-fragmentation, burring, and fuzzing. These damages decrease the properties and performances of manufactured components and could cause catastrophic incidents and significant costs in aerospace industries. Therefore, the prediction, evaluation and study of those damages are vital to prevent such disasters. Although there are many researches that have been carried out on drilling and trimming of CFRP materials, there are few researches regarding surface machining of these materials. Hence, a comprehensive study of the surface machining of CFRP process is necessary.

Making use of the developments in computer related technologies, many researchers have attempted to use different modeling methods to study the milling process of CFRPs. Previous researches have focused their efforts on the use of artificial neural networks (Kalla, Sheikh-Ahmad et Twomey, 2010) and empirical methods (Karpat, Bahtiyar et Değer, 2012; Zaghbani et al., 2012a). However, these models are not able to predict the mechanism of chip formation and the underlying machining damages. The numerical modeling of CRFP milling process taking into account the chip formation is thus required to understand the machining quality and cutting mechanisms.

In this research, the effects of different cutting conditions including the feed rate, cutting speed, tool lead angle, and fiber orientation on surface quality, cutting force and cutting temperature have been studied. In addition, a finite element model has been developed to study the cutting forces, chip formation and machining damages during CFRP milling. This research manuscript is divided into 7 chapters. In the first chapter, challenges description, objectives and the original contributions of this study are described. The second chapter gives a brief description of basic knowledge about CFRP materials. It also presents a short overview of milling process for composites and the previous experimental and modeling researches made on the milling of CFRP materials.

The third chapter is the first published journal paper. This paper presents an experimental research to study the optimum cutting conditions for multiaxis ball-end milling of multidirectional CFRP materials. It investigates the effects of different cutting conditions such as feed rate, cutting speed and tool lead angle on surface roughness and cutting forces. The findings of this chapter regarding the optimized cutting conditions (cutting speed, feed rate and lead angle) have been used in the next chapters.

The fourth chapter presents the second published journal paper. This chapter focuses on thermal aspects of CFRP milling. Milling experiments have been carried out on a unidirectional carbon fiber reinforced plastic to investigate the effects of fibers orientation and cutting speed on the cutting temperature, cutting force and surface damages. The ball-end milling tests were performed under the optimum cutting conditions found in the third chapter (moderate cutting speeds, low feed rate and zero degree lead angle).

Chapter five presents the third journal paper regarding the simulation of the CFRP milling process. According to the findings of chapters 3 and 4 for the ball-end milling, the best surface quality was achieved with a 0° tool lead angle. Based on this result, a new flat-end mill was selected and more experiments were carried out in 0° tool lead angle. Then, a combined micro-macro mechanical model has been developed to study the cutting forces, chip formation and machining damages during CFRP flat-end milling. The proposed model took the advantages of both macro (modeling the composite as an equivalent homogeneous material) and micro scales (use of adaptive meshing and related friction coefficient to fibers orientation) approaches to predict the cutting forces with good agreement to the experiments.

Finally, the last two chapters present the conclusions and recommendations that resulted from this study.

# CHAPTER 1

# CHALLENGE DESCRIPTION, OBJECTIVES AND ORIGINAL CONTRIBUTIONS

## 1.1 Challenge description

Applications of CFRP in aerospace industry is rapidly increasing due to their special properties such as high strength, high stiffness, long fatigue life, low density, good corrosion resistance and wear resistance. In spite of having these advantages, CFRP machining is still a big challenge due to their inhomogeneous and anisotropic nature that result in machining problems such as delamination, fibers pullout, fiber-fragmentation, burring, and fuzzing. Occurrence of these defects even in a small extent may cause catastrophic incidents in aerospace applications where parts are undergoing cyclic and dynamic loadings. Furthermore, tool wear is one of the major problems in CFRP machining due to extremely abrasive characteristics. Poor cutting conditions can accelerate tool wear rate and as a result increase the machining costs. To achieve the high quality of machined surfaces, it is necessary to understand the cutting mechanism and investigate the effects of different machining parameters.

In addition to aforementioned challenges during machining, the experimental study of composite machining is time consuming and is an expensive process with some dangers to human health due to the production of carbon chips and dusts during the operation. Moreover, the interpretation of the experimental results of milling is difficult due to complexity of the process. Therefore, the finite element modeling of CFRP machining could be a good alternative method to study and investigate the machining process of CFRP composites including chip formation, cutting forces, and surface machining damages. Recently, with the improvement in computer technology and equipment, many researchers have focused on modeling of CFRP machining. But in spite of existing many proposed models for simulating CFRP orthogonal cutting, there is no numerical models for simulating the CFRP surface machining process such as milling process.

## 1.2 Research objectives

In order to promote the use of composite materials in aerospace industries, it is critical to overcome their machining limitations. Therefore, the main purpose of this research is to improve machining quality of CFRP materials and to provide a better understanding of their milling process. Cutting forces are among the important machining factors that influence the process stability, machining quality, cutting temperature, and tool conditions.

Hence, the objectives of this research are to investigate the effects of machining conditions such as cutting speeds, feed rate, and tool lead angle on cutting forces and surface quality, and to optimize the cutting conditions for surface milling of CFRP. Since cutting temperature is an influent factor on machining quality and tool wear, the other purpose of this work is to focus on the thermal aspects of CFRP milling process. Therefore, the effects of cutting parameters such as the cutting speed and fiber orientation on the cutting temperature and surface damage were studied. Another objective of this work is to develop a finite element model to analyse the CFRP milling process and predict the cutting forces, chip formation and machining damages.

## 1.3 Original contributions

The CFRP surface milling process is investigated in this research work using the experimental and modeling methods. The original contributions of this work can be summarized in the following main points:

- The effects of tool lead angle (the angle between the tool axis and the surface normal) on cutting force, surface roughness, and machining damages was studied during the surface milling of CFRP materials.

- The effects of the cutting conditions such as cutting speed and fiber orientation on the cutting temperature were investigated during the CFRP ball end milling process. Based on the experimental results, the influences of the cutting temperature on cutting force and machining quality were studied to provide a better knowledge of thermal aspect of CFRP milling and improve the machining quality.

- The first finite element model was developed to study flat-end milling of CFRP material. The composite material was modeled as an equivalent homogeneous material and the friction coefficient between the tool and workpiece was assumed dependent to fibers orientation. The model was able to predict cutting forces, chip formation mechanism and machining damages in good agreement with the experiments. The presented finite element mode was applied to study the effect of fiber orientation and machining direction on the cutting forces.

# CHAPTER 2

# LITERATURE REVIEW

## 2.1 Carbon fiber reinforced plastics

Carbon fiber reinforced plastics (CFRPs) are used widely in aerospace industries, due to their advantages such as high tensile and compressive strength, and high fatigue and corrosion resistances. However, CFRPs are expensive and difficult to machine compared to metals (Daniel et Ishai, 2006; Gudimani, 2011; Teti, 2002). As shown in Figure 2-1, the carbon fiber in CFRPs can be unidirectional (unidirectional lamina or ply) or woven. To obtain quasi-isotropic properties, the individual lamina can be stacked with various orientations with respect to laminate global coordinate system (Daniel et Ishai, 2006).

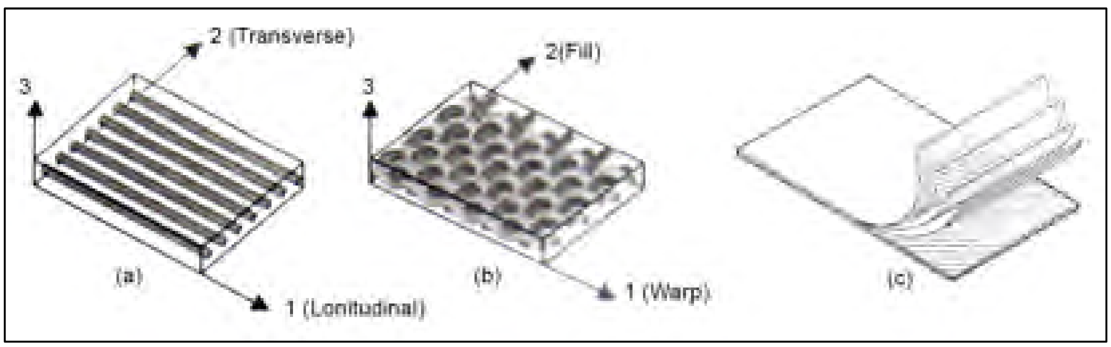


Figure 2-1 a) Unidirectional lamina, b) woven fibers c) laminate (Campbell, 2010; Daniel et Ishai, 2006)

## 2.2 Surface milling of CFRP

Milling processes are usually required to remove the excess of material and bring the parts to their final size and shape. In the milling operation, cutting is performed by a rotating multi-teeth cutter and often more than one cutting edge are cutting at the same time. Thus, the milling process is complex due to the variation of fiber orientation, chip size and cutting forces with tool rotation. The different aspects of CFRP surface milling process, including milling geometry, chip formation, cutting forces and the quality of machined surfaces, are studied in section 2.2.

### 2.2.1 Milling Geometry

Figure 2-2 shows the face (end) milling process and the cutting geometry in end milling. Different parameters of milling are shown in this picture. The spindle speed shown by letter N in the Figure 2-2b is the number of revolutions of the milling tool per minute.

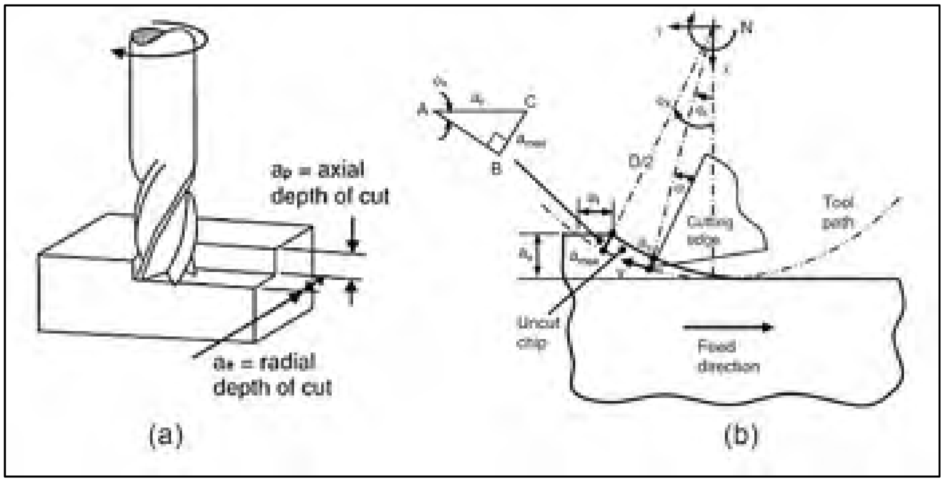


Figure 2-2 a) face milling, b) milling geometry (Sheikh-Ahmad, 2008)

Cutting speed ($v_C$) is an important parameter indicating the speed at which the cutting edge machines the workpiece and is defined by the following equation:

$$v_C = \frac{\pi \times D \times N}{1000} \ (m/min) \tag{1-1}$$

Where D and N represent the tool diameter and spindle speed, respectively. Feed speed ($v_f$) is the feed of the tool against the workpiece, in units of distance per time and feed per revolution (f) is a value used to determine finishing capacity. These two parameters are related by the following equation:

$$f = \frac{v_f}{N} \ (mm/rev) \tag{1-2}$$

Milling tools are multi-edge cutters, and the feed per tooth ($a_{f9}$), as a value for ensuring that each edge machines under satisfactory condition, is defined with the following equation:

$$a_f = \frac{v_f}{N \times z} \;\; (mm/tooth) \tag{1-3}$$

Where, z is number of edges of the tool.

### 2.2.2 Chip formation mechanism

The chip formation mechanism in CFRP milling is controlled by the fibers orientation. The fibers orientation varies continuously with tool rotation during milling process. Thus, different cutting mechanisms are responsible for chip formation process during mill rotation.

Figure 2-3 shows four types of chip formation mechanisms for different fiber orientations with respect to the cutting direction (Sheikh-Ahmad, 2008).

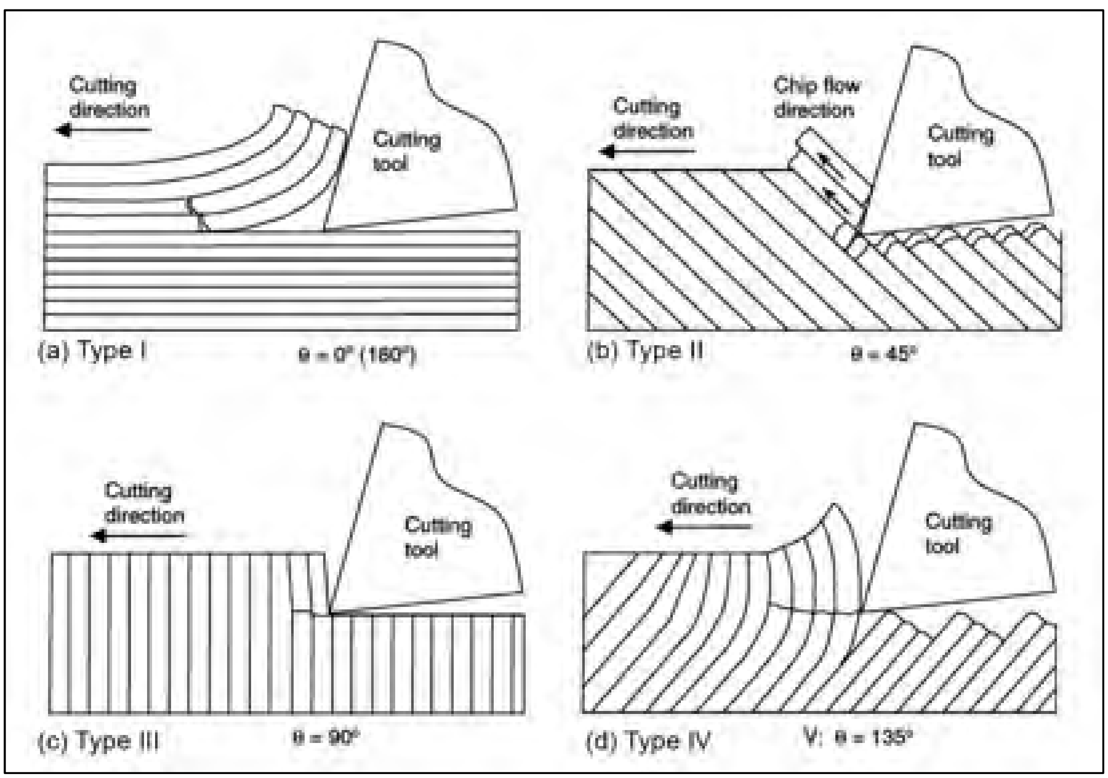


Figure 2-3 Cutting mechanisms in different fiber orientations (Sheikh-Ahmad, 2008)

For fibers oriented at 0° (Figure 2-3a), a crack initiates at the contact point of the workpiece and tool; and it propagates along the fiber-matrix interface. When the tool advances into the workpiece, the peeled layers bend and compress in the opposite direction to fibers. The fiber-matrix debonding continues until the bending stress in the fibers increases up to failure stress, and fiber failure occurs ahead of the cutting tool. The chip formation mode in 0° fibers orientation is of delamination type.

The second type of chip formation is fiber cutting (with continuous chip), that occurs for fiber orientations between 0° and 90° (Figure 2-3b). The chip formation mechanism consists of fracture from compression-induced shear perpendicular to fiber axis followed by shear fracture along the fiber–matrix interface occurring with the cutting edge movement. The cracks generated in the fibers above and below the cutting plane during the compression stage of the chip formation remain after machining and cause low quality machined surfaces.

For fibers at 90° (Figure2-3 c), fibers crush and fail at the contact point of the tool and the workpiece and each fiber is cut separately. The chip formation mechanism in this case is called fiber cutting type (with discontinuous chip).

For large fiber orientation angles (105–150°) where the tool enters the workpiece and catches on a peeled fiber, the fiber-matrix interfacial failure occurs below the cutting plane (Figure 2-3d). Fiber failure below the cutting plane occurs when the bending stresses that develop in the fibers below the surface of the cut are large enough for fracture. In this type of chip formation (type V- macrofracture) discontinuous chips are formed. A poor surface quality results from this orientation because of extensive fiber pull-out and delamination cracking (Sheikh-Ahmad, 2008; Teti, 2002)

### 2.2.3 Cutting forces in CFRP machining

Cutting forces are one of the important factors influencing the process stability, part quality, cutting temperature, and the tool conditions. A number of studies have been carried out about cutting forces and the effect of parameters such as fiber orientation, cutting speed and tool geometry on them. These studies show large fluctuations in the cutting forces during machining of fiber reinforced polymers. Cutting and thrust forces are strongly dependent on fiber orientation, while the operating conditions and the tool geometry will also have influence on them. Figure 2-4 shows typical cutting force evolutions during trimming (edge milling) of CFRP and GFRP (Glass fiber reinforced plastic) with different cutting conditions (Sheikh-Ahmad, 2008).

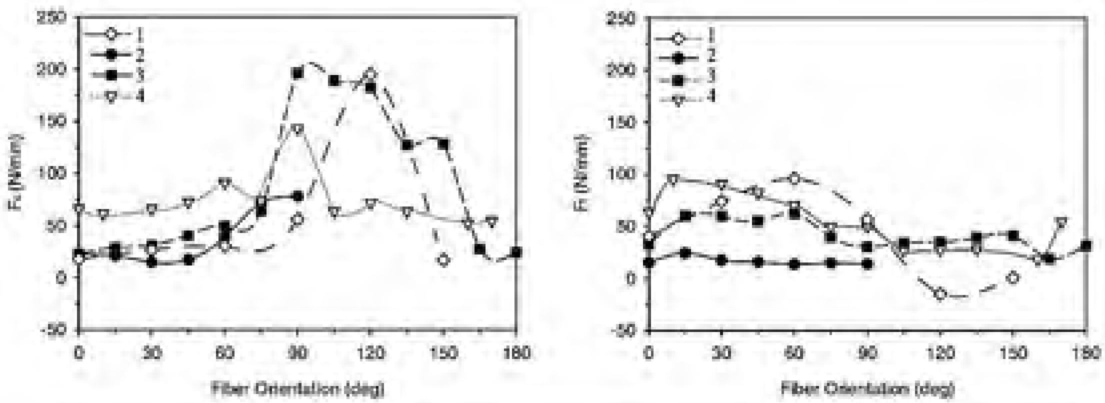


| Test | V (m/min) | $a_c$ (mm) | $a_w$ (mm) | Cutting tool | $\alpha_o$ (deg) | $\gamma_o$ (deg) | $r_a$ (µm) |
|---|---|---|---|---|---|---|---|
| 1 | 1.00 | 0.05 | 4.00 | – | 20 | 7 | 50 |
| 2 | 0.02 | 0.10 | 2.28 | K10 | 10 | 10 | 2 |
| 3 | 4.00 | 0.25 | 4.00 | PCD | 10 | 17 | – |
| 4 | 1.18 | 0.25 | 2.20 | K20 | 12 | – | – |

Figure 2-4 Variation of cutting and thrust forces per unit width with fiber orientation, 1-Carbon F593/epoxy, 2- Carbon (Torayca T300), 3-Graphite IM6/epoxy, 4-Carbon T300/epoxy (Sheikh-Ahmad, 2008)

As can be seen in Figure 2-4, generally the cutting force remains almost constant up to fiber orientations of approximately 60°, then it rapidly increases with fiber orientations up to 90°. Then the cutting force decreases with more increase in fiber orientation with a significant decrease occurring between 100° and 165° (Sheikh-Ahmad, 2008). The results of other studies on orthogonal cutting of FRP materials also showed that cutting and trust forces are highly dependent on fiber orientation (Dandekar et Shin, 2008; Gao et al., 2015; Ramulu, 1997; Rao, Mahajan et Bhatnagar, 2008; Rao, Mahajan et Bhatnagar, 2007b; Santiuste et al., 2014; Santiuste, Soldani et Miguélez, 2010; Wang, Ramulu et Arola, 1995; Zenia et al., 2015).

Fiber orientation is the most important factor influencing the cutting forces, but tool geometry, tool rake (the angle between the cutting face of the tool and a line perpendicular to the work piece), clearance angle (the angle between the flank face of the tool and the workpiece) and cutting parameters such as depth of cut and material removal rate also have effects on cutting forces. Cutting and thrust forces are decreased by increasing the rake angle; however the effect of rake angle is not as significant as fiber orientation and depth of cut (Wang et Zhang, 2003). Generally, cutting and thrust forces are decreased by increasing the clearance angle (Calzada et al., 2012).

Chatelain et al. investigated the effects of tool geometry on cutting forces in trimming of CFRP. The results of their studies showed that tool geometry (number of flute, helix and rake angle) has a significant effect on cutting forces (Chatelain et Zaghbani, 2011). In another study, Zaghbani et al. (Zaghbani et al., 2012b) showed that the force amplitude is dictated by the tool geometry, the type of machining operation, and material properties (the fiber orientation) in milling of CFRP. They also concluded that the cutting force profile does not significantly depend on fibers orientation. Karpat et al. (Karpat, Bahtiyar et Değer, 2012) presented a mechanistic cutting force model for milling CFRPs. In contrast to the finding of Zaghbani et al., they showed that fiber orientation significantly affects the cutting force profile and amplitude.

Cutting parameters such as cutting speed, depth of cut, and feed rate are other factors influencing the cutting forces. Generally, cutting forces are increased by the material removal rate. Therefore, thrust and cutting forces rise with increasing the feed rate and depth of cut during machining of CFRP (Rusinek, 2010). Experimental studies showed that the variation of cutting forces is not uniform over the variation of cutting speeds. As shown in Figure 2-5, moderate cutting speeds (between 200-300 m/min) were more suited for the machining of CFRPs.

### 2.2.4 Machining Induced Damage and Surface Integrity

Several aspects including subsurface damage and surface roughness are considered to characterize the results of surface machining process such as milling and trimming. The surface profile is typically described by its lay (the main direction of the surface texture), waviness, and roughness. The conceptual opposite from smoothness of a technical surface is designated as roughness. Waviness is the characteristic form of topographical variations that are measurable on the part profile in an actual or imaginary cross section (Figure 2-6a).

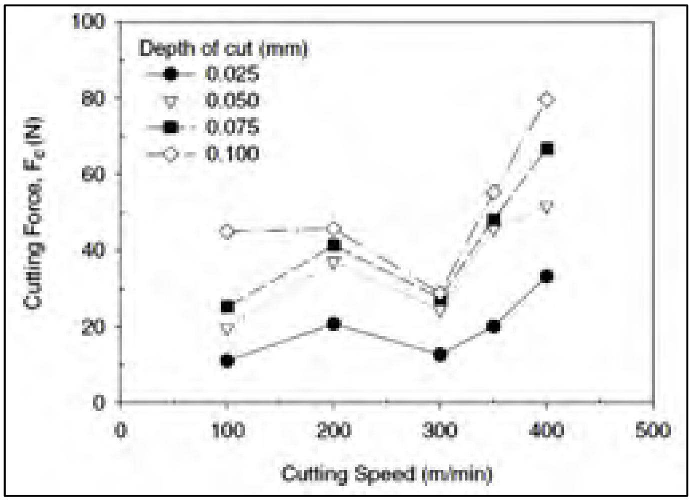


Figure 2-5 Variation of the cutting force with different cutting speeds and feed rates in machining CFRP with PCD tool(Sheikh-Ahmad, 2008)

Lay is the macroscopic contour of the surface and describes the direction of the predominant surface pattern. The surface waviness, profile and surface roughness parameters (arithmetic mean value $R_a$, maximum peak to valley height $R_t$, maximum peak to mean height $R_p$, mean to valley height $R_v$, and ten point average height $R_z$) are shown in Figure 2-6b (Farago et Curtis, 1994).

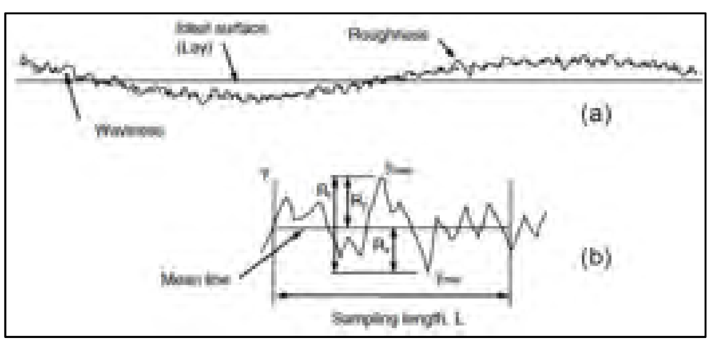


Figure 2-6 Surface characters, lay, waviness, and roughness (Sheikh-Ahmad, 2008)

The roughness of a machined surface is affected by machining parameters (feed rate, cutting speed, and depth of cut), tool geometry, tool wear, and fiber orientation. Generally, the value of $R_a$ and $R_z$ increases by increasing the feed rate and decreases by increasing the cutting speed. However, the effect of cutting speed is not as significant as feed rate (Chatelain, Zaghbani et Monier, 2011; Chatelain, Zaghbani et Monier, 2012; Davim et Reis, 2005; Davim, Reis et António, 2004). Wang and Zhang found that a smaller depth of cut generates less sub surface damages (Wang et Zhang, 2003).

El-Hofy et al. (El-Hofy et al., 2011) investigated the effects of different slotting parameters such as tool materials (WC & PCD) and cutting environment (chilled air and dry) on the surface roughness and integrity using 3D roughness parameters ($S_a$ and $S_t$). According to their results, the combination of low cutting speed and high feed rate was recommended for an improved surface roughness. By using analysis of variance (ANOVA), they showed that tool material was not a statistically significant factor; with a relatively low PCR of 5.44%. They also studied the effects of fiber orientation on surface roughness. The fibers fractured by buckling were removed cleanly, with the least surface damage, for a fiber orientation of 0°. Wavy surfaces were observed for plies oriented at 45° while those at 90° and 135° suffered matrix cracking and fiber pull out due to the high cutting forces and softening of the resin (Figure 2-7).

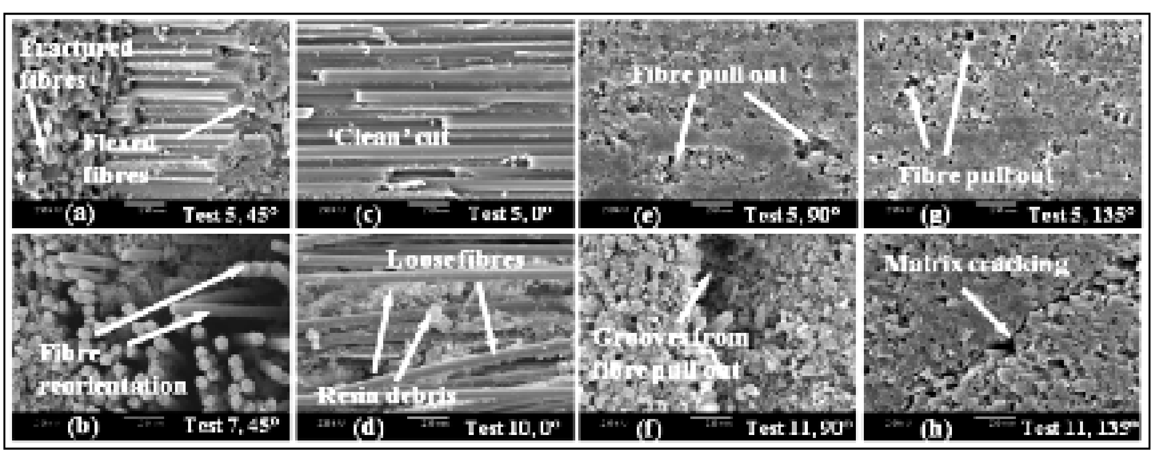


Figure 2-7 Damage at different fiber orientations; (a-b) 45°; (c-d) 0°; (e-f) 90°; (g-h) 135° (El-Hofy et al., 2011)

Sheikh-Ahmad et al. (Sheikh-Ahmad, Urban et Cheraghi, 2012) carried out an experimental study to determine the effects of cutting conditions on machining quality during edge trimming of CFRP. They demonstrated that the surface roughness and average delamination depth increase with an increase in feed rate and decrease with an increase in spindle speed. Feed rate had the highest influence on the surface roughness and delamination followed by cutting distance and cutting speed.

Machined CFRPs have roughness and subsurface damages that are influenced by fiber orientation. Ramulu (Ramulu, 1997) studied the effect of fibers orientation on surface quality and concluded, by measuring the average surface roughness in both longitudinal and transverse directions, that for fiber orientations between 15 to 60° good surface qualities can be obtained. He deduced that for an orientation of 135°, extensive fiber pull-out and delamination cracking occurred. Therefore, poor surface quality was obtained for this orientation. A recent study that has been carried out by Chatelain et al. (Chatelain, Zaghbani et Monier, 2012) confirmed the results of Ramulu's work. They showed that all roughness parameters ($R_a$, $R_p$, $R_q$, $R_v$, and $R_z$) were worse at 135° than for other orientations. The best surface quality was obtained for fibers at 45°.

The cutting of CFRPs is difficult due to diverse fiber and matrix properties, inhomogeneous nature of the material, and the presence of a high volume fraction of hard abrasive fibers in the matrix. They are especially vulnerable to the generation of damages such as delamination, fiber pull-out and matrix thermal degradation during machining. Davim et al. (Davim et Reis, 2005) investigated the influence of cutting parameters (cutting velocity and feed rate) and tool geometry on delamination. They showed that delamination increases with increasing feed rate and cutting speed. They also found that a two flute end mill presents less delamination compared to a six flute end mill.

### 2.2.5 Cutting temperature in CFRP milling

The cutting temperature is an important factor in the machining of composite materials that influences the quality of the machined surface and tool wear. However, only a few papers have covered the effect of cutting temperature in the surface milling of CFRP.

Yashiro et al. (Yashiro, Ogawa et Sasahara, 2013) studied the cutting temperature in CFRP milling. They found that the tool-workpiece contact point temperature increased up to 180 °C (the glass transition temperature) when the cutting speed reached 25 m/min, and up to 300 °C for a cutting speed of 50 m/min. The cutting temperature tends to stabilize and remain constant when the cutting speed was increased further.

In a recent research, Liu et al. (Liu et al., 2014) developed a mathematical model to predict the spatial and temporal distribution of the temperature in helical milling of CFRP. They concluded that the workpiece temperature increases with the spindle speed and axial depth of cut. The axial cutting depth had more influence than spindle speed on temperature variation of the workpiece, while the influence of tangential feed per tooth was less than the other factors.

## 2.3 Finite element modeling of CFRP machining

Recently, many researchers have focused on investigation of CFRP machining using modeling to decrease the experiments, which are time consuming and expensive. But in the literature, very few works attempt to model the cutting forces in surface milling of fiber reinforced composites. Generally, the modeling methods of FRP machining can be classified in two general approaches: (I) theoretical and empirical models and (II) numerical models. Theoretical and empirical models were used to study the FRP milling process (Karpat, Bahtiyar et Değer, 2012; Zaghbani et al., 2012a), but using these models is very complicated because of the highly nonlinear and inhomogeneous nature of composite materials. Another problem is the lack of cutting force coefficients that are necessary for these modeling techniques, especially for modelling oblique cutting for different tool/workpiece combinations (Calzada, 2010; Kalla, Sheikh-Ahmad et Twomey, 2010). In addition, these models are not able to predict machining damages and cutting mechanism.

More recently, with the improvement in computer technology, many researchers have focused on studying composite machining by numerical methods such as finite element modeling. Finite element models are able to predict the cutting forces, chip formation mechanisms, and material damage in the machining of a complex multi-phase and anisotropic material (Calzada, 2010). In spite of existing many models for simulating CFRP orthogonal cutting, there is no finite element model for simulating the complicated surface machining process of CFRP such as the surface milling process.

### 2.3.1 Finite element formulations

For machining simulations using finite element modeling, three formulations have been used: Eulerian, Lagrangian, and Arbitrary lagrangian eulerian (ALE) (Figure 2-8).

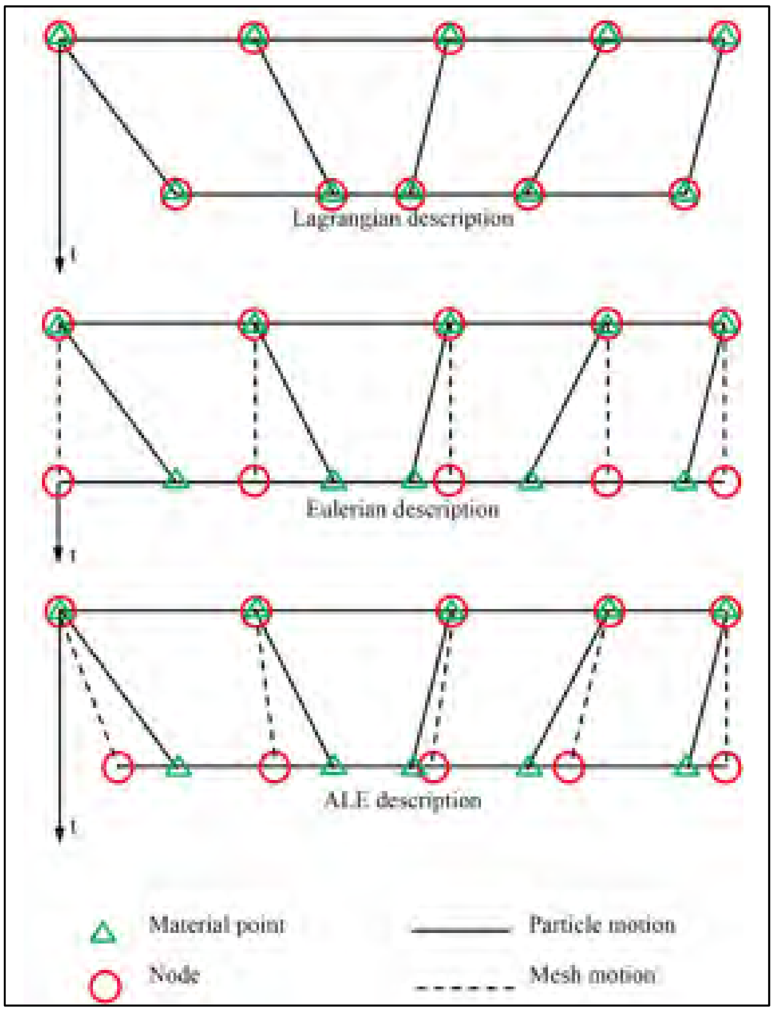


Figure 2-8 One dimensional example of Eulerian, Lagrangian and arbitrary lagrangian eulerian (ALE) mesh (Stein, de Borst et Hughes, 2004)

In the Eulerian method, the mesh is spatially fixed in order to eliminate excessive element distortion, but material can flow through a meshed control volume. In this method, cutting is simulated in the steady state and therefore there is no need for chip separation criteria. The disadvantage of this method is that the initial shape of the chip and the contact conditions must be known.

In Lagrangian method, the mesh is attached to the workpiece and the elements can deform similarly to actual machining. Knowing the chip geometry is not necessary using this formulation. Lagrangian mesh always contains the same material particles. From a computational viewpoint, it is one of significant advantages of this method, especially in problems involving materials with history-dependent behaviors. The disadvantages of this method are the excessive element distortion that reduces the accuracy in large material deformation and the need for frequent remeshing.

In order to have the advantages of both Eulerian and Lagrangian approaches, the arbitrary lagrangian eulerian (ALE) method was developed. In this method, the finite element mesh is neither fixed nor attached to the workpiece material (Stein, de Borst et Hughes, 2004).

### 2.3.2 Definition of CFRP material in finite element method (FEM)

The numerical modeling of fiber reinforced composites can be classified in two general approaches: (I) micromechanical approach where the composite is modeled as multi-phase material and (II) macro mechanical approach where the composite is modeled as an equivalent homogeneous material (EHM).

The micromechanical approach was used successfully to predict cutting forces and local defects in orthogonal cutting of FRP (such as debonding) (Calzada et al., 2012; Dandekar et Shin, 2008; Nayak, Bhatnagar et Mahajan, 2005; Rao, Mahajan et Bhatnagar, 2007a; Rao, Mahajan et Bhatnagar, 2007b). Despite the advantages of the micromechanical approach, such as good accuracy of predicted cutting force and damages, it has some limitations. The micro modeling is more complex than macro modeling and needs very high calculation time and precise details of fibers, fiber-matrix arrangements and their interfacial and physical properties (Dandekar et Shin, 2012). Because of these limitations, the macro mechanical modeling is preferable for modeling complex processes such as milling.

The first macro-mechanical FEM analysis of fiber-reinforced composites was developed by Arola and Ramulu (Arola et Ramulu, 1997) in 1995. The predicted values of principal cutting force agreed well with the experimental values but the predicted thrust force was much lower than experiments. The results of other studies also confirm the shortcoming of macromechanical modeling to predict the thrust forces (Arola, Sultan et Ramulu, 2002; Lasri, Nouari et El Mansori, 2009; Nayak, Bhatnagar et Mahajan, 2005; Santiuste, Soldani et Miguélez, 2010). Mkaddem et al. (Mkaddem et El Mansori, 2009; Mkaddem, Demirci et Mansori, 2008) developed a micro-macro model to get the advantages of both approaches. The composite was modeled as a homogeneous material with anisotropic effective friction coefficients. The model incorporates the adaptive mesh technique and density effect to analyse composite machining. It successfully predicted the sub-surface damages, cutting and thrust forces with lower mean errors (6% for cutting forces and 26% for thrust forces) than another macromechanical model presented by Nayak et al. (17% for cutting forces 44% for thrust forces) (Nayak, Bhatnagar et Mahajan, 2005).

### 2.3.3 Friction at the tool/workpiece interface

Friction is another important parameter in machining simulation. An accurate modeling of the coefficient of friction allows for accurate prediction of cutting forces and temperature distributions. Mahdi and Zhang (Mahdi et Zhang, 2001a) assumed that tool-workpiece friction is negligible but in most researches, a Coulomb friction law has been used to describe the contact between tool and workpiece.

In some researches, the coefficient of friction was assumed constant and equal to 0.3 (Arola et Ramulu, 1997; Rao, Mahajan et Bhatnagar, 2008; Rao, Mahajan et Bhatnagar, 2007b; Rentsch, Pecat et Brinksmeier, 2011), 0.4 (Arola, Sultan et Ramulu, 2002), or 0.5 (Lasri, Nouari et El Mansori, 2009; Santiuste, Soldani et Miguélez, 2010). Nayak and Bhatnagar (Nayak, Bhatnagar et Mahajan, 2005) and Mkaddem (Mkaddem et El Mansori, 2009; Mkaddem, Demirci et Mansori, 2008) used various friction coefficients for different fibre orientations to improve the predicted cutting forces in orthogonal cutting of FRP materials.

### 2.3.4 Failure criteria and chip formation

In the Lagrangian or ALE analysis, it is necessary to define a chip separation criterion (Dandekar et Shin, 2012). Different mechanisms may cause failure in machining of CFRP materials including fiber buckling (compression), fiber breakage (tensile), matrix cracking, matrix crushing and delamination, or a combination of these factors (Figure 2-9). Under longitudinal compression, the flexural stresses in fiber due to buckling lead to the formation of kink zones that can create fracture planes in the carbon fibers (Figure 2-9a). Buckling does not necessarily lead to immediate failure because the surrounding matrix supports the fibers. Under longitudinal tension, the fibers with lower ultimate strain than matrix will fail first. When a fiber breaks in tensile stress, the matrix transmits the load across the gap created by the breakage from the broken to the adjacent fibers. The broken fibers increase gradually in density with increasing load. Stress concentrations thus created by the broken fibers produces failure of adjacent fibers up to the point where catastrophic failure occurs in the composite (Figure 2-9b). (Daniel et Ishai, 2006)

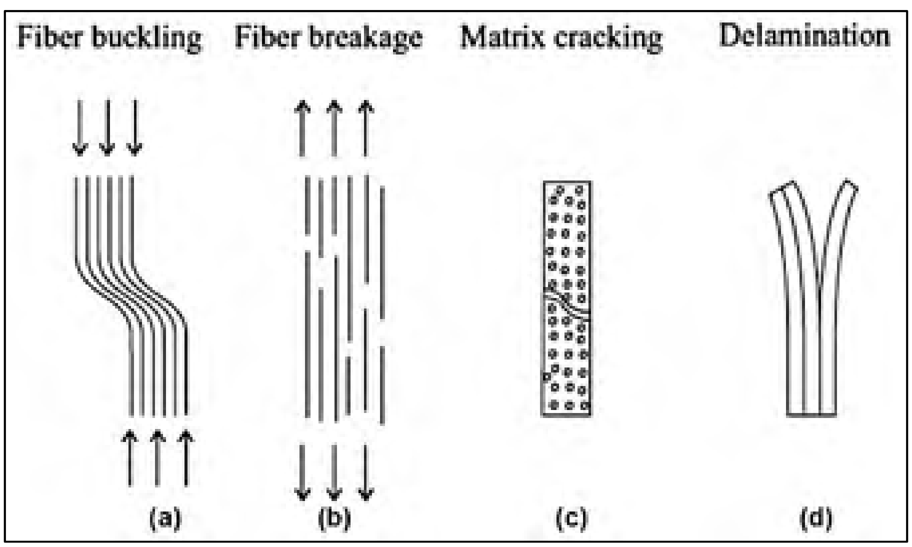


Figure 2-9 Failure modes in machining of CFRP (Kollár et Springer, 2003)

Matrix cracking (Figure 2-9c) frequently occurs in composite laminates and is usually accompanied by other damages, thus it generally does not result in ultimate failure of a laminate. Delamination reduces the bending stiffness and strength as well as the load carrying capability of the laminate under compression. The size of the delamination may increase to a critical point under repeated loading and cause laminate failure (Kollár et Springer, 2003).

There are several theories describing the failure of composite materials such as: (a) maximum stress theory, (b) maximum strain theory, (c) Energy-based interaction theory (Tsai-Hill), (d)Tsai-Wu failure theory, (e) Hoffman failure theory, and (f) Hashin failure theory. According to maximum stress theory, failure occurs when at least one stress component along one of the principal material axis exceeds the corresponding strength in that direction. Lasri et al. (Lasri, Nouari et El Mansori, 2009) used this failure criteria for modeling orthogonal cutting of GFRP in 45º fiber orientation. They found that using maximum stress failure criteria, fiber-matrix debonding was the first damage initiated ahead of cutting tool tip and developed during chip formation process. Matrix failure initiated later and gradually developed in the vicinity of the cutting tool edge. Fiber fracture was the last failure mode occurring during chip formation.

Because failure of composite materials cannot be predicted by the Von Mises yield criterion (this criterion is applicable only for isotropic material), Hill modified the von Mises criterion for ductile and anisotropic materials (Daniel et Ishai, 2006). Tsai-Hill or maximum work criteria is a failure criteria based on Hill criterion that has been used widely in several studies for modeling of CFRP machining (Arola et Ramulu, 1997; Mahdi et Zhang, 2001b; Mkaddem et El Mansori, 2009; Mkaddem, Demirci et Mansori, 2008; Nayak, Bhatnagar et Mahajan, 2005; Rao, Mahajan et Bhatnagar, 2008). Rao et al. (Rao, Mahajan et Bhatnagar, 2008) used this criterion in a three-dimensional modeling of CFRP orthogonal cutting. Their model successfully predicted the cutting forces and chip formation when compared to experiments. The main disadvantage of Tsai-Hill failure theory is that it does not distinguish between tensile and compressive strengths. Tsai-Wu criterion is a modification of Tsai-Hill criterion to overcome this shortcoming. Mkaddem et al. (Mkaddem, Demirci et Mansori,

2008) developed a micro-macro mechanical model using Tsai-Hill criterion to investigate orthogonal machining of composite materials.

Figure 2-10 shows the predicted cutting and thrust forces of their combined micro–macro model. They concluded that the chip size, chip geometry and the cutting forces are significantly dependent on the fiber orientation.

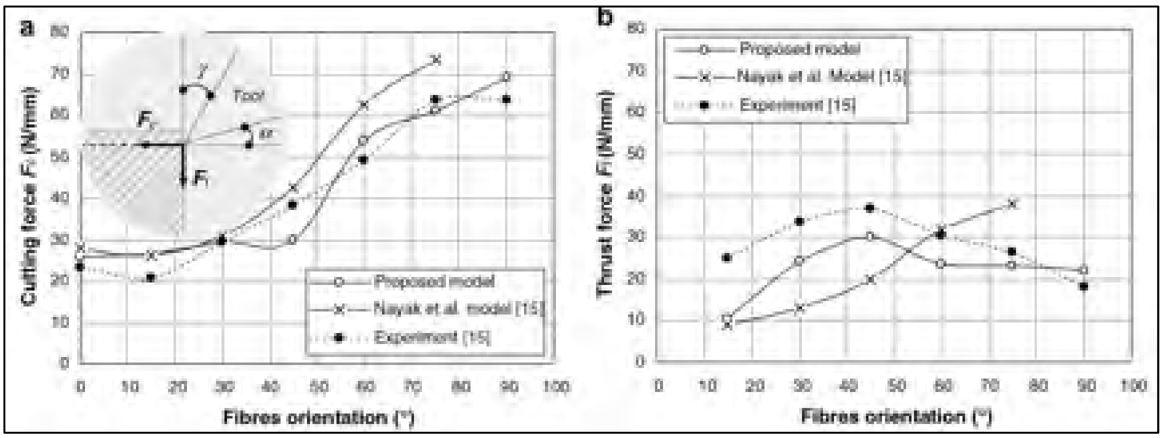


Figure 2-10 Measured and predicted values of a) cutting force $F_c$ ,and b) thrust force $F_t$ (depth of cut= 0.2mm) (Mkaddem, Demirci et Mansori, 2008)

Hoffman also modified Hill's equation by adding linear terms to eliminate the Hill's theory limitation on tensile and compressive strengths (Schellekens et De Borst, 1990). Hashin proposed failure criteria for unidirectional composite materials that include four different failure modes for fiber tensile failure, fiber compressive failure, matrix cracking, and matrix crushing. The Hashin's failure criterion has been extensively used to study FRP orthogonal cutting.

Lasri et al. (Lasri, Nouari et El Mansori, 2009) investigated the orthogonal cutting of glass fiber reinforced plastics (GFRP) using Hashin, Maximum stress, and Hoffman failure criteria. They found that the principal cutting forces simulated with Hashin criterion were closer to the experimental results than other criteria (Figure 2-11a) However, the predicted thrust forces for all failure criteria were much less than experiments (Figure 2-11b). They also observed that chip formation is highly dependent on fiber orientation. For all failure criteria, damage started near the cutting tool edge and propagated parallel and perpendicular to the direction of fibers inside the workpiece.

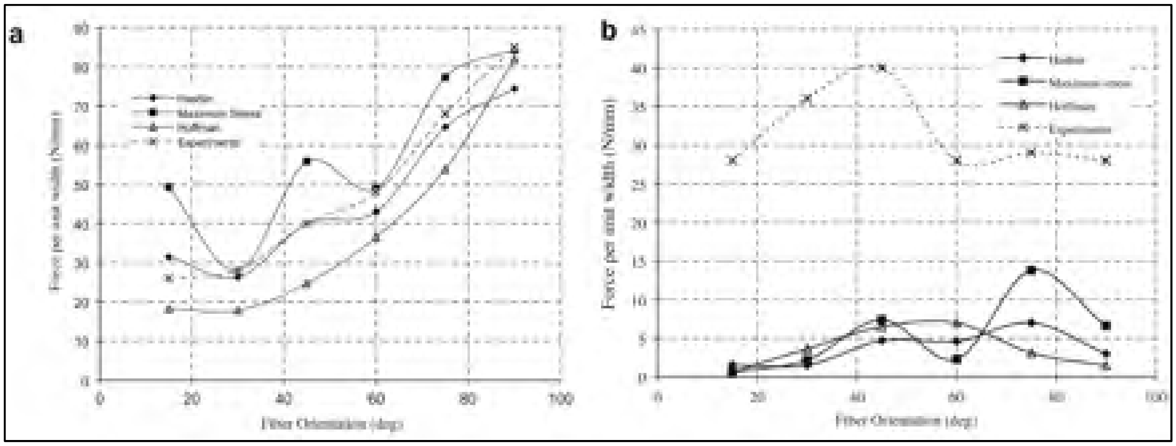


Figure 2-11 Comparison between experimental and predicted values of cutting force using Hashin, Maximum stress, and Hoffman failure criteria, (a) Principal cutting force, (b) Thrust cutting force (Lasri, Nouari et El Mansori, 2009)

## 2.4 Summary

This section presented a review of previous researches on CFRP machining. The effects of different cutting conditions on machining quality and cutting forces were explained. Though numerous studies have been carried out on the machining of CFRP materials, less attention has been given to the tool lead angle in surface milling of CFRPs. Next chapter presents an experimental study on the effect of tool angle and other cutting conditions (such as cutting speed and feed rate) on the cutting forces and machining quality.

The thermal aspect of CFRP milling was discussed in few researches as reported in this literature review. More research is required to determine the effects of different parameters, especially fiber orientation, on the cutting temperature in CFRP surface milling operation. An experimental investigation on cutting temperature in ball-end milling of unidirectional CFRP is carried out in chapter 4, where the effects of cutting conditions (cutting speed and feed rate) and fiber orientation on cutting temperature, cutting forces and machining quality are demonstrated.

The importance of milling modeling was highlighted and different approaches in machining modeling were briefly introduced. The literature review showed that few studies focused on modeling of fiber reinforced plastics milling. The available models for CFRP milling were limited to empirical, semi-analytical, and neural networks based models and no study was found on finite element modeling of CFRP milling process. Since these force models are unable to predict the chip formation and machining damages, an appropriate numerical model is essential in order to study the complicated milling process. A modeling study of CFRP milling is presented in chapter 5 where a combined micro-macro mechanical model is used to provide a better understanding of CFRP surface milling and explain the chip formation mechanism and machining damages in this operation.

# CHAPTER 3

## EFFECT OF CUTTING TOOL LEAD ANGLE ON MACHINING FORCES AND SURFACE FINISH OF CFRP LAMINATES

S.B. Ghafarizadeh[a], J.F. Chatelain[b], G. Lebrun[c]

[a,b] Department of Mechanical Engineering, École de Technologie Supérieure,
1100 Notre-Dame West, Montreal, Québec, Canada H3C 1K3
[c] Department of Mechanical Engineering, Université du Québec à Trois-Rivières
C.P. 500, Trois-Rivières, Québec, G9A 5H7

This article is published
in *Science and Engineering of Composite, April 2015 (APPENDIX I)*

### 3.1 Abstract

Machining is one of the most practical processes for finishing operations of composite components, allowing high quality surface and controlled tolerances. The high precision surface milling of Carbon Fiber Reinforced Plastics (CFRP) is particularly applicable in the assembly of complex components requiring accurate mating surfaces, as well as for surface repair or mold finishing. CFRP Surface milling is a challenging operation because of the heterogeneity and anisotropy of these materials, which are the source of several types of damage, such as delamination, fibers pullout, and fiber-fragmentation. In order to minimize the machining problems of CFRP milling and improve the surface quality, this research focuses on the effect of multi axis machining parameters, such as the feed rate, cutting speed, and lead angle, on cutting forces and surface roughness. The results show that the surface roughness and cutting forces increase with the feed rate, while their variations are not uniform when changing the cutting speed. Generally, a lower surface roughness was achieved by using lower cutting feed rate (0.063 mm/rev) and higher cutting speeds (250-500 m/min). It was also found that the cutting forces and surface roughness vary significantly and non-linearly with the lead angle of the cutting tool with respect to the surface.

**Keywords:** Carbon fiber reinforced plastic, surface machining, milling, surface quality

## 3.2 Introduction

In recent years, the use of Carbon Fiber Reinforced Plastics (CFRP) has increased considerably, especially in aerospace industries. Nowadays, many aircraft parts are made of this composite material. For example, about 50% of the weight of the Boeing 787 aircraft is made from composite materials such as carbon/epoxy and graphite/ titanium (Daniel et Ishai, 2006). CFRP composites are widely used for different parts of aircrafts such as wing boxes, fuselages, ailerons, wings, spoilers, vertical stabilizers, traps and struts (Gay et Hoa, 2007). CFRP materials present many advantages compared to other materials, including higher strength and stiffness, longer fatigue life, low density and better corrosion and wear resistance. Because of a negative coefficient of thermal expansion along the axis of carbon fibers, carbon reinforced composites can be patterned to minimize the thermal expansion over a wide range of temperatures. This is very important for aerospace structures (Sheikh-Ahmad, 2008).

CFRP components are usually produced to near net-shape, but machining is often required to remove excess material and produce high quality surfaces with controlled tolerances. In particular, drilling and trimming are extensively used to remove excessive material, produce cutouts, or holes that are required for the product function or to assemble components. The high precision surface milling of Carbon Fiber Reinforced Plastics is particularly useful for the assembly of complex components requiring accurate mating surfaces, as well as for surface repair and mold finishing. CFRP surface milling is a challenging operation because of the heterogeneous and anisotropic nature of these composites, which can cause some damages such as delamination, fibers pullout, fiber-fragmentation, burring, fuzzing, or thermally affected matrix which in turn may affect the surface finish and properties of the material (Ferreira, Coppini et Miranda, 1999; Wang et Zhang, 2003). In addition, these composites are extremely abrasive; consequently tool wear is one of the major problems encountered in CFRP machining. Poor cutting conditions produce increased specific cutting energies and higher tool temperatures, resulting in higher tool wear rates (Boothroyd et Knight, 2006). Choosing the appropriate conditions, such as feed rate, cutting speed, and lead angle, in the case of multi axis machining is thus very important.

In recent years, many studies have been carried out to provide a better understanding regarding the effects of cutting conditions in CFRP machining on the quality of machined surfaces. Devim and Reis (Davim et Reis, 2005) investigated the effects of milling parameters on surface roughness and machining damage. They concluded that surface roughness (Ra) increases with the feed rate and decreases with the cutting speed. It was also found that the feed rate presents the highest statistical and physical influence on surface roughness and on delamination factor, respectively. In another study, El-Hofy et al. (El-Hofy et al., 2011) investigated the effects of different slotting parameters, such as tool materials (WC & PCD) and the cutting environment (chilled air& dry) on the surface roughness and integrity, using 3D roughness parameters (arithmetical mean height Sa and maximum peak to valley height St). According to the results of their research, the combination of low cutting speeds and high feed rates was recommended in view of improving surface roughness, with the feed rate being a significant factor. The effect of the feed rate on the surface roughness was also found to be significant from a study that was carried out by Chatelain et al. (Chatelain, Zaghbani et Monier, 2012). Sheikh-Ahmad et al. (Sheikh-Ahmad, Urban et Cheraghi, 2012) carried out an experimental study aimed to determine the effects of cutting conditions on machining quality during the edge trimming of CFRP. They demonstrated that the surface roughness and average delamination depth increase with an increase in the feed rate and decreases with an increase in the spindle speed.

Cutting forces are among the important factors in machining. They influence the process stability, part quality, cutting temperature, and tool wearing condition (Zaghbani et al., 2012a). Colligan and Ramulu (Colligan et Ramulu, 1999) studied the edge trimming of graphite/epoxy with diamond abrasive cutters and demonstrated that cutting forces increase with the material removal rate (where, V is cutting speed, f is feed rate and d is depth of cut).

Sreejith et al.'s (Sreejith et al., 2000) experiments examining the face turning of FRP showed that variations of cutting forces/specific cutting pressure is not uniform over the cutting speed, and the moderate cutting speeds (200-300 m/min) are more suited for the machining of CFRP. Zhang (Zhang, 2009) investigated the machining of long fiber reinforced polymer matrix composites and found that cutting forces became greater when the depth of cut increases. Rusinek (Rusinek, 2010) studied the milling process of CFRP and concluded that the cutting force rises with an increase in the feed rate. Wang et al. (Wang et al., 2011) studied CFRP milling using a PCD tool, and showed that good surface quality and low delamination could be achieved in high speed milling of CFRP by using PCD tool. They found that cutting forces are an important factor for controlling surface roughness; they also observed that the surface roughness tends to increase with the cutting forces up to 250 N, followed by a decrease when the cutting forces continue to rise from 250N to 400 N.

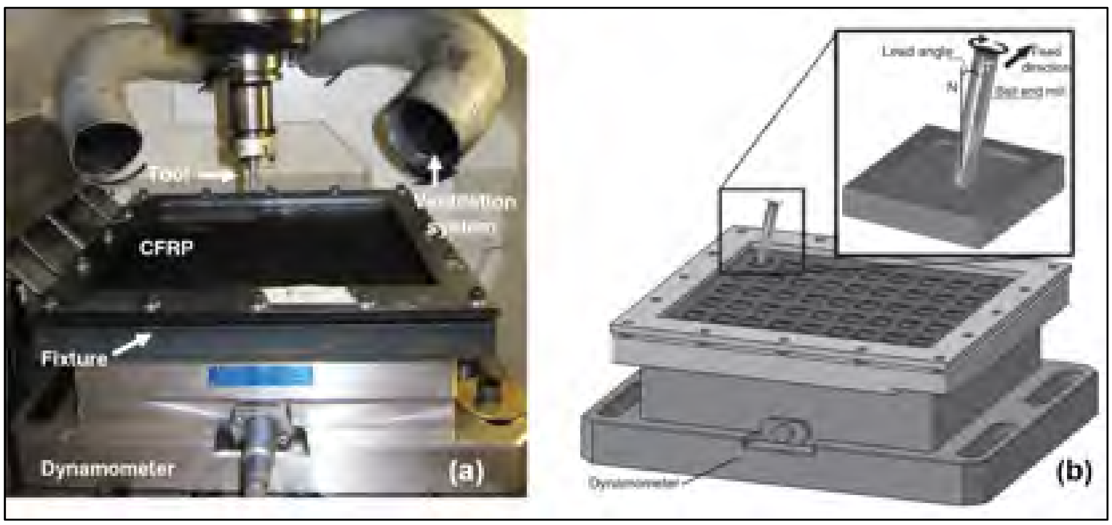


Figure 3-1 CFRP milling, a) experimental setup, b) tool lead angle

The lead angle is the rotation of the tool axis about the cross-feed axis (Ozturk, Tunc et Budak, 2009) (Figure 3-1). This angle has a significant effect on process mechanics and dynamics, which have not been studied in CFRP milling until now. The study of the effect of the lead angle on metal milling has shown that the cutting geometry, mechanics, and dynamics vary drastically and non-linearly with the lead angle (Ozturk, Tunc et Budak, 2009). Despite of all the researches that have been carried out to provide a better understanding of the machining of fiber reinforced polymers, there are still many challenges with CFRP machining.

This work presents some experiments that have been carried out on CFRP to study the optimum condition for the multi-axis milling of these materials and investigates the effects of different parameters such as the cutting speed, the feed rate, and the lead angle on the resulting cutting forces, surface quality, and machining damages.

### 3.3 Materials and methods

A set of experiments was carried out to provide a better understanding of the effects of machining parameters on surface quality and cutting forces. A high performance carbon fiber epoxy prepreg having a 64% fiber volume content was used to produce stacks of 24 plies that were autoclave-cured to obtain composite plates with a final average thickness of approximately 3.5 mm. Quasi-isotopic laminates are an important class of composites, and those that are most familiar to aerospace industries. With such laminates, the elastic properties are independent of orientation and stiffness, compliance and all engineering constants are almost identical in all directions (Daniel et Ishai, 2006; Soden, Hinton et Kaddour, 1998). The symmetric stacking sequence [90/-45/45/0/(±45)2/0/-45/45/90]s of the plies was such as to provide a laminate with in-plane quasi-isotropic properties (Figure 3-2).

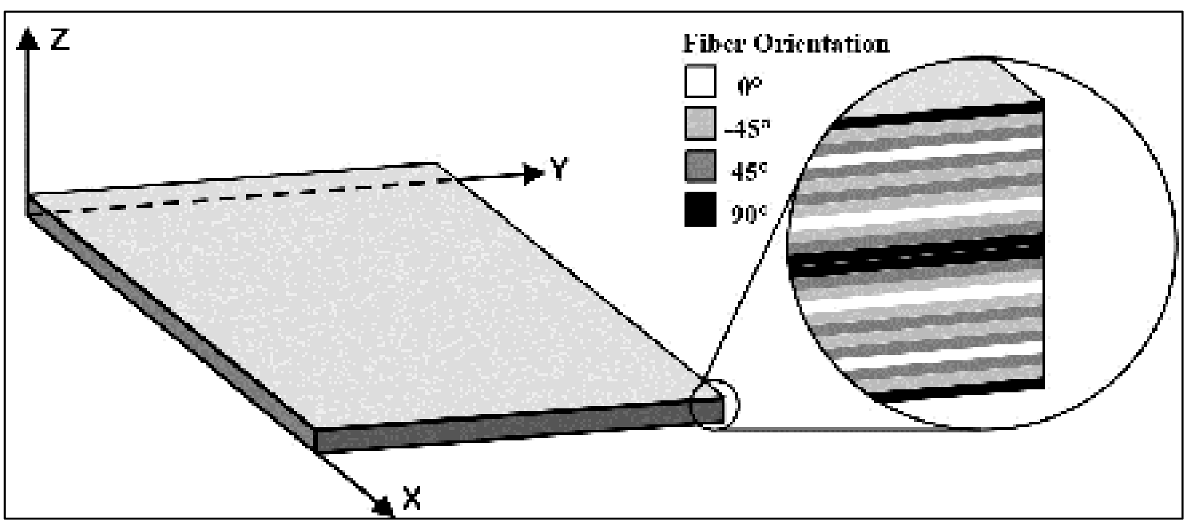


Figure 3-2 The layup of multidirectional CFRP

This layup is balanced and symmetric, and as a result, extension/bending coupling ($B_{ij}$) and shear coupling stiffnesses ($A_{is}$) are zero, and because of the fine ply distribution, the torsion coupling ($D_{is}$) is relatively low (i, j= x, y, s; the subscript s denotes shear stress in the x-y plane, and subscripts the x and y denote normal strains in the x- and y- directions, respectively). Because of these characteristics, warpage and unexpected distortion are avoided and interlaminar stresses reduced (Daniel et Ishai, 2006).

The experiments were carried out using a Huron K2X8 five-axis CNC machine with a maximum spindle speed of 24,000 rpm under different cutting speeds, feed rates and lead angles under dry cutting condition, while keeping the axial depth of cut and radial depth of cut (or width of cut: distance between milling passes) constant and equal to 1.4 and 0.71 mm, respectively.

Table 3-1 Description of tool geometries

| **Tool material** | **Number of flouts** | **Shank diameter** | **Flute Length** | **Overall length** | **Helix angle** | **Rake angle** | **Overall length** |
|---|---|---|---|---|---|---|---|
| PCD brazed inserts | 2 | 3/8" | 1/2" | 4" | 0 | 24° | 4" |

The cutting mode was up-milling with a 3/8 inch diameter ball end mill (LMT. ONSRUD, Waukegan, USA) having two flutes with polycrystalline diamond (PCD) brazed inserts (Figure 3-3). Table 3-1details the tool geometry. Different cutting conditions were studied including: the cutting speed (100 to 500 m/min), the feed rate (0.063 to 0.254 mm/rev) and the lead angle (-10 to +10º), as can be seen in Table 3-2. In this table, the cutting speed levels are calculated from the tool shank diameter. Each experimental run was repeated three times, with the same conditions, to evaluate the repeatability of the experiments.

Figure 3-3 Two-flute polycrystalline diamond (PCD) ball end mills

A Kistler 9255B(#3) three-axis dynamometer table (Kistler Group, Winterthur, Switzerland), connected to charge amplifiers, type Kistler 5010, was used for measuring the cutting forces during machining. The experimental setup is shown in Figure 3-1.

Commercially available dynamometers typically specify a bandwidth below the first natural frequency of the dynamometer structure (Burton et al., 2004). The Kistler 9255B dynamometer table has a nominal natural frequency ($f_n$) equal to 2 kHz in x- and y- directions and 3.3 kHz in the z- direction (Kistler-Group, 2009).

Table 3-2 Cutting parameters

| Cutting speed (m/min) | Spindle speed (RPM) | Feed rate (mm/rev) | Lead angle (º) |
|---|---|---|---|
| 100 | 3341 | 0.063 | -10 |
| 175 | 5848 | 0.158 | -5 |
| 250 | 8354 | 0.254 | 0 |
| 375 | 12531 | | 5 |
| 500 | 16709 | | 10 |

Any machining operations reaching this range may lead to cutting force signals which are distorted because of the influence of the dynamic behavior of the dynamometer. Thus, the determination of the passing bandwidth is a very important step for an accurate force measurement during milling with high cutting speed. Zaghbani et al. (Zaghbani et al., 2012a) studied the dynamometer behavior of the Kistler 9255B (3#) dynamometer table with the same setup and calibration method as the ones used in the present study. They showed that the cutting force measurement setup has a passing bandwidth less than 1 kHz in the z- direction and 2 kHz in x- and y- directions. In the case of the z- direction (lower passing bandwidth) , the highest tooth passing frequency should therefore not be higher than 1 kHz, which corresponds to a spindle speed of 450 Hz for a two-tooth cutter (27000 r/min). In this study, all spindle speeds were lower than 27000 RPM (800 m/min for a tool with 3/8 inch diameter), according to Table 3-2. The roughness of the machined surfaces was measured using a Mitutoyo SJ400 contact profilometer (Mitutoyo Corporation, Tokyo, Japan) (Figure 3-4).


Figure 3-4 Measuring of surface roughness

Three readings were taken for each surface over an evaluation length of 12.5 mm, at regular intervals in a transverse direction to the cutting (feed direction), and their average was calculated. The measured values of Ra (arithmetic average height) and Rt (total height of the roughness profile) in different cutting conditions were compared in order to investigate the effect of cutting conditions on the surface quality.

Table 3-3 indicates the average of measured resultant cutting forces and surface roughness for three times repetition of each condition. The surfaces were also examined using a Keyence VHC-500F type digital microscope (Keyence Corporation, Osaka, Japan), as well as Hitachi S-3600N electronic microscope (Hitachi Science Systems Ltd, Tokyo, Japan) [scanning electron microscopy (SEM)].

## 3.4 Results

### 3.4.1 Effects of feed rate and cutting speed on surface roughness

Surface morphology and integrity depend on the machining process and workpiece characteristics such as the cutting speed, the feed rate, the fiber type and volume content, the fiber orientation and the matrix type (Sheikh-Ahmad, 2008).

Figure 3-5 and Figure 3-6 show the effects of the feed rate and cutting speed on the average surface roughness ($R_a$) and total roughness ($R_t$), respectively. When comparing both figures, it is obvious that the variations of $R_t$ and $R_a$ with the cutting speed follow the same trends. All the roughness results will therefore be discussed for Ra values alone. As can be seen, Ra increases with an increase in the feed rate.

Table 3-3 Values of resultant cutting force ($F_c$) and surface roughness ($R_a$) as a function of the cutting parameters (average of three times repetition)

| **Test No.** | **Cutting speed (m/min)** | **Feed rate (mm/rev)** | **Lead angle (°)** | **$F_c$ (N)** | **$R_a$ (μm)** |
|---|---|---|---|---|---|
| 1 | 100 | 0.063 | 0 | 60.30 | 2.69 |
| 2 | 175 | 0.063 | 0 | 62.66 | 2.30 |
| 3 | 250 | 0.063 | 0 | 81.52 | 1.89 |
| 4 | 375 | 0.063 | 0 | 97.79 | 1.75 |
| 5 | 500 | 0.063 | 0 | 94.05 | 1.87 |
| 6 | 100 | 0.158 | 0 | 83.02 | 4.70 |
| 7 | 175 | 0.158 | 0 | 69.80 | 3.44 |
| 8 | 250 | 0.158 | 0 | 90.05 | 2.73 |
| 9 | 375 | 0.158 | 0 | 120.42 | 2.82 |
| 10 | 500 | 0.158 | 0 | 116.69 | 2.74 |
| 11 | 100 | 0.254 | 0 | 80.90 | 4.76 |
| 12 | 175 | 0.254 | 0 | 84.04 | 4.19 |
| 13 | 250 | 0.254 | 0 | 123.44 | 4.53 |
| 14 | 375 | 0.254 | 0 | 145.63 | 5.38 |
| 15 | 500 | 0.254 | 0 | 138.17 | 5.01 |
| 16 | 100 | 0.063 | -10 | 65.94 | 2.50 |
| 17 | 175 | 0.063 | -10 | 70.76 | 2.68 |
| 18 | 250 | 0.063 | -10 | 62.51 | 2.22 |
| 19 | 375 | 0.063 | -10 | 75.37 | 2.21 |
| 20 | 500 | 0.063 | -10 | 80.00 | 2.56 |
| 21 | 100 | 0.063 | -5 | 75.86 | 3.31 |
| 22 | 175 | 0.063 | -5 | 81.25 | 3.59 |
| 23 | 250 | 0.063 | -5 | 68.16 | 3.04 |
| 24 | 375 | 0.063 | -5 | 95.48 | 2.24 |
| 25 | 500 | 0.063 | -5 | 82.39 | 2.28 |
| 26 | 100 | 0.063 | 5 | 83.57 | 1.85 |
| 27 | 175 | 0.063 | 5 | 93.86 | 1.86 |
| 28 | 250 | 0.063 | 5 | 96.32 | 2.07 |
| 29 | 375 | 0.063 | 5 | 131.73 | 1.96 |
| 30 | 500 | 0.063 | 5 | 90.37 | 2.02 |
| 31 | 100 | 0.063 | 10 | 74.83 | 2.25 |
| 32 | 175 | 0.063 | 10 | 72.57 | 2.17 |
| 33 | 250 | 0.063 | 10 | 79.06 | 2.22 |
| 35 | 375 | 0.063 | 10 | 96.09 | 2.40 |
| 35 | 500 | 0.063 | 10 | 90.26 | 2.25 |

The dependence of the surface roughness on the cutting speed is more complex. However, it could generally be concluded that for lower cutting speeds (100 and 175 m/min), the surface roughness decreases by increasing the cutting speed.

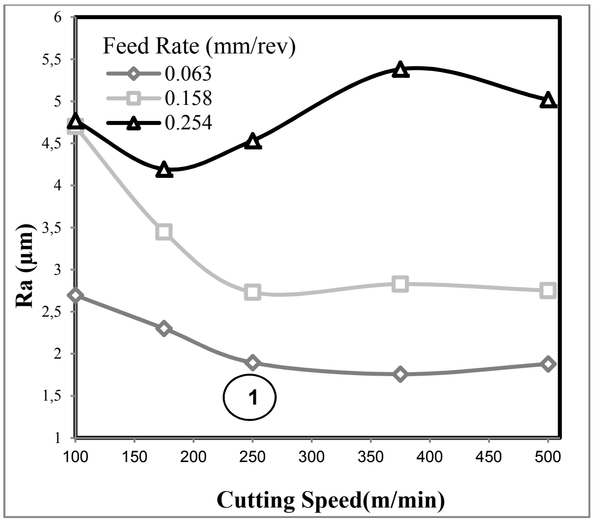


Figure 3-5 Effects of feed rate and cutting speed on the $R_a$, 0º lead angle

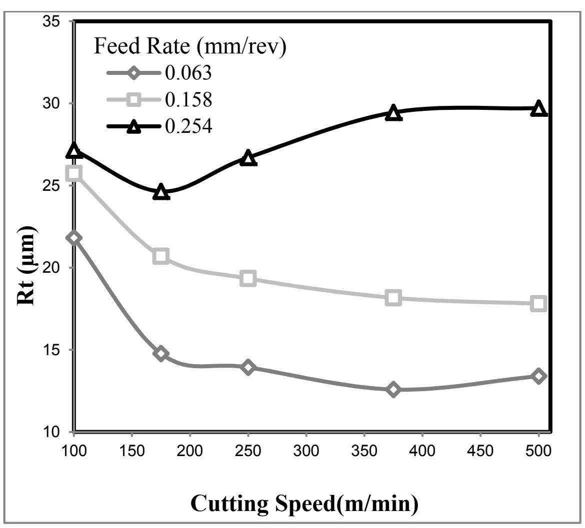


Figure 3-6 Effect of feed rate and cutting speed on the $R_t$, 0º lead angle

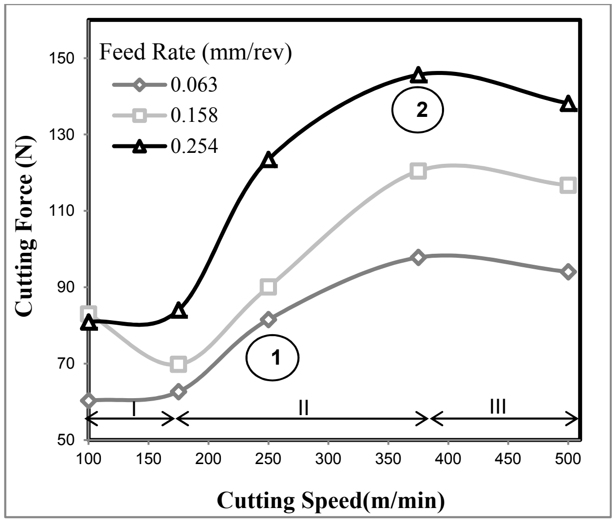


Figure 3-7 Effects of feed rate and cutting speed on the cutting force, 0º lead angle

Increasing the cutting speed to more than 250 m/min does not have a significant effect on the surface roughness for lower feed rates (0.063 and 0.158 mm/rev). The minimum surface roughness values were achieved with a low feed rate (0.063 mm/rev) and higher cutting speed (250-500 m/min). For a higher feed rate (0.254 mm/rev), the roughness diagram has a minimum point at 175 m/min and a maximum point (point 2) at 375 m/min cutting speed. Increasing the feed rate and cutting speed increases the cutting temperature (Sreejith et al., 2000), which can lead to softening and burning of the matrix material (Hamedanianpour et Chatelain, 2013). Therefore, decreasing the surface roughness for higher feed rates (0.158 and 0.254 mm/rev) at a 500 m/min cutting speed might be explained by adhering of the uncut fibers to the softened matrix under high cutting temperatures.

### 3.4.2 Effects of feed rate and cutting speed on cutting force

According to the literature, cutting forces generally increase with an increase in the feed rate, but the dependence of cutting forces on the cutting speed is not uniform for different types of fiber reinforced plastics (Sheikh-Ahmad, 2008). Figure 3-7 illustrates the effect of the feed rate and cutting speed on the resultant cutting force in our experiments. It can be seen that the cutting force increases with an increase in the feed rate, and there is a greater influence on the cutting force for higher cutting speeds.

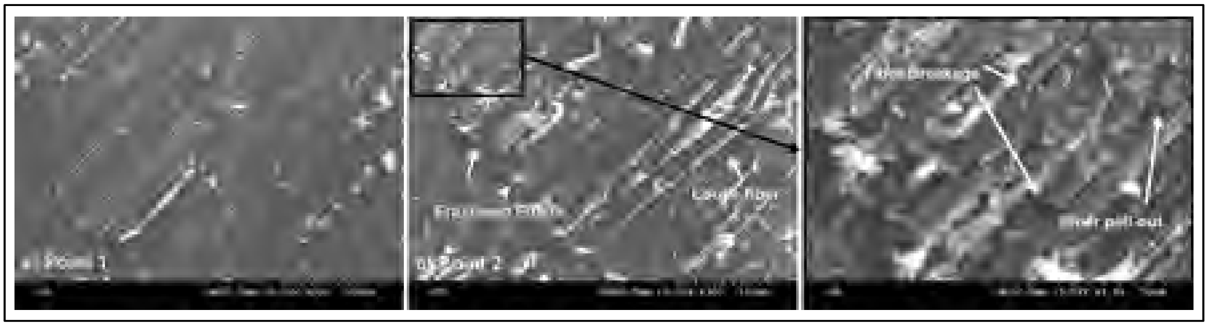

Figure 3-8 Effect of cutting speed on the quality of machined surface, lead angle 0º, a) Cutting speed 250 m/min, feed rate 0.063 mm/rev, b) Cutting speed: 375 m/min, feed rate=0.254 mm/rev

The variation of cutting forces is not uniform over the cutting speed and can be studied in three cutting speed ranges, including I. low cutting speeds (100-175 m/min), II. moderate cutting speeds (175-375 m/min), and III. high cutting speeds (375-500 m/min). In range I, the effect of cutting speed on resultant cutting force is not significant, but in range II, the cutting force rises with the cutting speed. In the third range, the cutting force diminishes when the cutting speed increases. The non-uniform variation of the cutting force to cutting speed is consistent with other studies (Hamedanianpour et Chatelain, 2013; Sheikh-Ahmad, 2008; Zhang, 2009). The rate of variation of the cutting forces with the cutting speed is related to cutting temperatures. At low cutting speeds, the cutting temperatures are not high enough to soften the polymer matrix, and dry friction predominates. The softening/degrading of the matrix in the cutting zone occurs at a critical speed and causes a reduction in cutting forces (Sheikh-Ahmad, 2008). Figure 3-7 shows that this critical speed is probably reached in range III, where the cutting forces become almost independent of the cutting speed.

Among the conditions resulting in lower roughness (feed rate 0.063 mm/rev and cutting speeds 250-500 m/min), point 1 in Figure 3-5 and Figure 3-7 has the lowest cutting force, which produces greater process stability and part quality. Therefore, this condition is recommended for the surface machining of CFRP with this cutting tool. A comparison of the surface quality in point 1 with that in point 2 (the point with the highest surface roughness and cutting force) in Figure 3-8 shows that much damage occurs using a high feed rate.

### 3.4.3 Effects of lead angle on surface roughness and cutting force

The study of the effect of the lead angle on the surface roughness showed that it varies non-linearly with the lead angle and that variation depends on the cutting speed. Figure 3-9 shows the effect of the lead angle on the surface roughness for different cutting speeds and a feed rate of 0.0635 mm/rev.

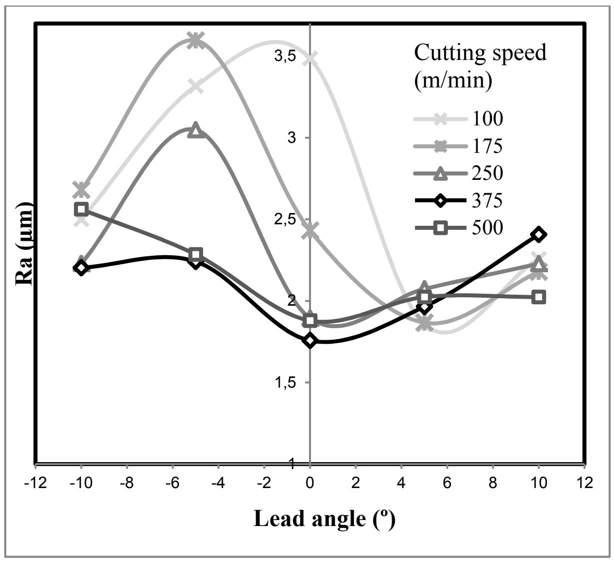


Figure 3-9 Effect of lead angle on the roughness $R_a$ for different cutting speeds (feed=0.0635 mm/rev)

The minimum Ra is achieved for a lead angle of 5° for low cutting speeds (100 and 175 m/min) and 0° for higher cutting speeds (250-500 m/min). The diagram in Figure 3-9 illustrates that the variability in roughness curves is higher for negative lead angles. It is shown that the roughness curves for lower cutting speeds (100, 175 and 250 m/min) have high amplitudes as compared to those for higher cutting speeds (375 and 500 m/min). In other words, the sensitivity of roughness to the lead angle is higher for the low cutting speeds. Figure 3-10 shows the effect of the lead angle on the resultant cutting forces for different cutting speeds and a feed rate of 0.063 mm/rev. As can be seen, the variation of the cutting force with the lead angle is not uniform for all cutting speeds. However, the minimum cutting forces were achieved at the lead angle 0º for low cutting speeds (100, and 175 m/min) and -10º for higher cutting speeds (250, 375 and 500 m/min).

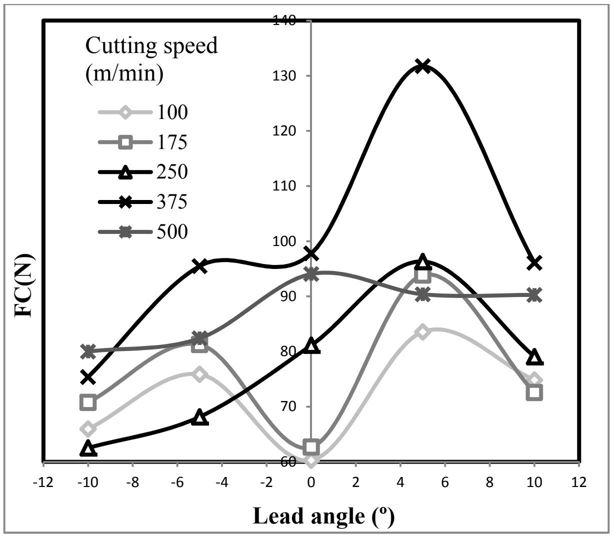


Figure 3-10 Effect of lead angle on the cutting force, (feed= 0.063 mm/rev)

Figure 3-11 shows the SEM images of a machined surface with different lead angles. As can be seen, the best quality surface was achieved with a lead angle equal to 0 and -10 degree where the roughness and cutting force are respectively at minimum values. More damage, such as fiber breakage, fiber de-cohesion and matrix damage is observed in the case of 5º lead angle while the roughness and cutting force have maximum values.

### 3.5 Conclusions

In this paper, surface milling experiments were carried out on carbon fiber reinforced laminates in order to study the effects of cutting parameters on the cutting force and surface quality, and to find the optimum conditions for this operation type using a PCD two-flute ball nose end mill. Based on the presented results, the following conclusions are drawn:

- The surface roughness increases with an increase in the feed rate for all cutting speeds.
- At lower cutting speeds (100 and 175 m/min), the surface roughness decreases with an increase in the cutting speed, while increasing the cutting speed to more than 250 m/min has no significant effect on the surface roughness for lower feed rates (0.063 and 0.158 mm/rev).

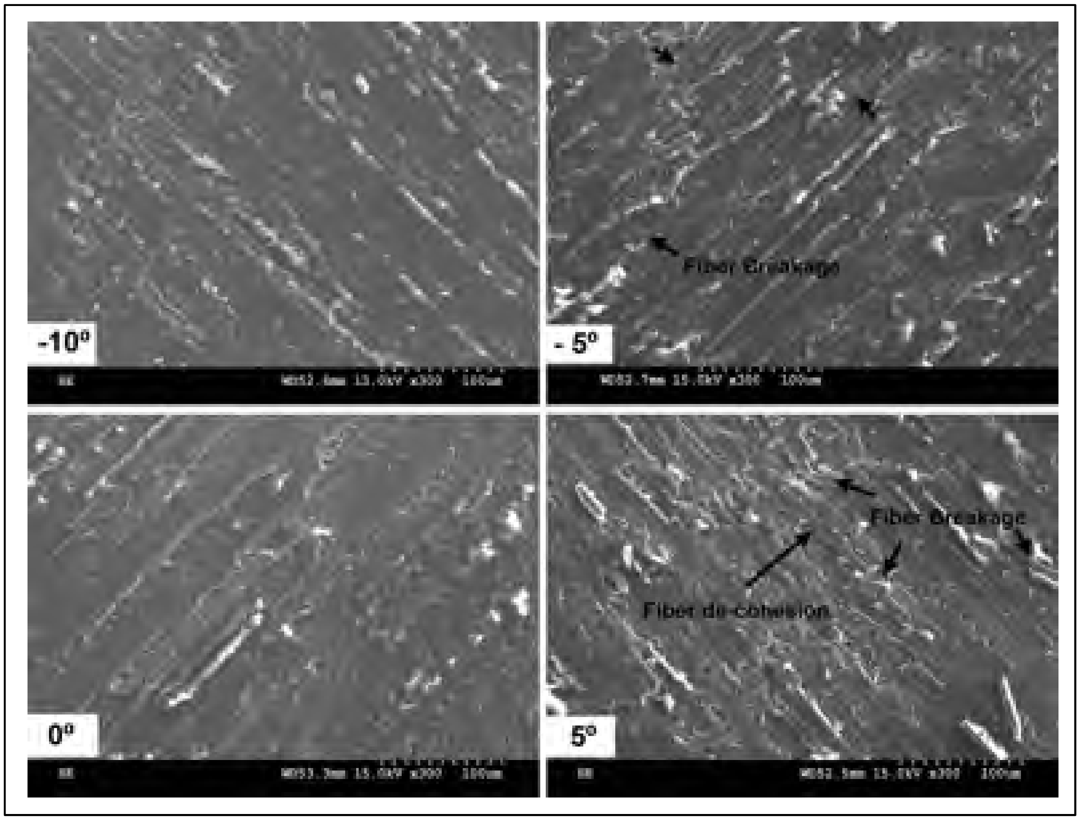


Figure 3-11 SEM images of machined surface with different lead angles (cutting speed 250 m/min, feed rate 0.063 mm/rev)

- The cutting force increases with the feed rate, but the variation of cutting forces showed no consistent trend over the cutting speed range evaluated. However, the effect of the cutting speed on cutting force is more significant for moderate cutting speed values (175-375 m/min), while improving the cutting force.

- The variation of the cutting force and surface roughness with the lead angle is non-linear and the minimum values are found at the 250 m/min speed and 0.0635 mm/rev feed rate, for lead angles equal to 0º and -10º, respectively. This latter value is unexpected since it is quite an unusual lead angle in multi-axis machining.

- Instability in the roughness diagram increases when using a negative lead angle. On the other hand, using a positive lead angle produces higher cutting forces.

### 3.6 Acknowledgment

This research was funded by the Consortium for Research and Innovation in Aerospace in Quebec (CRIAQ) and its partners, the Natural Sciences and Engineering Research Council of Canada (NSERC), MITACS, Bombardier Aerospace, Avior Integrated Products, Delastek and AV&R Vision & Robotics.

### 3.7 References

Boothroyd, G, et WA Knight. 2006. *Fundamentals of Machining and Machine Tools*, CRC Publication. ISBN 1-57444-659-2.

Burton, David, G Scott Duncan, John C Ziegert et Tony L Schmitz. 2004. « High frequency, low force dynamometer for micro-milling force measurement ». *In 19th annual meeting on American Society for Precision Engineering (ASPE 2004*). (University of Florida), p. 221–224.

Chatelain, Jean François, Imed Zaghbani et Joseph Monier. 2012. « Effect of Ply Orientation on Roughness for the Trimming Process of CFRP Laminates ». *C. World Academy of Science, Engineering and Technology*, vol. 68, p. 1204-1210.

Colligan, K, et M Ramulu. 1999. « Edge trimming of graphite/epoxy with diamond abrasive cutters ». *Journal of Manufacturing Science and Engineering*, vol. 121, n° 4, p. 647-655.

Daniel, I.M., et O. Ishai. 2006. *Engineering mechanics of composite materials*, second edition. New York, USA: Oxford university press.

Davim, J.P., et P. Reis. 2005. « Damage and dimensional precision on milling carbon fiber-reinforced plastics using design experiments ». *Journal of Materials Processing Technology*, vol. 160, no 2, p. 160-167.

El-Hofy, MH, SL Soo, DK Aspinwall, WM Sim, D Pearson et P Harden. 2011. « Factors affecting workpiece surface integrity in slotting of CFRP ». *Procedia Engineering*, vol. 19, p. 94-99.

Ferreira, JR, NL Coppini et GWA Miranda. 1999. « Machining optimisation in carbon fibre reinforced composite materials ». *Journal of Materials Processing Technology*, vol. 92, p. 135-140.

Gay, D, et SV Hoa. 2007. *Composite materials: design and applications*, 2nd. CRC Press.

Hamedanianpour, Hossein, et Jean François Chatelain. 2013. « Effect of Tool Wear on Quality of Carbon Fiber Reinforced Polymer Laminate during Edge Trimming ». *In Applied Mechanics and Materials.* Vol. 325, p. 34-39.

Kistler-Group. 2009. *Cutting Force Measuring Catalog*, Data sheet: 9255B_000-148. Switzerland: Kistler Group.

Ozturk, Erdem, L Taner Tunc et Erhan Budak. 2009. « Investigation of lead and tilt angle effects in 5-axis ball-end milling processes ». *International Journal of Machine Tools and Manufacture*, vol. 49, n$^{o}$ 14, p. 1053-1062.

Rusinek, Rafal. 2010. « Cutting process of composite materials: An experimental study ». *International Journal of Non-Linear Mechanics*, vol. 45, n$^{o}$ 4, p. 458-462.

Sheikh-Ahmad, J.Y. 2008. *Machining of Polymer Composites*. Springer Verlag.

Sheikh-Ahmad, Jamal, Nebu Urban et Hossein Cheraghi. 2012. « Machining damage in edge trimming of CFRP ». *Materials and Manufacturing Processes*, vol. 27, n$^{o}$ 7, p. 802-808.

Soden, PD, MJ Hinton et AS Kaddour. 1998. « Lamina properties, lay-up configurations and loading conditions for a range of fibre-reinforced composite laminates ». *Composites Science and Technology*, vol. 58, n$^{o}$ 7, p. 1011-1022.

Sreejith, PS, R Krishnamurthy, SK Malhotra et K Narayanasamy. 2000. « Evaluation of PCD tool performance during machining of carbon/phenolic ablative composites ». *Journal of Materials Processing Technology*, vol. 104, n$^{o}$ 1, p. 53-58.

Wang, XM, et LC Zhang. 2003. « An experimental investigation into the orthogonal cutting of unidirectional fibre reinforced plastics ». *International Journal of Machine Tools and Manufacture*, vol. 43, n$^{o}$ 10, p. 1015-1022.

Wang, Yong Guo, Xiang Ping Yan, XG Chen, Chang Yu Sun et G Liu. 2011. « Cutting performance of carbon fiber reinforced plastics using PCD tool ». *In Advanced Materials Research*. Vol. 215, p. 14-18.

Zaghbani, Imed, Jean-François Chatelain, Victor Songmene, Sébastien Bérubé et Abdelatif Atarsia. 2012. « A comprehensive analysis of cutting forces during routing of carbon fiber-reinforced polymer laminates ». *Journal of Composite Materials*, p. 0021998311428362.

Zhang, LC. 2009. « Cutting composites: A discussion on mechanics modelling ». *Journal of materials processing technology*, vol. 209, n$^{o}$ 9, p. 4548-4552.

## CHAPTER 4

# EXPERIMENTAL INVESTIGATION OF THE CUTTING TEMPERATURE AND SURFACE QUALITY DURING MILLING OF UNIDIRECTIONAL CARBON FIBER REINFORCED PLASTIC

S.B. Ghafarizadeh[a], G. Lebrun[b], J.F. Chatelain[c]

[a,c] Department of Mechanical Engineering, École de Technologie Supérieure,
1100 Notre-Dame West, Montreal, Québec, Canada H3C 1K3
[b] Department of Mechanical Engineering, Université du Québec à Trois-Rivières
C.P. 500, Trois-Rivières, Québec, G9A 5H7

This article is published
in *Journal of Composite Materials, May 2015*

### 4.1 Abstract

The surface machining of Carbon Fiber Reinforced Plastics (CFRP) materials is a challenging process, given the heterogeneity and anisotropic nature of composites, which, combined with the abrasiveness of the fibers, can produce some surface damage and extensive tool wear. The cutting temperature is one of the most important factors associated with the tool wear rate and machinability of these materials, which are also affected by the mechanical and thermal properties of the workpiece material and the cutting conditions. In this work, the cutting temperature, cutting forces and composite surface roughness were measured under different cutting conditions for the end milling of unidirectional CFRP. Cutting speeds ranging from 200 to 350 m/min, a feed rate of 0.063 mm/rev, fiber orientations of 0, 45, 90 and 135 degrees, and a 0.5 mm depth of cut were considered. The results show that the cutting speed and fiber orientation have a significant influence on the cutting temperature and cutting forces. The maximum and minimum cutting forces and temperatures were achieved for fiber orientations of 90 and 0 degrees, respectively.

**Keywords:** Surface machining, carbon fiber reinforced plastics, cutting temperature, cutting forces, surface roughness

## 4.2 Introduction

Carbon Fiber Reinforced Plastics (CFRP) constitute an important class of composite materials in the aerospace industry due to their superior properties, such as high strength and stiffness, a long fatigue life, a low density and high corrosion and wear resistances. Because of their low (close to zero) linear thermal expansion coefficient, CFRP materials have a high degree of dimensional stability in a wide range of temperatures (Gay et Hoa, 2007; Shalin, 2012). Combined to their excellent mechanical properties, these composites are largely used for structural parts of airplanes. For example, 52% of the weight of Airbus A350, 50% of the Boeing 787, and 46% of the Bombardier CSeries consist of composite materials such as CFRP. They are increasingly used for different aircraft parts, such as wing boxes, fuselages, ailerons, wings, spoilers, vertical stabilizers, cowlings, traps and struts (Daniel et Ishai, 2006; Girot et al., 2009). About 80% of CSeries wing is in composite materials, specifically the torque box and wing skins that are made of CFRP (Marsh, 2011).

Even though CFRP components are usually produced to near net-shape, for several manufacturing processes, part machining, trimming, milling, and drilling are often required to remove excess materials and ensure the components meet the dimensional requirements. This is required not only for assembly, but also to produce high quality part surfaces with controlled tolerances (Sheikh-Ahmad, 2008). Despite the unique physical and mechanical properties of CFRP, their machining is difficult because the fibers are brittle, they are heterogeneous and their behavior is anisotropic at the ply scale (Isbilir et Ghassemieh, 2012). Damages such as fiber pullout, fiber fragmentation, matrix softening/melting, stress concentrations, micro cracking, burring, fuzzing, and delamination are mainly observed after machining (Ferreira, Coppini et Miranda, 1999; Ghafarizadeh, Chatelain et Lebrun, 2014; Isbilir et Ghassemieh, 2012; Wang et Zhang, 2003).

A number of researchers have studied the machining of CFRP materials in order to provide a better understanding of the effects of different cutting parameters on the cutting force, machining quality and cutting temperature. Devim and Reis (Davim et Reis, 2005) studied the effects of milling parameters on surface roughness and machining damages. Their results showed that surface roughness increases with the feed rate and decreases with the cutting speed. Lopez De Lacalle et al. (De Lacalle et al., 2009) investigated the cutting forces during CFRP milling and concluded that the specific cutting force for CFRP milling is much lower than that of steel or aluminum alloys. They suggested that high cutting force and the abrasive nature of the reinforcement causes high tool wear rate. El-Hofy et al. (El-Hofy et al., 2011) also found that the fiber orientation, feed rate, and cutting speed have significant effects on machined surface roughness and integrity. According to their results, while high cutting speeds and low feed rates are recommended for CFRP edge trimming, a combination of low cutting speeds and high feed rates was recommended for reducing surface roughness during CFRP slot milling, with the feed rate being a significant factor. Wavy surfaces were observed for plies oriented at 45°, while those at 90° and 135° suffered from matrix cracking and fiber pull-out due to high cutting forces and matrix softening. The best surface was achieved where the fibers were parallel to the cutting direction (0°). In another research, Sheikh-Ahmad et al. (Sheikh-Ahmad, Urban et Cheraghi, 2012) studied the effects of cutting conditions on machining quality during the edge trimming of a multidirectional CFRP laminate. They concluded that the best surface quality in terms of surface roughness (in a direction parallel to machined edge) and delamination depth is obtained using small feed rates and high cutting speeds. Through experimentations, Rusinek (Rusinek, 2010) described the relations between the cutting forces and cutting process parameters in the milling of a carbon fiber reinforced plastics (CFRP) using epoxy as matrix. He showed that the cutting force rises with an increase of the feed rate for the milling of CFRP. Ghafarizadeh et al. (Ghafarizadeh, Chatelain et Lebrun, 2014) studied the effects of different cutting conditions on surface quality and cutting forces in CFRP milling. The best surface quality in terms of surface roughness and damage was achieved using moderate cutting speeds (250-375 m/min), lower feed rates (0.063 and 0.158 mm/rev) and a 0° lead angle.

The cutting temperature is an important factor in the machining of composite materials. It influences the quality of the machined surface and tool wear. Cutting temperatures are influenced by the cutting speed, the depth of cut, the tool and workpiece materials, the feed rate, and the fibers orientation (Sheikh-Ahmad, 2008). Experimental investigations on drilling of CFRP composite laminates carried out by Chen (Chen, 1997) showed that the flank surface temperature of a drill increases with increasing cutting speed and decreasing feed rate. Yashiro et al. (Yashiro, Ogawa et Sasahara, 2013) measured the cutting temperature during machining of a CFRP composite laminate and the temperature distribution through the laminate thickness during machining. They used three measurement methods: one using an infrared camera, a second one using a tool-workpiece thermocouple, and a third one using embedded thermocouples between the layers of the composite. Their observations showed that the temperature at the tool-workpiece contact point reached 180 °C (the glass transition temperature) at 25 m/min of cutting speed, and then increased to 300 °C at 50 m/min. The cutting temperature tends to stabilize and remain constant when the cutting speed was increased further. The cutting temperature in the workpiece material was relatively low (104 °C) compared to the tool-workpiece contact point, even at high cutting speeds (300 m/min). In a recent research, Liu et al. (Liu et al., 2014) investigated the workpiece temperature variation in helical milling of CFRP. They concluded that the workpiece temperature increases with increasing spindle speed and axial cutting depth. They also showed that the axial cutting depth has more influence on the temperature variation of the workpiece than spindle speed, while the influence of the tangential feed per tooth is less than the other factors.

Notwithstanding all the research that has been carried out on some machining process such as trimming and drilling of fiber reinforced polymers, few papers have covered the effect of cutting temperature in the surface milling of CFRP. In contrast to other machining processes such as trimming and drilling, the machined plane is parallel to the stack of plies. This work presents the results of experiments carried out on a CFRP laminate to study the effects of different parameters, especially the cutting speed and fiber orientation, on the resulting cutting forces, cutting temperature, surface quality, and machining damages. The objective is to provide a better understanding of the relationship between these parameters and the surface quality. Based on SEM observations, this study also explains the effects of cutting forces on the surface integrity and machining damages during surface milling of CFRP materials.

## 4.3 Methodology

A high performance carbon fiber epoxy unidirectional prepreg (P2053F-10) with fiber volume content ($V_f$) of 60% was used to obtain unidirectional fiber composite plates having a final average thickness of approximately 6.3 mm. The prepreg has a surface density of 100 g/m$^2$ and the fiber weight content ($W_f$) of 70%. The plates were cured in autoclave following the cure cycle recommended by the supplier. Table 4-1 shows the mechanical properties obtained from the supplier for the unidirectional laminate and the physical properties of the carbon fiber used in the composite for the surface milling experiments.

Table 4-1 Mechanical and physical properties of CFRP (reported by supplier)

| **CFRP unidirectional laminate (TC-09-U)** | | | **Carbon Fiber T800HB-12000 (C 96 %)** | |
|---|---|---|---|---|
| | Fiber direction | Transverse direction | Tensile strength (MPa) | 5490 |
| Tensile strength (MPa) | 1388.0 | 48.2 | Tensile modulus (GPa) | 294 |
| Tensile modulus (GPa) | 122.6 | 7.010 | Elongation (%) | 1.9 |
| Compressive strength (MPa) | 551.69 | | Density (g/cm$^3$) | 1.81 |
| Compressive modulus (GPa) | 60.9 | | Specific Heat (Cal/g·˚C) | 0.18 |
| Apparent interlaminar shear strength (N/mm²) | 45.9 | | coefficient of thermal expansion ($\alpha \cdot 10^{-6}$/˚C) | -0.56 |
| Specific gravity (g/cm$^3$) | 1.552 | | Thermal Conductivity (Cal/cm·s·˚C) | 0.0839 |

The experiments were carried out on a Huron K2X10 three-axis CNC machine with a maximum spindle speed of 28,000 rev/min. In the previous research of Ghafarizadeh et al. (Ghafarizadeh, Chatelain et Lebrun, 2014), the effects of different lead angle on the cutting forces, surface quality and damages were studied using ball end mill and its results showed that the best surface quality was achieved with a lead angle equal to 0 degree.

As a continuation of our previous work, machining experiments were carried out in 0 degree lead angle and with a ball end mill. The up-milling cutting mode was used, along with a 10 mm diameter solid carbide ball end mill with CVD (chemical vapor deposition) diamond coating, made of two flutes with a 30 degree helix angle.


Figure 4-1 CFRP milling setup

Figure 4-1 shows the CFRP milling setup. Two K-type thermocouples (made from nickel-chromium wires each of 0.076 mm diameter (0.003 inch), as in BS1041 code for temperature measurement, were used for measuring the temperature during machining. The thermocouples were installed on both edges of the tool, at 0.7 mm from the tool tip. For all experiments, the axial depth of cut was maintained constant at 0.5 mm, so the thermocouples were located at a distance of 0.2 mm from the cutting area. For this axial depth of cut (0.5 mm), the tool radial engagement into the workpiece was maintained to 2.534mm (shown in Figure 4-2).

The tips of the thermocouples were mounted on the edges of the tool using a high thermal conductivity paste (1.59 W/m-K) as shown in Figure 4-3. The temperature data were transmitted from the tool to the stationary receiver (M320 transmitters and receivers provided by the Michigan Scientific Corporation) via a radio frequency (RF) signal. After detection by the receiving antennas, the signals were converted to analog signals corresponding to the temperature. A low pass filter in the receiver provided a bandwidth of 1000 or 100 Hz.

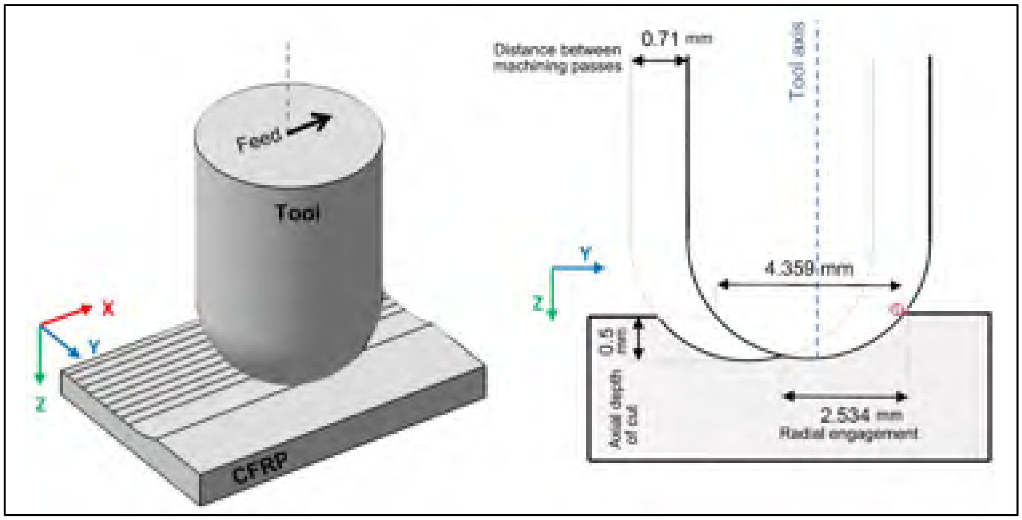


Figure 4-2 The schematic of the milling process geometry

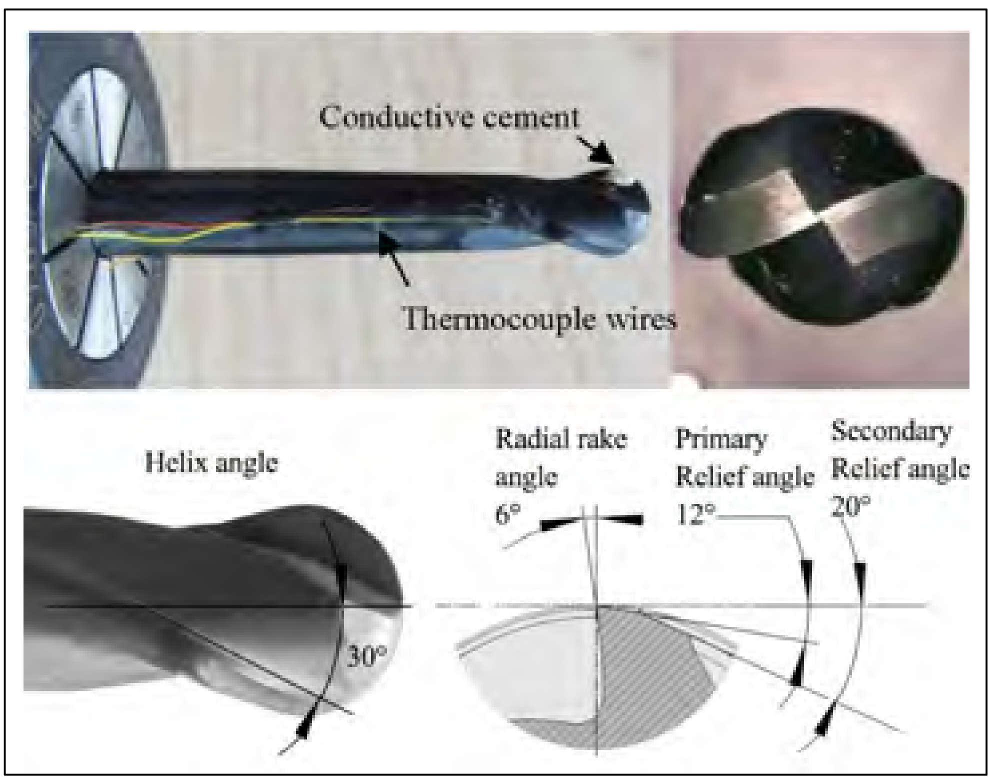


Figure 4-3 Cutting tool

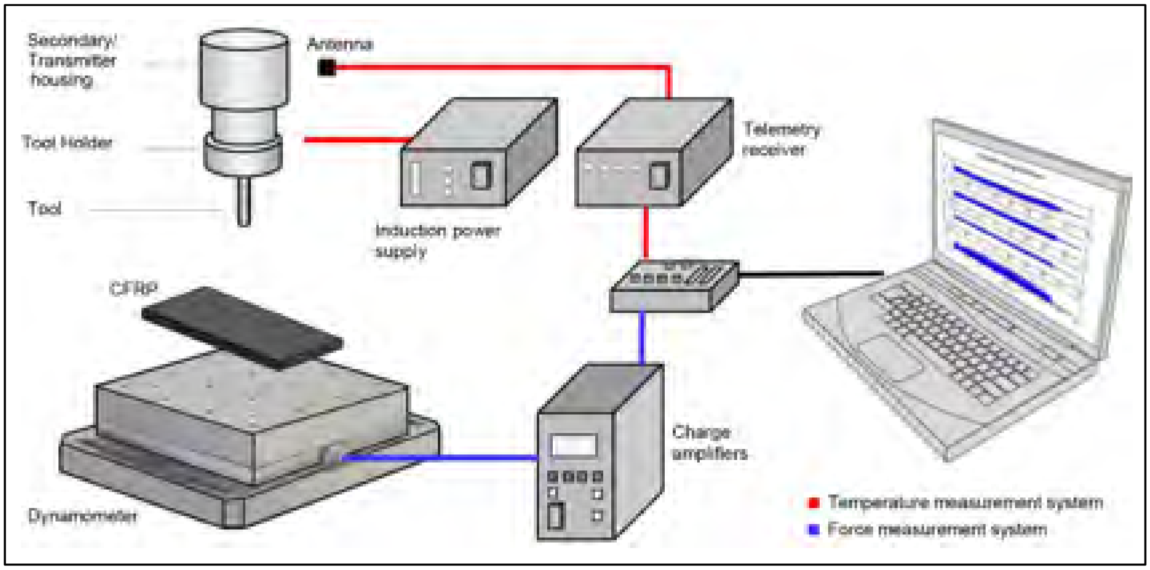


Figure 4-4 Measuring of cutting temperature and cutting force

Figure 4-4 shows the cutting forces and temperature measurement system used during machining. Previous research showed the effects of different cutting conditions, such as the cutting speed, the feed rate, and the lead angle, on the cutting forces and surface quality (Ghafarizadeh, Chatelain et Lebrun, 2014). A better surface quality was achieved using a moderate cutting speed and a lower feed rate when milling CFRP.

In the present work, the cutting speeds were therefore selected between 200-375 m/min (moderate cutting speeds), while the feed rate was kept constant at 0.063 mm/rev (lowest feed rate). The milling experiments are carried out with four different fiber orientations (the angle between carbon fibers and feed direction) of 0, 45, 90 and 135 degrees as described in Figure 4-5.

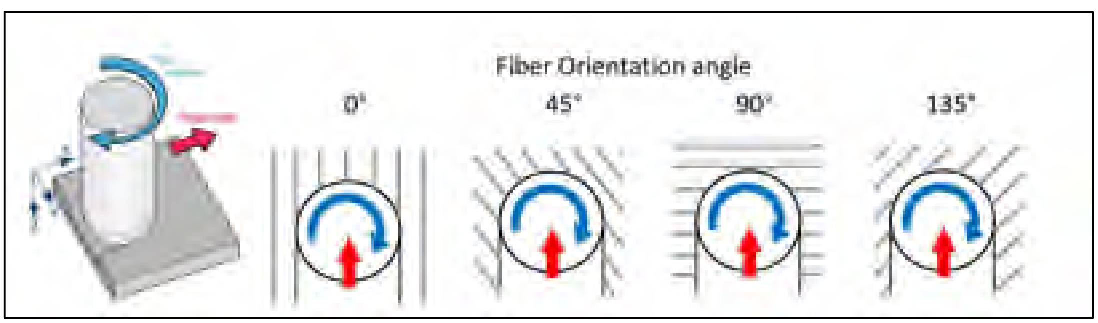


Figure 4-5 Fiber orientation angle in milling experiments

Table 4-2 Cutting conditions

| **Cutting speed (m/min)** | **Spindle speed (RPM)** | **Maximum effective cutting speeds (m/min)*** | **Fiber orientation (°)** | **Feed rate (mm/rev)** | **Cutting condition** |
|---|---|---|---|---|---|
| 200 | 6366 | 87.1 | 0 | 0.063 | Dry |
| 250 | 7958 | 108.9 | 45 | | |
| 300 | 9549 | 130.7 | 90 | | |
| 375 | 11937 | 163.4 | 135 | | |

* The effective cutting speed in the maximum diameter of tool engaged into the workpiece (4.359 mm)

Table 4-2 details the cutting conditions used for the experiments. In this table, the cutting speed levels are calculated from the tool shank diameter. The effective cutting speed varies with tool diameter from zero in the tool tip to its maximum amount in the maximum diameter of tool engaged into the workpiece (point 1 in the Figure 4-2). The maximum effective cutting speeds are given in Table 4.2. A Kistler 9255B(#3) three-axis dynamometer table, connected to a Kistler type 5010 charge amplifier, was used for measuring the cutting forces during machining (Figure 4-4) The roughness of the machined surfaces was measured using a Mitutoyo SJ400 contact profilometer. Three readings were taken at regular intervals for each surface; each reading having 0.8 mm in length perpendicular to the feed direction, and an average value was calculated from the three readings (Figure 4-6). The measured values of $R_a$ (arithmetic average height) under different cutting conditions were compared in order to investigate the effect of cutting conditions on the surface quality. The surfaces were also examined using a Keyence VHC-500F type digital microscope, Olympus LEXT OLS4000 3D confocal laser microscope, as well as Hitachi S-3600N electronic microscope (scanning electron microscopy - SEM).

## 4.4 Results and discussion

### 4.4.1 Effects of cutting speed on the cutting force and cutting temperature

CFRP composites are sensitive to moisture and using cooling lubricants in the machining of composites can cause some problems, such as swelling of the polymer and a chemical reaction of the polymer and coolant. CFRP are thus often machined in dry conditions, without coolants (Turner, Scaife et El-Dessouky, 2015).

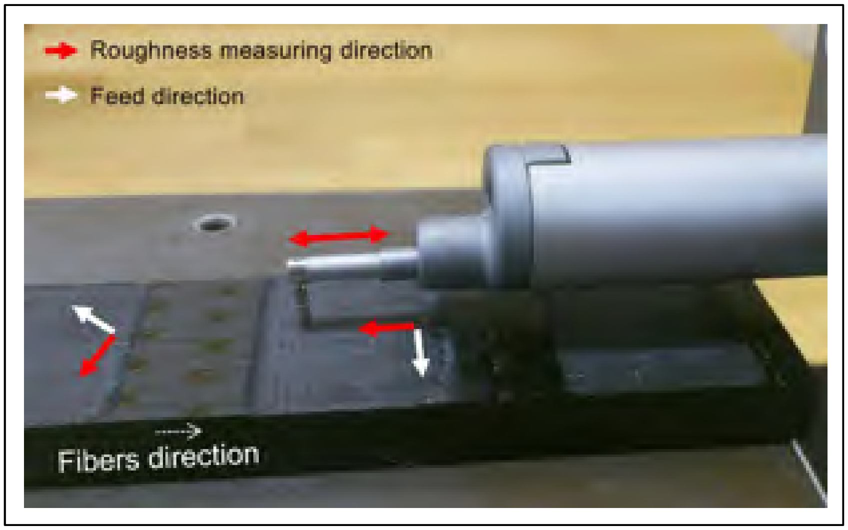


Figure 4-6 Measuring of surface roughness using contact profilometer

Dry machining produces an increase in temperature and generates thermal damage of machined surfaces (Weiert et Kempann, 2004). The cutting temperature is also a major factor that directly affects tool life (Li, Wang et Chu, 2013). Figure 4-7 shows the effect of the cutting speed on the maximum cutting temperature at different fiber orientations. As can be seen, the cutting temperature increases linearly with the cutting speed for all fiber orientations. The measured milling temperature in this research is lower than the cutting temperatures reported in other machining processes, such as drilling (Li, Wang et Chu, 2013; Weiert et Kempann, 2004; Yashiro, Ogawa et Sasahara, 2013), because of a lower axial depth of cut and a more efficient heat transfer in milling as compared to drilling. Because the temperatures were measured at 0.2 mm from the cutting edge; it could be argued that the temperature is higher at the cutting edge. However, because of the extremely high thermal conductivity of the CVD diamond coated film ($1300<\kappa<2000$ (Miranzo et al., 2002)), the measured temperature may be assumed representative of the cutting temperature at the cutting edge. Because of the brittle nature of CFRP, plastic deformation does not represent an important portion of the heat generated during machining compared to friction. Therefore, the main source of heat generation is the frictional work at the tool rake face and at the clearance face (Yashiro, Ogawa et Sasahara, 2013).

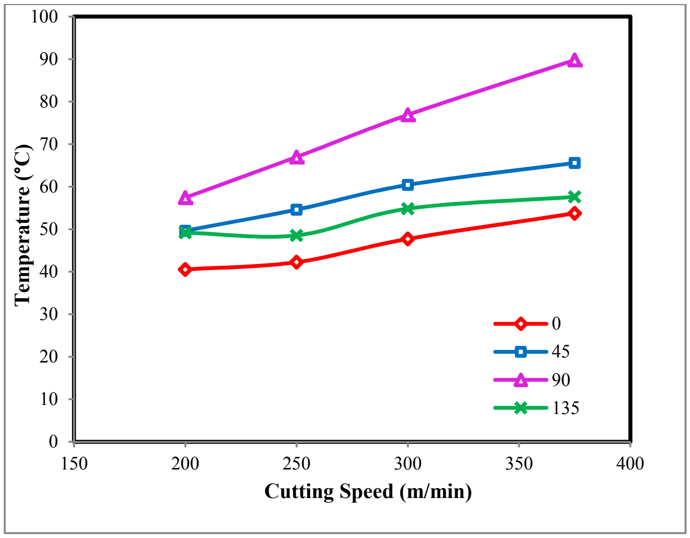


Figure 4-7 Effect of cutting speed on the maximum cutting temperature for different fiber orientations

When the surfaces slide one over the other under load, the energy dissipated per unit time is the product of the friction force (F) and sliding speed (V), and this energy is converted into heat according to equation (4-1) (Shaw, 2005);

$$U = F \times V = \mu \times P \times V \qquad (4\text{-}1)$$

Where P is the applied load and μ the friction coefficient. Increasing the cutting speed raises the sliding speed of the tool on the workpiece surface, thus increasing heat generation according to the above equation. Because the temperature measured is lower than the glass transition temperature ($T_g$) of epoxy matrix (Figure 4-7) ; thus, and as mentioned by Yashiro et al. (Yashiro, Ogawa et Sasahara, 2013), heat energy generated is not consumed for phase transition, and the temperature increases at an approximately constant rate when increasing the cutting speed. The dependence between the cutting temperature ($\theta_c$) and the cutting speed can also be expressed by:

$$\theta_c \propto V^b \qquad (4\text{-}2)$$

Where b depends on the material (Sreejith et al., 2000). As can be seen in Figure 4-7, the cutting temperature increases linearly with the cutting speed over the 200-375 m/min cutting speed range; therefore, b in equation (4-2) is equal to 1.

The lines slope in Figure 4-7 indicate the rate of increase in temperature with the cutting speed. This rate is not constant for different fiber orientations, and this might be explained by the variation of friction coefficients (equation (4-1)) for different fiber orientations. The friction coefficient (μ) is not a constant parameter, and varies from 0.09 to 0.9 (for CFRP material), depending of machining parameters such as sliding speed, temperature, normal applied load, workpiece and tool materials, and fiber orientation. Generally, the friction coefficient increases with increasing fibers angle, temperature, and applied load, and decreases when increasing the sliding speed (Chardon et al., 2015; Cheng et al., 2009; Kukureka et al., 1999; Muhammad Nuruzzaman, Asaduzzaman Chowdhury et Lutfar Rahaman, 2011; Nak-Ho et Suh, 1979; Suresha et al., 2006).

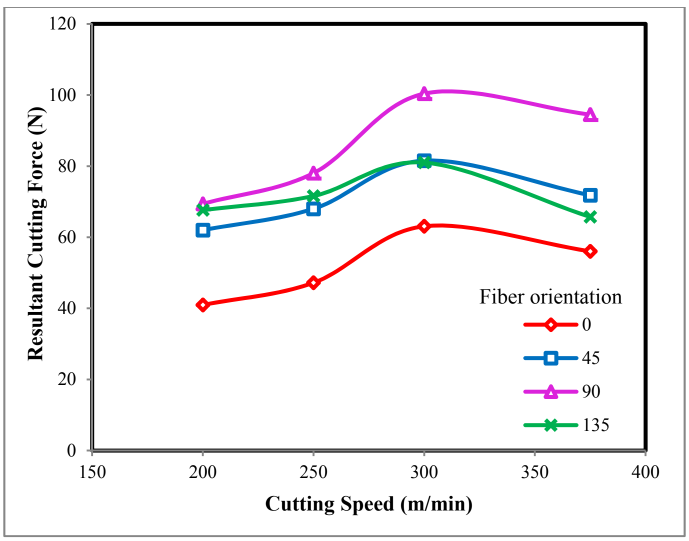


Figure 4-8 Effect of cutting speed on the maximum resultant cutting force for different fiber orientations

The cutting forces constitute one of the important factors in machining. They influence the process stability, part quality, cutting temperature, and tool wearing condition (Zaghbani et al., 2012a). Figure 4-8 illustrates the effect of the cutting speed on the maximum resultant cutting force for different fiber orientations. The trend is the same for all fiber orientations, similar to the results reported in previous milling experiments on a quasi-isotopic multidirectional CFRP laminate (Ghafarizadeh, Chatelain et Lebrun, 2014). As shown in Figure 4-8, the cutting force increases with the cutting speed for speeds ranging from 200 to

300 m/min, and then decreases above 300 m/min. Because the cutting temperature increases with an increase in the cutting speed (Figure 4-7), this can influence the cutting force considering the influence of temperature on the mechanical properties of polymers.

Generally, the mechanical properties of CFRP materials are function of the mechanical properties of the matrix and carbon fibers and decrease when the temperature increases. The strength of a CFRP composite made of epoxy decreases much more rapidly at higher temperatures (over 100° C) (Shalin, 2012). Therefore, decreases in the cutting force at higher cutting speeds might be explained by the softening of the material as cutting speed increases.

### 4.4.2 Effects of fibers orientation on the cutting temperature and cutting force

The cutting force and temperature are strongly influenced by the reinforcement volume fraction, reinforcement geometry, and orientation (Sheikh-Ahmad, 2008). Figure 4-9 illustrates the effect of fiber orientation on the resultant cutting force. As shown, the maximum and minimum cutting forces are achieved for the 90 and 0 degree fiber orientations, respectively.

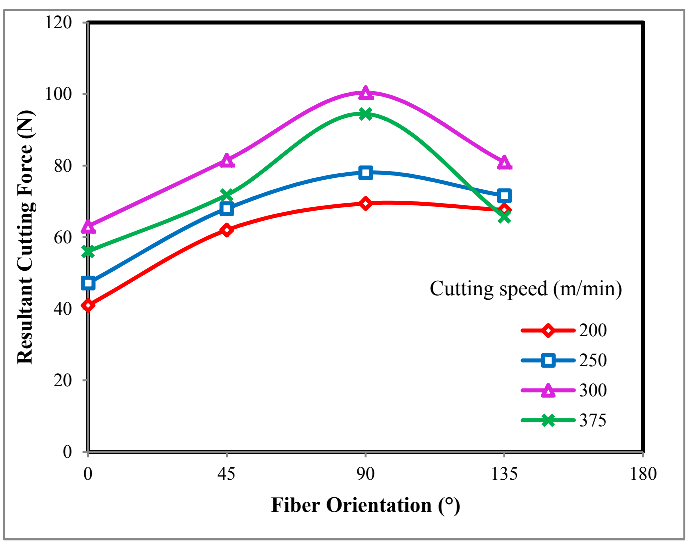


Figure 4-9 Effect of fiber orientation on the maximum resultant cutting force for different cutting speeds

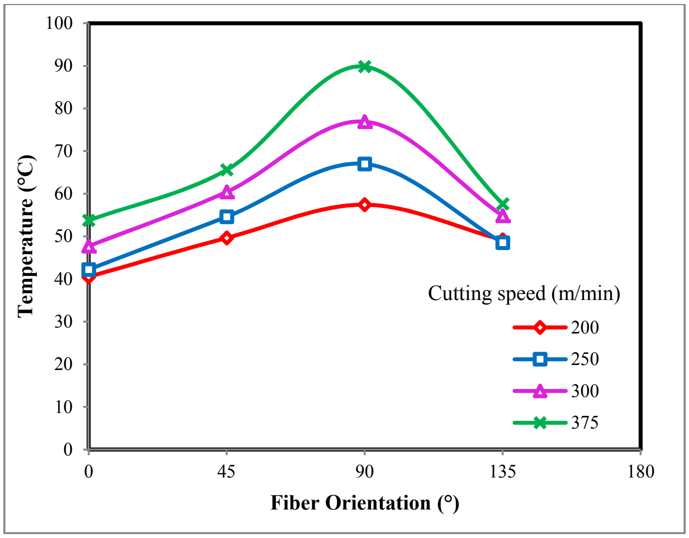


Figure 4-10 Effect of fiber orientation on the maximum cutting temperature at different cutting speeds

This is consistent with the results of Figure 4-7 and Figure 4-8 for the temperature and cutting force. Figure 4-10 shows the effect of fiber orientation on the cutting temperature at different cutting speeds. As can be seen, the fiber orientation has a significant effect on the cutting temperature. This temperature increases with the fiber orientation from 0 to 90 degrees, and then decreases with a further increase to 135 degrees. A comparison of Figure 4-9 and Figure 4-10 demonstrates that both diagrams follow the same trends. The maximum temperature was measured when milling with a 90 degree fiber orientation (Figure 4-10), orientation for which the maximum force was observed (Figure 4-9). The maximum temperature and milling force are almost the same when comparing the results at 45° and 135° fiber orientations.

### 4.4.3 Effects of fibers orientation and cutting speed on surface quality

Surface morphology and integrity depend on the machining process and workpiece characteristics, such as the cutting speed, the feed rate, the fiber type and volume content, the fiber orientation and the matrix type (Sheikh-Ahmad, 2008).

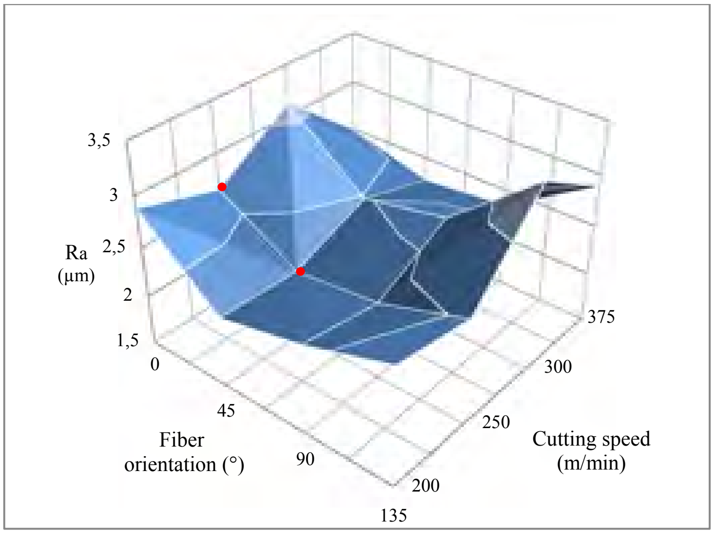


Figure 4-11 Effects of fiber orientation and cutting speed on surface roughness (standard deviations (σ) of 0.06 to 0.33 μm)

Figure 4-11 shows the effects of the fiber orientation and cutting speed on surface roughness. The machined surface roughness ($R_a$) was measured between 2.17 and 3.35 μm with corresponding standard deviations (σ) of 0.06 to 0.33 μm. The minimum surface roughness is achieved for 45° and 90° fiber orientations and a cutting speed of 250 m/min, and the maximum surface roughness for a fiber orientation of 135° and a cutting speed of 300 m/min.

As illustrated in Figure 4-7 and Figure 4-8, the resultant cutting force and cutting temperature for the fiber orientations of 45° and 135° are close to each other but the measured surface roughness for these orientations was completely different.

Figure 4-12 illustrates the SEM photographs of machined surface as function of fibers orientation and cutting speed. It can be noticed their significant effects on machining damages and surface quality. As can be seen, more surface damages (including fiber fracture, fiber pullout, and fiber-matrix debonding) are observed at higher cutting speeds. The best surfaces were produced for 0 and 90 degree fiber orientations at lower cutting speeds (Figure 4-12 (a), (c) and (e)).

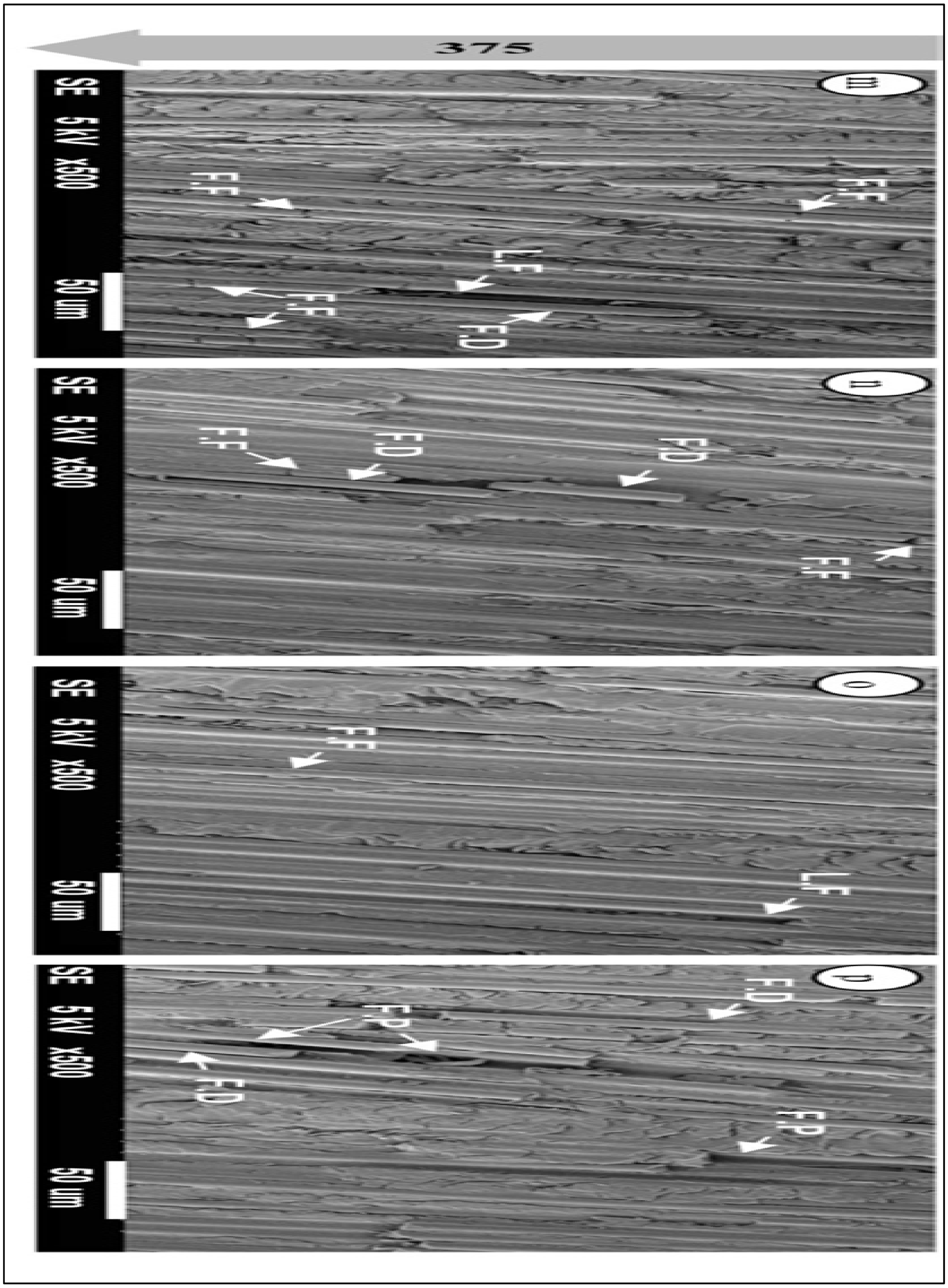

Figure 4-12 Surface damages at different cutting speeds and Fiber orientation angle: Fiber fracture (F.F), fiber pullout (F.P), fiber/Matrix de-cohesion (F.D), loss of fibers (L.F)

A comparison of the surface roughness diagram (Figure 4-11) and SEM images of Figure 4-12 demonstrates that the surface roughness alone may not be a sufficient indicator to evaluate the quality of the machined surfaces of CFRP materials. For example, for a cutting speed of 250 m/min, the measured surface roughness at 45° (point 2 in Figure 4-11) was lower than that at 0° (point 1 in Figure 4-11) but the observed surface quality seems better at 0° (compare Figure 4-12 (e) and (f)). In contrast to other machining processes such as trimming and drilling, the machined plane in surface milling is parallel to the stack of plies. As can be seen in SEM images of the machined surface (Figure 4-12), less major machining damages such as delamination and fiber pull out was observed in surface milling compared to the other machining process such as slotting (El-Hofy et al., 2011), trimming (Sheikh-Ahmad, Urban et Cheraghi, 2012) and drilling (Merino-Pérez et al., 2015).

Figure 4-13 presents the cutting forces in the x, y and z directions during 0.022 second of milling as function of fibers orientation and cutting speed, in the steady state period. During this period, the tool makes 2.3, 2.9, 3.5, and 4.3 revolutions for 200, 250, 300 and 375 m/min cutting speeds respectively. The forces profile for each passing tooth of the tool and forces magnitude in different directions can be clearly identified. Each peak of the force profile presents the passage of a tooth. The horizontal and vertical axes (on the top and left side of the figure) represent the fiber orientation and cutting speeds, respectively. A comparison of the Figure 4-13 a-p demonstrates that the cutting force profiles vary with the cutting speed and fiber orientation angle. From the results presented in Figure 4-12 and Figure 4-13, it is noticed that lower cutting forces produce a better surface integrity. Figure 4-13 (f), (j), and (k) show higher cutting forces fluctuations (marked by double-headed arrows in Figure 4-13) compared to other cutting conditions. The high fluctuations observed under these conditions (especially in the z direction) are most probably due to a dynamic instability. The peak-to-peak amplitude can be used to evaluate the force fluctuation. The highest peak-to-peak amplitude in the z direction was recorded for fibers at 45° with a cutting speed of 250 m/min (Figure 4-13 (f)). This axial cutting force is two times higher than that of clean cut conditions (Figure 4-12 (a) and (e)). As shown in Figure 4-12 (f), for these conditions, the cutting process occurred in several layers and a poor surface quality was produced.

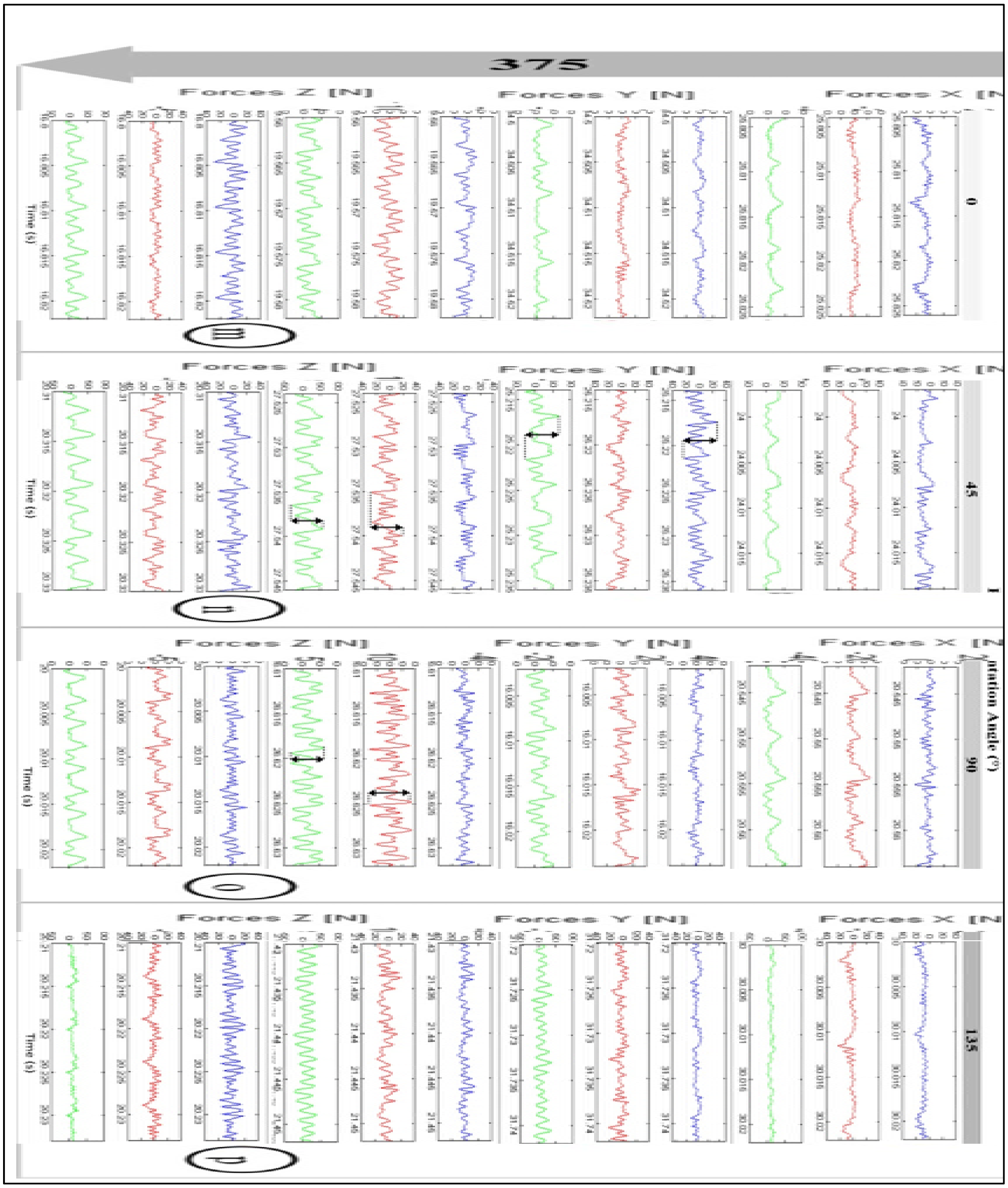


Figure 4-13 Cutting forces for different cutting speeds and fiber orientations

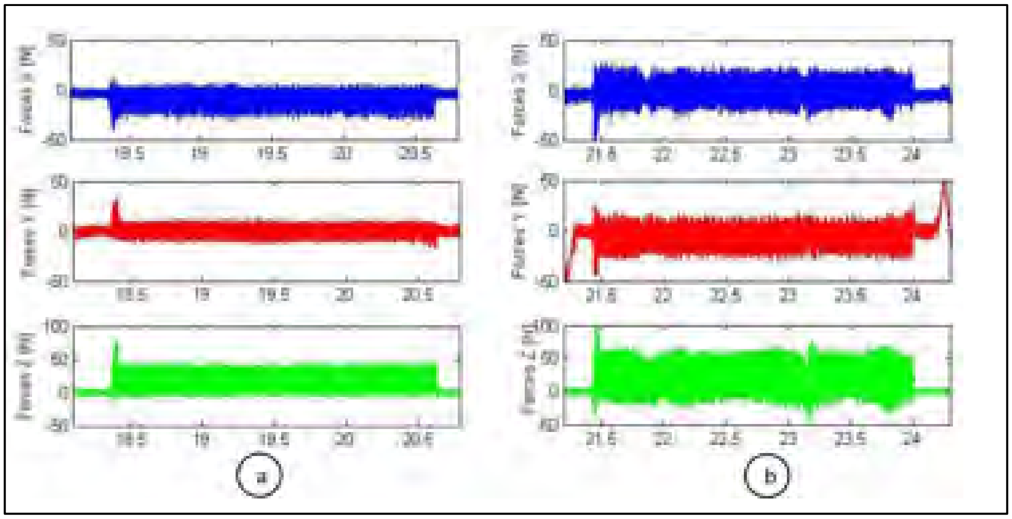


Figure 4-14 Cutting forces in time domain a) Fiber orientation angle 0° and cutting speed 200 m/min), b) fiber orientation angle 45° and cutting speed 250 m/min

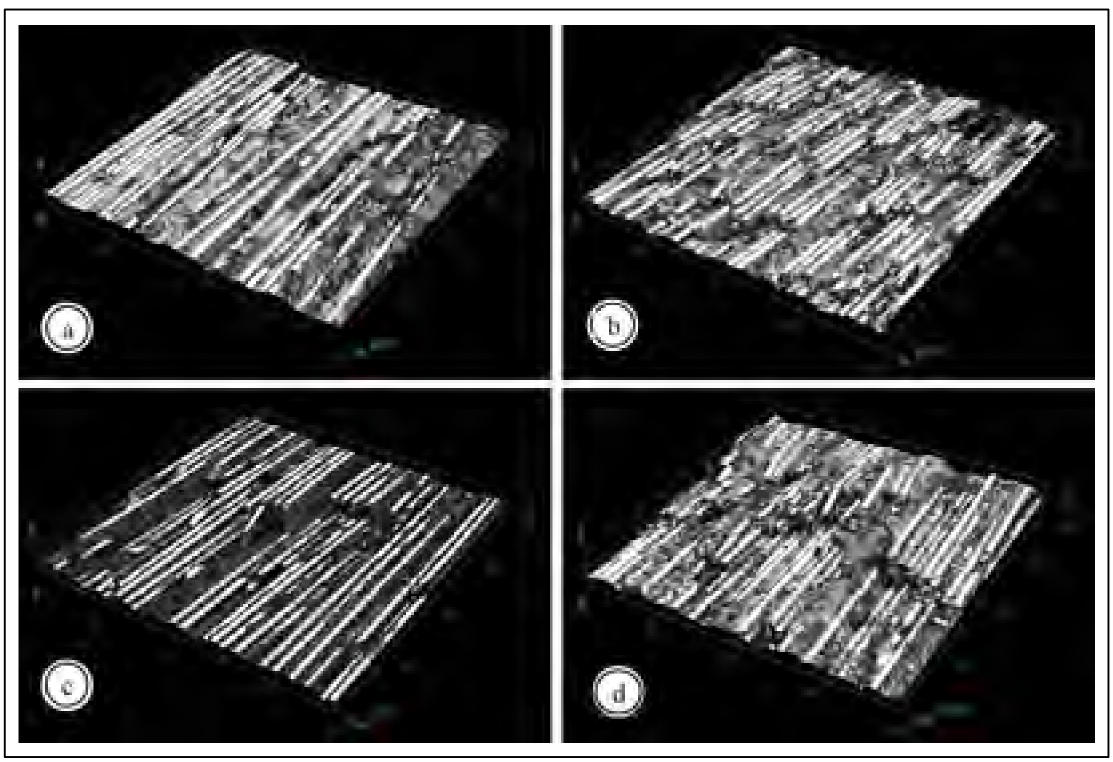


Figure 4-15 3D topography of surfaces machined with confocal laser microscope a) cutting speed 200 m/min and fiber orientation 0°, b) cutting speed 300 m/min and fiber orientation 45°, c) cutting speed 375 m/min and fiber orientation 45°, d) cutting speed 375 m/min and fiber orientation 90°

A stable cut is also characterized by a clean cutting force spectrum. Figure 4-14 shows the cutting forces in the time domain for a clean cutting condition (Figure 4-14(a): fiber orientation of 0° and cutting speed of 200 m/min) and an unstable cutting condition (Figure 4-14 (b)) corresponding to the conditions of Figure 4-12 (f). The inharmonic cutting forces spectra in Figure 4-14 (b) confirms the process instability for this cutting condition, in contrast to the harmonic cutting forces spectra for a clean cut (Figure 4-14 (a)). 3D images of the machined surfaces by laser confocal microscope better show the surface topography in different conditions and confirm the observations made from the micrographs in Figure 4-12. For example, Figure 4-15 illustrates the surface topography for the clean cutting (a: cutting speed 200 m/min and fiber orientation 0°), the dynamic unstable cutting (b: cutting speed 300 m/min and fiber orientation 45°) and the damaged surfaces obtained for a high cutting speed (c and d: cutting speed 375 m/min). Also, many damages such as fiber fracture, fiber pullout, and fiber/matrix debonding are observed in Figure 4-15 (c) and (d) for a high cutting speed.

## 4.5 Conclusion

In this paper, surface milling experiments were carried out on unidirectional carbon fiber reinforced laminates in order to study the effects of cutting parameters, such as the fiber orientation and cutting speed, on the cutting force, the cutting temperature, and surface quality. Based on the presented results, the following conclusions are drawn:

- The cutting temperature increases linearly with the cutting speed for cutting speeds ranging from 200 to 375 m/min.

- The maximum resultant cutting force is influenced by the cutting speed. The cutting force increases as the cutting speed increases from 200 to 300 m/min, and then decreases, with a further increase in cutting speed above 300 m/min.

- The fiber orientation has significant effects on the cutting force and cutting temperature. Maximum and minimum cutting forces and cutting temperatures values are achieved at fiber orientations of 90 and 0 degrees, respectively.

- The minimum and maximum surface roughness values are achieved for 45° and 135° fiber orientations, respectively.

- Based on SEM images, the best surface integrity produced using 0 and 90 degree fiber orientation angle and lower cutting speeds (200 and 250 m/min).

### 4.6 Acknowledgments

This research was funded by the Consortium for Research and Innovation in Aerospace in Quebec (CRIAQ) and its partners, the Natural Sciences and Engineering Research Council of Canada (NSERC), MITACS, Bombardier Aerospace, Avior Integrated Products, Delastek and AV&R Vision & Robotics.

### 4.7 References

Chardon, Grégory, Olga Klinkova, Joël Rech, Sylvain Drapier et Jean-Michel Bergheau. 2015. « Characterization of friction properties at the work material/cutting tool interface during the machining of randomly structured carbon fibers reinforced polymer with Poly Crystalline Diamond tool under dry conditions ». *Tribology International*, vol. 81, p. 300-308.

Chen, Wen-Chou. 1997. « Some experimental investigations in the drilling of carbon fiber-reinforced plastic (CFRP) composite laminates ». *International Journal of Machine Tools and Manufacture*, vol. 37, n° 8, p. 1097-1108.

Cheng, Du-qing, Xue-tao Wang, Jian Zhu, Dong-hua Qiu, Xiu-wei Cheng et Qing-feng Guan. 2009. « Friction and wear behavior of carbon fiber reinforced brake materials ». *Frontiers of Materials Science in China*, vol. 3, n° 1, p. 56-60.

Daniel, Isaac M, et Ori Ishai. 2006. *Engineering mechanics of composite materials*, 2nd. New York: Oxford university press New York.

Davim, J.P., et P. Reis. 2005. « Damage and dimensional precision on milling carbon fiber-reinforced plastics using design experiments ». *Journal of Materials Processing Technology*, vol. 160, n° 2, p. 160-167.

De Lacalle, LN Lopez, A Lamikiz, FJ Campa, A Fdz Valdivielso et I Etxeberria. 2009. « Desing and test of a multitooth tool for CFRP milling ». *Journal of Composite Materials,* vol. 46, n° 16, p. 1955-1971.

El-Hofy, MH, SL Soo, DK Aspinwall, WM Sim, D Pearson et P Harden. 2011. « Factors affecting workpiece surface integrity in slotting of CFRP ». *Procedia Engineering*, vol. 19, p. 94-99.

Ferreira, JR, NL Coppini et GWA Miranda. 1999. « Machining optimisation in carbon fibre reinforced composite materials ». *Journal of Materials Processing Technology*, vol. 92, p. 135-140.

Gay, D, et SV Hoa. 2007. *Composite materials: design and applications*, 2nd. CRC Press.

Ghafarizadeh, Seyedbehzad, Jean-François Chatelain et Gilbert Lebrun. 2014. « Effect of cutting tool lead angle on machining forces and surface finish of CFRP laminates ». *Science and Engineering of Composite Materials,* DOI: 10.1515/secm-2013-0188.

Girot, F, LN López de Lacalle, A Lamikiz, D Iliescu et ME Gutiérrez. 2009. « *Machinability aspects of polymer matrix composites in machining composites materials* ». Wiley& Sons, New York (USA).

Isbilir, Ozden, et Elaheh Ghassemieh. 2012. « Finite element analysis of drilling of carbon fibre reinforced composites ». *Applied Composite Materials*, vol. 19, n° 3-4, p. 637-656.

Kukureka, SN, CJ Hooke, M Rao, P Liao et YK Chen. 1999. « The effect of fibre reinforcement on the friction and wear of polyamide 66 under dry rolling–sliding contact ». *Tribology International*, vol. 32, n° 2, p. 107-116.

Li, Kuan-Ming, Chia Wang et Wei-Ying Chu. 2013. « An improved remote sensing technique for estimating tool–chip interface temperatures in turning ». *Journal of Materials Processing Technology*, vol. 213, n° 10, p. 1772-1781.

Liu, Jie, Guang Chen, Chunhui Ji, Xuda Qin, Hao Li et Chengzu Ren. 2014. « An investigation of workpiece temperature variation of helical milling for carbon fiber reinforced plastics (CFRP) ». *International Journal of Machine Tools and Manufacture*, vol. 86, p. 89-103.

Marsh, George. 2011. « Bombardier throws down the gauntlet with CSeries airliner ». *Reinforced Plastics*, vol. 55, n° 6, p. 22-26.

Merino-Pérez, JL, R Royer, S Ayvar-Soberanis, E Merson et A Hodzic. 2015. « On the temperatures developed in CFRP drilling using uncoated WC-Co tools Part I: Workpiece constituents, cutting speed and heat dissipation ». *Composite Structures*, vol. 123, p. 161-168.

Miranzo, P, MI Osendi, E Garcia, AJS Fernandes, VA Silva, FM Costa et RF Silva. 2002. « Thermal conductivity enhancement in cutting tools by chemical vapor deposition diamond coating ». *Diamond and Related Materials*, vol. 11, n° 3, p. 703-707.

Muhammad Nuruzzaman, Dewan, Mohammad Asaduzzaman Chowdhury et Mohammad Lutfar Rahaman. 2011. « Effect of duration of rubbing and normal load on friction coefficient for polymer and composite materials ». *Industrial Lubrication and Tribology*, vol. 63, n° 5, p. 320-326.

Nak-Ho, Sung, et Nam P Suh. 1979. « Effect of fiber orientation on friction and wear of fiber reinforced polymeric composites ». *Wear*, vol. 53, n° 1, p. 129-141.

Rusinek, Rafal. 2010. « Cutting process of composite materials: An experimental study ». *International Journal of Non-Linear Mechanics*, vol. 45, n° 4, p. 458-462.

Shalin, Radiĭ Evgen′evich. 2012. *Polymer matrix composites*, 4. Springer Science & Business Media.

Shaw, Milton Clayton. 2005. *Metal cutting principles*, 2. New York: Oxford university press

Sheikh-Ahmad, J.Y. 2008. *Machining of polymer composites*. Springer Verlag.

Sheikh-Ahmad, Jamal, Nebu Urban et Hossein Cheraghi. 2012. « Machining damage in edge trimming of CFRP ». *Materials and Manufacturing Processes*, vol. 27, n° 7, p. 802-808.

Sreejith, PS, R Krishnamurthy, SK Malhotra et K Narayanasamy. 2000. « Evaluation of PCD tool performance during machining of carbon/phenolic ablative composites ». *Journal of Materials Processing Technology*, vol. 104, n° 1, p. 53-58.

Suresha, B, G Chandramohan, P Samapthkumaran, S Seetharamu et S Vynatheya. 2006. « Friction and wear characteristics of carbon-epoxy and glass-epoxy woven roving fiber composites ». *Journal of Reinforced Plastics and Composites*, vol. 25, n° 7, p. 771-782.

Turner, J, RJ Scaife et HM El-Dessouky. 2015. « Effect of machining coolant on integrity of CFRP composites ». *Advanced Manufacturing: Polymer & Composites Science*, vol. 1, no 1, p. 54-60.

Wang, XM, et LC Zhang. 2003. « An experimental investigation into the orthogonal cutting of unidirectional fibre reinforced plastics ». *International Journal of Machine Tools and Manufacture*, vol. 43, n° 10, p. 1015-1022.

Weiert, K, et C Kempann. 2004. « Cutting temperature and their effects on machining behavior in drilling reinforced plastics composites ». *Advanced Engineering Materials*, vol. 6, p. 684-689.

Yashiro, Takeshi, Takayuki Ogawa et Hiroyuki Sasahara. 2013. « Temperature measurement of cutting tool and machined surface layer in milling of CFRP ». *International Journal of Machine Tools and Manufacture*, vol. 70, p. 63-69.

Zaghbani, Imed, Jean-François Chatelain, Victor Songmene, Sébastien Bérubé et Abdelatif Atarsia. 2012. « A comprehensive analysis of cutting forces during routing of carbon fiber-reinforced polymer laminates ». *Journal of Composite Materials*, p. 0021998311428362.

## CHAPTER 5

# FINITE ELEMENT ANALYSIS OF SURFACE MACHINING OF CARBON FIBER REINFORCED COMPOSITES

S.B. Ghafarizadeh[a], J.F. Chatelain[b], G. Lebrun[c]

[a,b] Department of Mechanical Engineering, École de Technologie Supérieure,
1100 Notre-Dame West, Montreal, Québec, Canada H3C 1K3
[c] Department of Mechanical Engineering, Université du Québec à Trois-Rivières
C.P. 500, Trois-Rivières, Québec, G9A 5H7

This paper has been submitted for publication
in *International Journal of Advanced Manufacturing and Technology.*

## 5.1 Abstract

Despite increased applications of carbon fiber reinforced plastic (CFRP) materials in many industries, such as aerospace, their machining is still a challenge due to their heterogeneity and anisotropic nature. In this research, a finite element model is used to investigate the cutting forces, chip formation mechanism and machining damage present during the flat end milling of unidirectional CFRP. The material is modeled as an equivalent orthotropic homogeneous material, and Hashin theory is used to characterize failure in plane stress conditions. The friction coefficient between the tool and the composite material was assumed dependent on the carbon fiber orientation. A comparison of modeling and experimental results indicates that the model successfully predicts the cutting forces. The numerical model predictions of machining damage around the cutting area due to fiber compression damage and matrix cracking and the relation between damage extension and fiber orientation are confirmed through a comparison with SEM images of machined edges and surfaces.

**Keywords**: Carbon fiber reinforced plastics, milling, finite element method, machining damage, cutting forces

## 5.2 Introduction

Carbon fiber reinforced plastics offer high strength and stiffness-to-weight ratio, long fatigue life, low density and high corrosion and wear resistances, which make them an important class of composite materials in the many industries such as aerospace, construction, and transportation industries, as well as medical and military applications (Daniel et Ishai, 2006; Sheikh-Ahmad, 2008). CFRP components are usually produced to near net-shape, but some machining processes such as milling, drilling and trimming are often required to remove excess materials and bring the parts to the final size and shape (Davim, 2015). Machining CFRP materials is a challenging process, due to their heterogeneity and anisotropic nature, and can generate some damages such as fiber pullout, fiber fragmentation, matrix softening/melting, stress concentrations, matrix cracking, burring, and delamination.

Experimental research of composite machining is not only time consuming and expensive, but also the carbon chips that are produced during machining of CFRP are dangerous for human health. In addition, interpretation of the experimental results is difficult due to complexity of the process and anisotropy of the composites (Soldani et al., 2011). Therefore, in recent years and with the improvement of computer technology, many researchers have focused on numerical modeling to study CFRP machining. The numerical modeling of fiber reinforced composites can be classified in two general approaches: (I) micromechanical approach where the composite is modeled as multi-phase material and (II) macro mechanical approach where the composite is modeled as an equivalent homogeneous material (EHM) (Dandekar et Shin, 2012). The micromechanical approach was used successfully to predict local defects (such as debonding) and cutting forces (Calzada et al., 2012; Dandekar et Shin, 2008; Nayak, Bhatnagar et Mahajan, 2005; Rao, Mahajan et Bhatnagar, 2007a; Rao, Mahajan et Bhatnagar, 2007b). Nayak et al. (Nayak, Bhatnagar et Mahajan, 2005) presented two micro and macromechanical models and compared the predicted forces of both models with experimental results. They concluded that both models are able to predict the principal cutting force with good accuracy but the micromechanical models offer better estimations of thrust forces. They also indicated that the sub-surface damages and cutting forces increase with fibers angle.

Despite the advantages of the micromechanical approach, it has some limitations. The micro modeling is more complex than macro modeling and needs very high calculation time and precise details of fibers, fiber-matrix arrangements and their interfacial and physical properties (Dandekar et Shin, 2012). Therefore, many researchers have applied macromechanical approaches to model fiber reinforced composite orthogonal cutting (Arola, Sultan et Ramulu, 2002; Lasri, Nouari et El Mansori, 2009; Mahdi et Zhang, 2001b; Rentsch, Pecat et Brinksmeier, 2011; Santiuste, Soldani et Miguélez, 2010; Soldani et al., 2011). Lasri et al. (Lasri, Nouari et El Mansori, 2009) investigated the cutting of glass fiber reinforced plastics (GFRP) using Hashin, Maximum stress, and Hoffman failure criteria. The simulated principal cutting forces with Hashin criterion were closer to the experimental measurements, but the predicted thrust forces for all failure criteria were much less than experiments. Santiuste (Santiuste, Soldani et Miguélez, 2010) and Soldani (Soldani et al., 2011) confirmed the shortcoming of macromechanical modeling in predicting the thrust forces in orthogonal cutting of fiber reinforced plastics. Mkaddem et al. (Mkaddem et El Mansori, 2009; Mkaddem, Demirci et Mansori, 2008) developed a micro-macro model to combine the advantages of both approaches. They considered the composite material as a homogeneous material but the friction coefficient between the tool and the workpiece was assumed dependent to fiber orientation. Their model successfully predicted the sub-surface damages, cutting and thrust forces with lower mean error (6% for cutting forces and 26% for thrust forces) than another macromechanical model presented by Nayak et al. (17% for cutting forces 44% for thrust forces) (Nayak, Bhatnagar et Mahajan, 2005). Their modeling result demonstrated that the cutting forces increase with an increase of fibers angle, while the thrust force increases with fibers angle up to 45° and decreases to its minimum at 90°.

To the authors' knowledge, in spite the existence of many models proposed for simulating the orthogonal cutting of CFRP, there is no numerical model simulating the machining of CFRP, such as the surface milling process. Therefore, this work is an attempt to present the first numerical model for CFRP milling. In this research, a combined micro-macro mechanical model has been developed to study the cutting forces, chip formation and machining damages during CFRP milling. In our approach, the composite material was modeled as an equivalent homogeneous material (like the macroscale approach). An adaptive meshing approach was employed in the cutting zone and the friction coefficient between the tool and workpiece was assumed dependent to fibers orientation (like the microscale approach). For validation purposes, experimental milling tests have been performed and compared to the modeling results.

## 5.3 Experimental procedure

### 5.3.1 Composite Materials

A high performance carbon fiber epoxy unidirectional prepreg (P2053F-10) from Toray Inc. with a surface density of 100 g/m$^2$ and fiber volume content ($V_f$) of 60% was used to produce unidirectional fiber composite plates with a final average thickness of approximately 6.3 mm. The plates were then post-cured in autoclave following the cure cycle recommended by the supplier. The mechanical and physical properties of the material were needed for the modeling. Therefore, compression, shear and tensile tests (according to ASTM D6641 (ASTM, 2009), ASTM D5379 (ASTM, 2012) and ASTM D3039 (ASTM, 2014), respectively) were carried out in both the fiber and transverse directions of the unidirectional composite, and the specific gravity, also required as a physical property, was measured based on ASTM D-792 (ASTM, 2008). The material properties used in the model are summarized in Table 5-1.

Table 5-1 Mechanical and physical properties of CFRP unidirectional laminate (TC-09-U)

| **Mechanical properties** | **CFRP** | **Method/ Reference** | **Mechanical properties** | **CFRP** | **Method/ Reference** |
|---|---|---|---|---|---|
| Longitudinal modulus, $E_1$ | 122.6 GPa | ASTM D3039 | Longitudinal shear strength, $S^L$ | 76.7 MPa | ASTM D5379 |
| Transverse modulus, $E_2$ | 7.01 GPa | ASTM D3039 | Transverse shear strength, $S^T$ | 45.9 MPa | ASTM D5379 |
| In-Plane shear modulus, $G_{12}$ | 12.6 GPa | ASTM D5379 | Fracture energy- fiber tension | 91.6 KJ/m$^2$ | [20] |
| Major Poisson's ratio $\nu_{12}$ | 0.27 | | Fracture energy-fiber compression | 79.9 KJ/m$^2$ | [20] |
| Longitudinal tensile strength, $X^T$ | 1388.0 Mpa | ASTM D3039 | Fracture energy-matrix cracking | 0.22 KJ/m$^2$ | [20] |
| Longitudinal compressive strength, $X^C$ | 551.6 Mpa | ASTM D6641 | Fracture energy-matrix crushing | 1.1 KJ/m$^2$ | [20] |
| Transverse tensile strength, $Y^T$ | 48.2 Mpa | ASTM D3039 | Specific gravity | 1.552 g/cm$^3$ | ASTM D 792 |
| Transverse compressive strength, $Y^C$ | 124.5 Mpa | ASTM D6641 | | | |

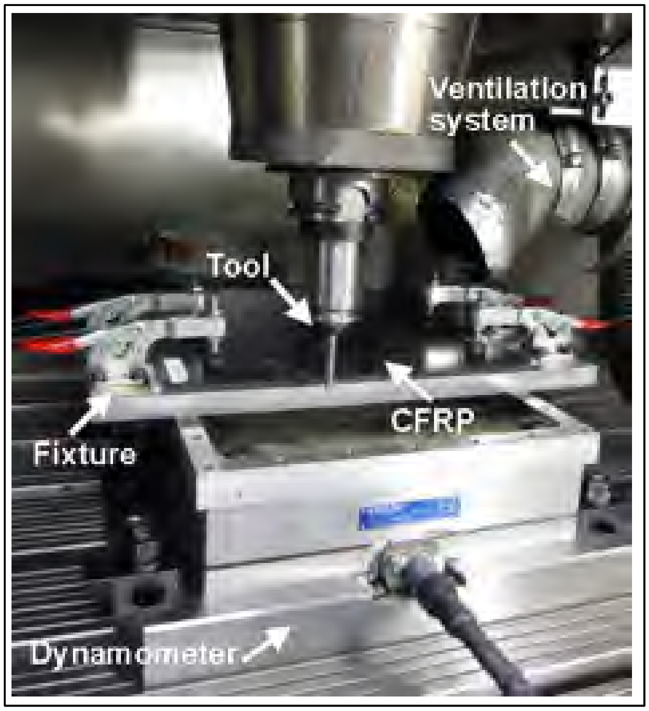


Figure 5-1 Milling experiments set-up

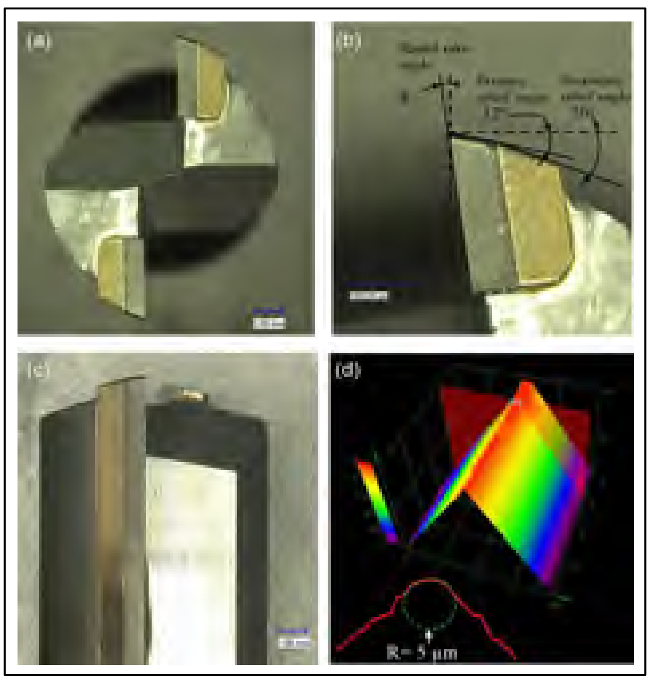


Figure 5-2 Cutting tool geometry

### 5.3.2 Milling process

The experiments were carried out on a Huron K2X10 three-axis CNC machine with a maximum spindle speed of 28,000 rev/min (Figure 5-1). A 3/8" Polycrystalline Diamond (PCD) flat end mill (Figure 5-2) was used for milling tests. Figure 5-2 (b) shows the tool geometry, including the rake and relief angles that were measured using a Keyence VHC-500F type digital microscope. The average tool edge radius of 5 µm was measured by an Olympus LEXT OLS4000 3D confocal laser microscope (Figure 5-2 (d)).

According to the results of the authors' previous research works (Ghafarizadeh, Chatelain et Lebrun, 2014; Ghafarizadeh, Lebrun et Chatelain, 2015), a better surface quality can be achieved using a moderate cutting speed and a lower feed rate when surface milling CFRP. Therefore, in the present work, a moderate cutting speed of 250 m/min was used, while the feed rate was kept constant at 0.063 mm/rev (lowest feed rate). The axial depth of cut was maintained constant at 0.5 mm for all milling tests. The milling experiments were carried out with four different machining directions (defined in Figure 5-3(b) by the angle between carbon fibers and the feed direction) of 0, 45, 90 and 135 degrees. A Kistler 9255B(#3) three-axis dynamometer table, connected to a Kistler type 5010 charge amplifier, was used for measuring the cutting forces during machining (Figure 5-1). The roughness of the machined surfaces was measured using a Mitutoyo SJ400 contact profilometer. The surfaces and edges of the machined slots were also examined using a Hitachi S-3600N electronic microscope (scanning electron microscopy - SEM).

## 5.4 Numerical modeling

### 5.4.1 Geometry, contact, meshing and analysis

CFRP Milling is a three-dimensional process and involves geometrically complex operations. Thus, its modeling is very complex and requires huge computation time. A simplified two-dimensional orthogonal cutting model can describe the milling process quite well with lower computation time than 3D modeling. During milling with a flat end mill, most of the cutting is performed by the periphery of the cutter (Figure 5-3 (a)).

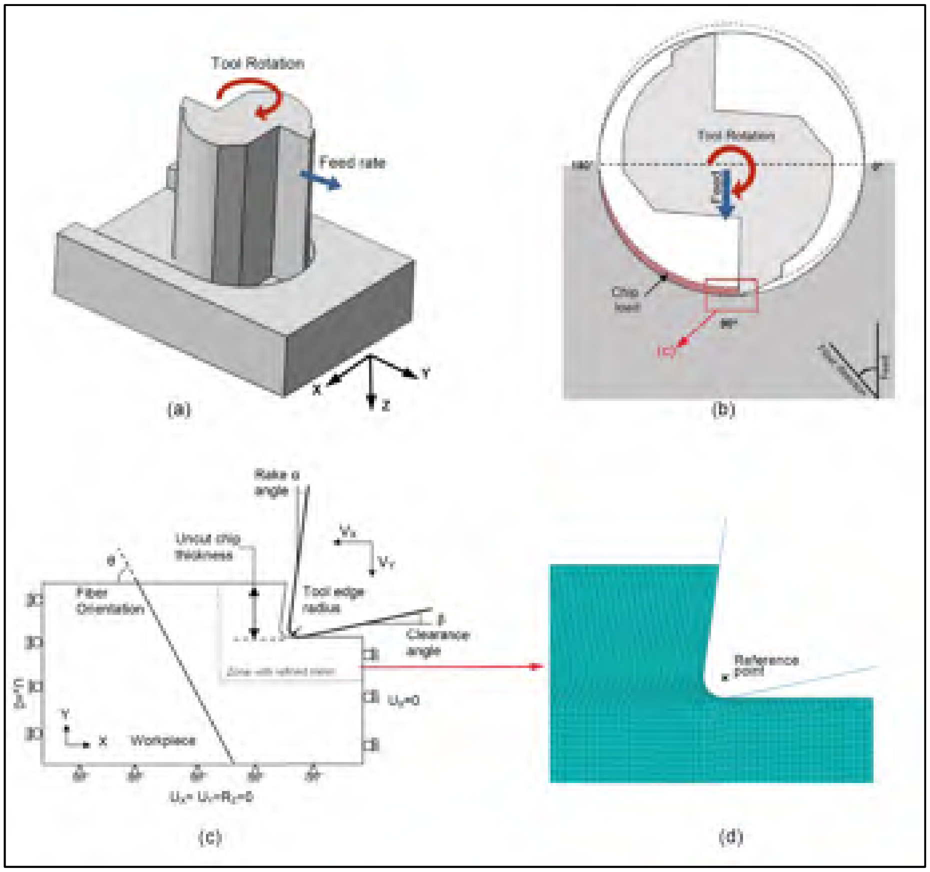


Figure 5-3 Numerical modeling set-up

As can be seen in Figure 5-3b, the flat end milling process can then be approximated as the sum of a deck of 2D deformation-process sections. To reduce the computation time, a simplified geometry of one cutting flute was modeled for a small portion (Figure 5-3(c)) of the tool rotation and for different tool rotation angles: 30, 45, 60, 90, 120, 135, and 150°. In the actual milling process, the cutting edge tip travels on a trochoidal path as the resultant of the feed rate and spindle rotation. However, this path can be assumed circular for small chip thickness values (Özel et Altan, 2000). The conventional uncut chip thickness ($h_n(\theta)$) was calculated for different tool rotation angles ($\theta$) by the following equation, based on the assumption of a circular tool path:

$$h_n(\theta) = f_z \sin\theta \qquad (5\text{-}1)$$

Where $f_z$ represents the feed per tooth ($f_z = f/Z$, Z: Number of teeth) (Li et al., 2007).

The displacement of the workpiece bottom in the cutting and perpendicular directions, and the displacement of the workpiece extremities in the machining direction were restrained (Figure 5-3 (c)). The unidirectional CFRP was modeled as a homogeneous orthotropic material. A plane strain model is not appropriate for composite materials due to the out-of-plane material displacement observed during the cutting process (Lasri, Nouari et El Mansori, 2009). A plane stress model was therefore considered, using continuum solid elements CPS4R available in the commercial finite element code ABAQUS/Explicit version 6.12, allowing linear interpolation, reduced integration and automatic hourglass control. The milling tool was assumed to be a rigid body in order to save computational time (the elastic modulus of Polycrystalline Diamond material is 6 times greater than the elastic modulus of CFRP in the fiber direction (Ramulu et al., 1991)). In many research works, the orthogonal cutting process is modeled based on quasi-static analysis, focusing on the initial instant of cutting process (Arola et Ramulu, 1997; Arola, Sultan et Ramulu, 2002; Lasri, Nouari et El Mansori, 2009; Nayak, Bhatnagar et Mahajan, 2005; Ramesh et al., 1998; Rao, Mahajan et Bhatnagar, 2007b; Soldani et al., 2011). The low strain rate dependence of CFRP materials due to their brittle nature supports this assumption (Lasri, Nouari et El Mansori, 2009). Thus, a quasi-static analysis was employed in the present study.

A reference point controlled the movement of the cutting tool (Figure 5-3(d)). The tool was modeled with the geometry described in the previous section, with a rake angle of 8°, a clearance angle of 12° and an edge radius of 5 µm. Wang and Zhang (Wang et Zhang, 2003) found that there is a difference between the real and nominal depths of cut due to the bouncing back phenomenon. This phenomenon occurs when a certain part of the material below the tool is pushed down without cutting, partially producing an elastic spring-back after the tool passes through. Thus, in this model, the workpiece was configured with a round corner ahead of the cutting tool in order to take the bouncing back effect during cutting into account. As can be seen in Figure 5-3(c), the mesh of the workpiece was refined in the cutting zone surrounding the tool edge tip (mesh size of 10 µm, approximately equal to the fiber diameter). This mesh size was selected for having a good balance between accuracy and computation time. Arbitrary Lagrangian-Eulerian (ALE) adaptive meshing is a general formulation that combines the features of pure Lagrangian and pure Eulerian analysis. This technique allows the mesh to move independently of the underlying material. Thus, it can control the element distortion and maintain a high-quality mesh, even in a process where large material deformations are involved, by allowing the mesh to move independently of the underlying material (Hibbitt, Karlsson et Sorensen, 2012). The ALE method was used in this research to reduce mesh distortion.

### 5.4.2 Contact modeling

The interaction between the work material and tool was modeled by using surface-node surface contact available in ABAQUS/Explicit. The tool was defined as the master object, and the workpiece as the slave object. Friction is an important phenomenon that affects the accuracy of predicted cutting forces in machining simulation. In the present model, the friction between the cutting tool and the workpiece was described by Coulomb's friction law (Equation 5-2), where the frictional stress ($\tau_n$) on the tool is proportional to the normal stress ($\sigma_n$) with a constant friction coefficient ($\mu$), such that:

$$\tau_n = \mu\sigma_n \tag{5-2}$$

Many researchers assume a constant coefficient of friction for all fiber orientations, such as 0.3 (Rao, Mahajan et Bhatnagar, 2007a; Rao, Mahajan et Bhatnagar, 2007b; Rentsch, Pecat et Brinksmeier, 2011), 0.4 (Arola, Sultan et Ramulu, 2002), or 0.5 (Lasri, Nouari et El Mansori, 2009; Santiuste, Soldani et Miguélez, 2010). Nayak and Bhatnagar (Nayak, Bhatnagar et Mahajan, 2005) showed that the friction coefficient increased by increasing the fibers angle using pin-on-disk tests (Figure 5-4). To enhance cutting force predictions, variable coefficients of friction (between 0.3 and 0.9) were determined for different fiber orientations according to Nayak et al.'s research (Nayak, Bhatnagar et Mahajan, 2005).

### 5.4.3 Failure criteria

Lasri et al. (Lasri, Nouari et El Mansori, 2009) compared the Hashin, Maximum stress and Hoffman failure criteria for the orthogonal cutting of FRP and concluded that cutting forces predicted using the Hashin failure criterion are closer to experimental results.

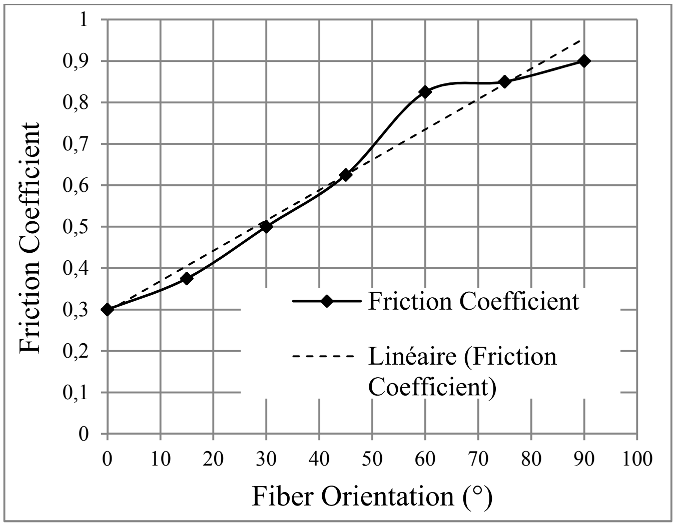


Figure 5-4 Variation of coefficient of friction with respect to fiber orientation (Mkaddem et El Mansori, 2009; Nayak, Bhatnagar et Mahajan, 2005)

Thus, Hashin theory was used to predict damage and failure modes in this research. This failure criterion presents four failure modes, including fiber tensile failure, fiber compressive failure, matrix cracking, and matrix crushing modes, according to the following equations (Hashin, 1980; Hashin et Rotem, 1973):

Tensile fiber failure for $\sigma_{11} \geq 0$

$$\left(\frac{\sigma_{11}}{X^T}\right)^2 + \alpha\left(\frac{\tau_{12}}{S^L}\right)^2 \leq 1 \tag{5-3}$$

Fiber compression ($\sigma_{11} < 0$)

$$\left(\frac{\sigma_{11}}{X^C}\right)^2 \leq 1 \tag{5-4}$$

Matrix cracking ($\sigma_{22} > 0$)

$$\left(\frac{\sigma_{22}}{Y^T}\right)^2 + \left(\frac{\tau_{12}}{S^L}\right)^2 \leq 1 \tag{5-5}$$

Matrix crushing ($\sigma_{22} > 0$)

$$\left(\frac{\sigma_{22}}{2S^T}\right)^2 + \left[\left(\frac{Y^C}{2S^T}\right)^2 - 1\right]\frac{\sigma_{22}}{Y^C} + \left(\frac{\tau_{12}}{S^L}\right)^2 \leq 1 \tag{5-6}$$

Where $\sigma_{11}$, $\sigma_{22}$, and $\sigma_{12}$ are the normal stresses in the fiber and transverse directions and the in-plane shear stress, respectively. All other variables ($X^T$, $X^C$, $Y^T$, $Y^C$, $S^L$, and $S^T$) are listed in Table 5-1. The onset of damage was predicted using Hashin's failure criterion and material degradation was modeled by reducing the material stiffness to zero. Reducing the stiffness to zero occurs gradually in the modeling process by controlling damage variables, varying between 0 for the undamaged state, to 1, for the fully damaged state. The evolution law of the damage variable is based on the fracture energy dissipated during the damage process (Lapczyk et Hurtado, 2007). The fracture energies used in the model for the different failure modes are presented in Table 5-1.

## 5.5 Results and discussion

### 5.5.1 Chip formation

In the model, the tool moves towards the workpiece until a complete chip is formed after reaching material failure on the free surface ahead of the cutting tool. Figure 5-5 shows the chip formation process for different tool rotation angles in CFRP milling with a machining direction of 0°. The horizontal and vertical axes (on the top and left sides of the figure) represent the failure modes and tool rotation angle, respectively. At low tool rotation angles (30, 45, and 60°), the fiber compressive failure and matrix crushing progressed in the fiber direction until completion of the chip formation. For higher tool rotation angles (90° and more), while the cutting tool progresses in the workpiece, a stressed zone is formed ahead of the tool edge, and matrix crushing damage is extended in the fiber direction until chip formation. The matrix cracking damage mode is illustrated in the last column of Figure 5-5. It can be seen that matrix cracking failure affected a relatively large zone of uncut material below the tool for all tool rotation angles. The second column of Figure 5-5 shows the fiber tensile failure mode for all tool rotation angles. The effect of this failure mode was almost negligible on the limited area ahead of the tool tip. Comparing the fiber compression damage mode of all tool rotation angles in Figure 5-5 (the first column) demonstrates that compression failure occurs in the direction of fibers. For 45° and 60° tool rotations, a large zone of uncut material is affected by this failure mode.

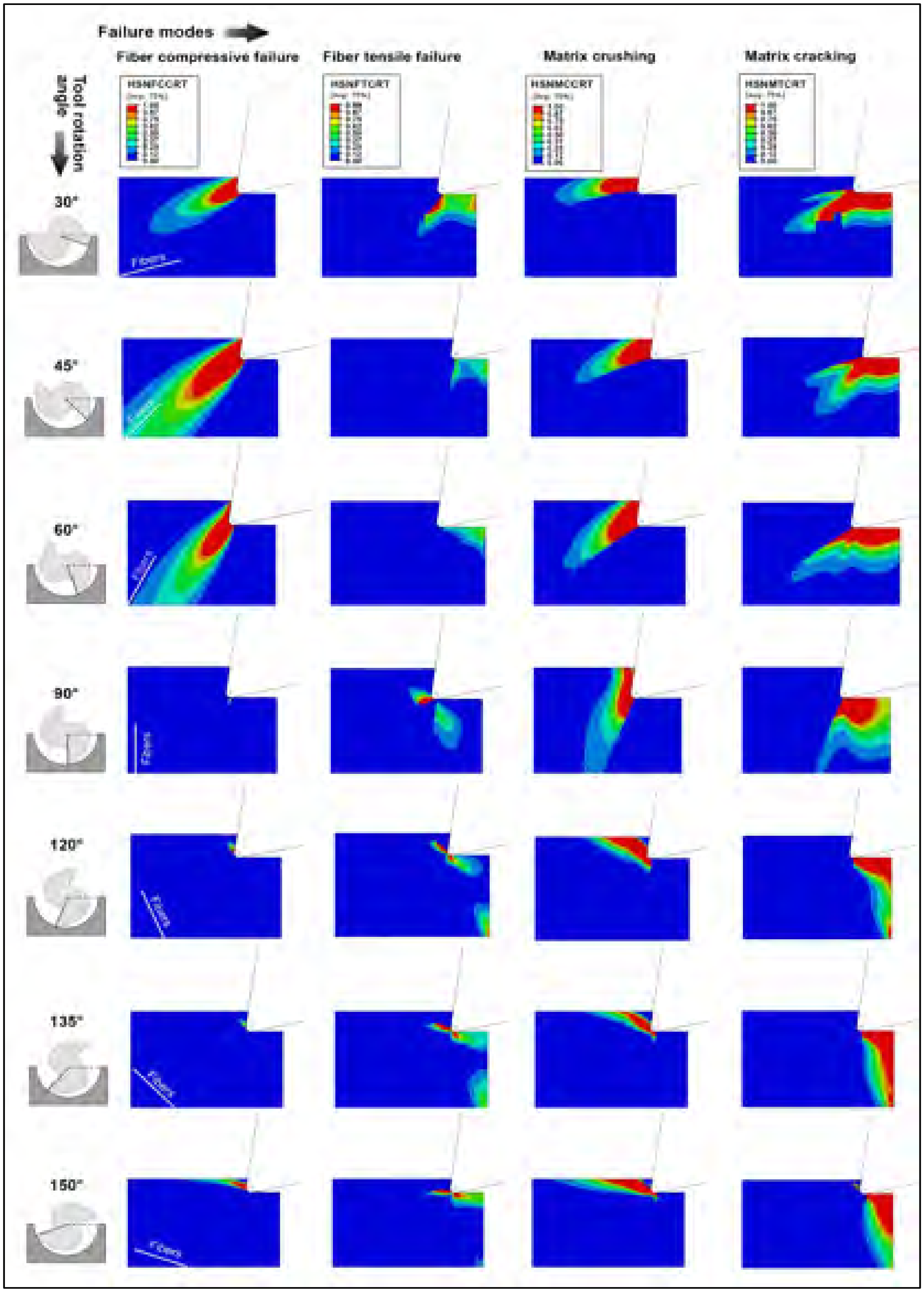


Figure 5-5 Chip formation mechanism in milling of CFRP with a 0° feed rate orientation, step time: 1.00E-4

The materials' behavior under load can generally be classified as ductile or brittle, based on their ability to undergo plastic deformation before fracture (Dieter et Bacon, 1986). Santiuste et al. (Santiuste, Soldani et Miguélez, 2010) found, from finite element analysis results, that glass fiber reinforced plastics behave like ductile materials by showing a progressive damage process, while CFRPs are brittle materials showing little or no progression of damage. These results are supported by the actual modeling results demonstrating that CFRPs undergo catastrophic failure with a negligible plastic deformation. The elements did not suffer significant deformation, and they broke when tool entered 1μm into the workpiece in step time 1.00E-4 s.

### 5.5.2 Cutting forces

Cutting forces in the x and y directions are calculated in the model from the reaction exerted by the workpiece material on the reference point of the tool (Figure 5-3(d)). The cutting forces obtained from the 0° and 90° milling directions are shown in Figures 5-6 and 5-7, respectively. These figures show a relatively good agreement between the experimental and predicted values of the cutting forces. The left images (Figure 5-6 (a) and Figure 5-7 (a)) show the cutting forces in the time domain for seven complete rotations of the tool (the two-flutes tool generating 14 peaks in the graph), and the right images (Figure 5-6 (b) and Figure 5-7 (b)) show the cutting forces of one tooth for a 180° rotation of the tool. So each peak of the force profile in Figure 5-6 (a) and Figure 5-7 (a) represents the passage of one tooth.

It is clearly shown that the force profiles for the two teeth of the tool are not completely similar. The small difference can be explained by the tool run-out during the milling process. Tool run-out affects the cutting force profile of conventional end-milling operations by affecting the feed per tooth of each tooth (Li et al., 2007). By comparing the cutting forces in Figure 5-6 (b) and Figure 5-7 (b), it can be observed that the cutting forces do not have similar profiles and amplitudes for different machining directions. It thus seems that fiber orientation has a significant effect on the cutting force profiles during machining of unidirectional CFRP. This can be explained by the anisotropic character of unidirectional fiber reinforced plastic materials.

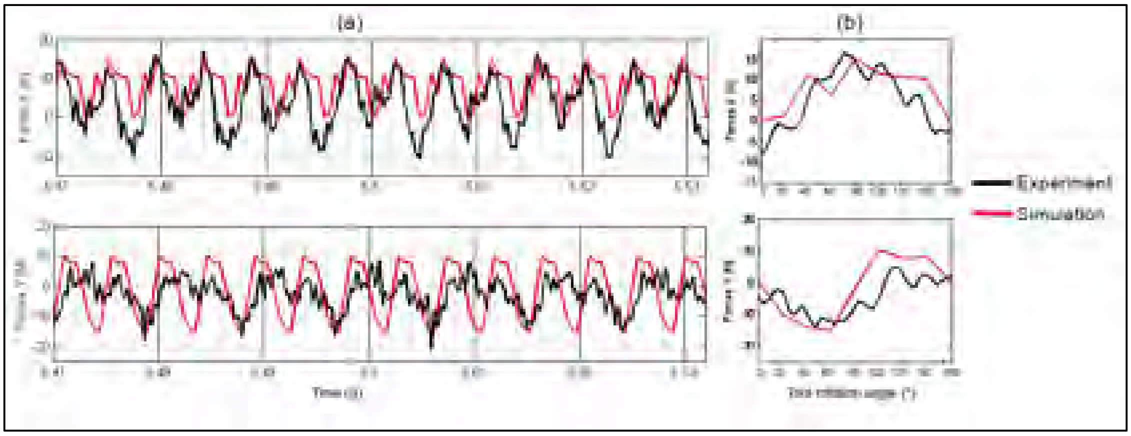


Figure 5-6 Comparison between experimental and simulated values of the cutting forces for a 0° machining direction, a 250 m/min cutting speed, a 0.063 mm/rev feed rate and a 0.5 mm depth of cut

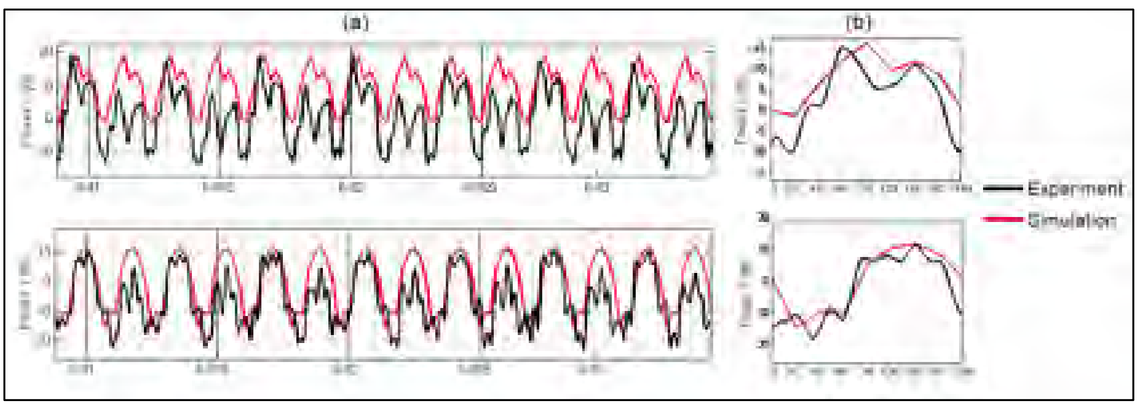


Figure 5-7 Comparison between experimental and simulated values of the cutting forces with 90° machining direction, 250 m/min cutting speed, 0.063 mm/rev feed rate, 0.5 mm depth of cut

### 5.5.3 Surface integrity

Figure 5-8 shows the CFRP machined surface for different machining directions of 0, 90, 45, and 135 degrees. The best surface quality in terms of surface roughness ($R_a$ - arithmetic average height) and lowest damage was achieved in the 0° machining direction. As shown in Figure 5-8 (d), many uncut fibers are observed in milling at 135°, fibers that protrude from the machined edges, resulting in a poor edge quality.

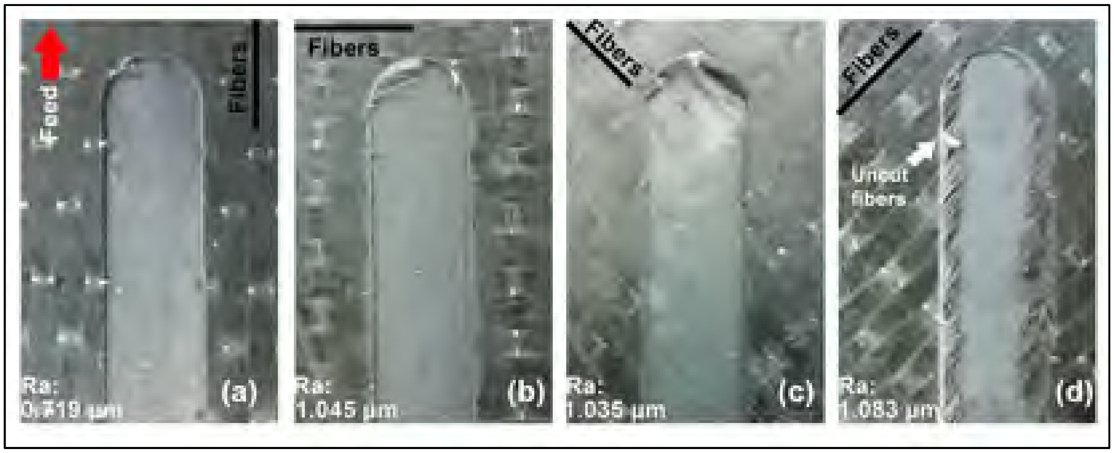


Figure 5-8 CFRP machined surface for different machining directions of 0 (a), 90 (b), 45 (c) and 135 (d) degrees, 250 m/min cutting speed, 0.063 mm/rev feed rate, 0.5 mm depth of cut

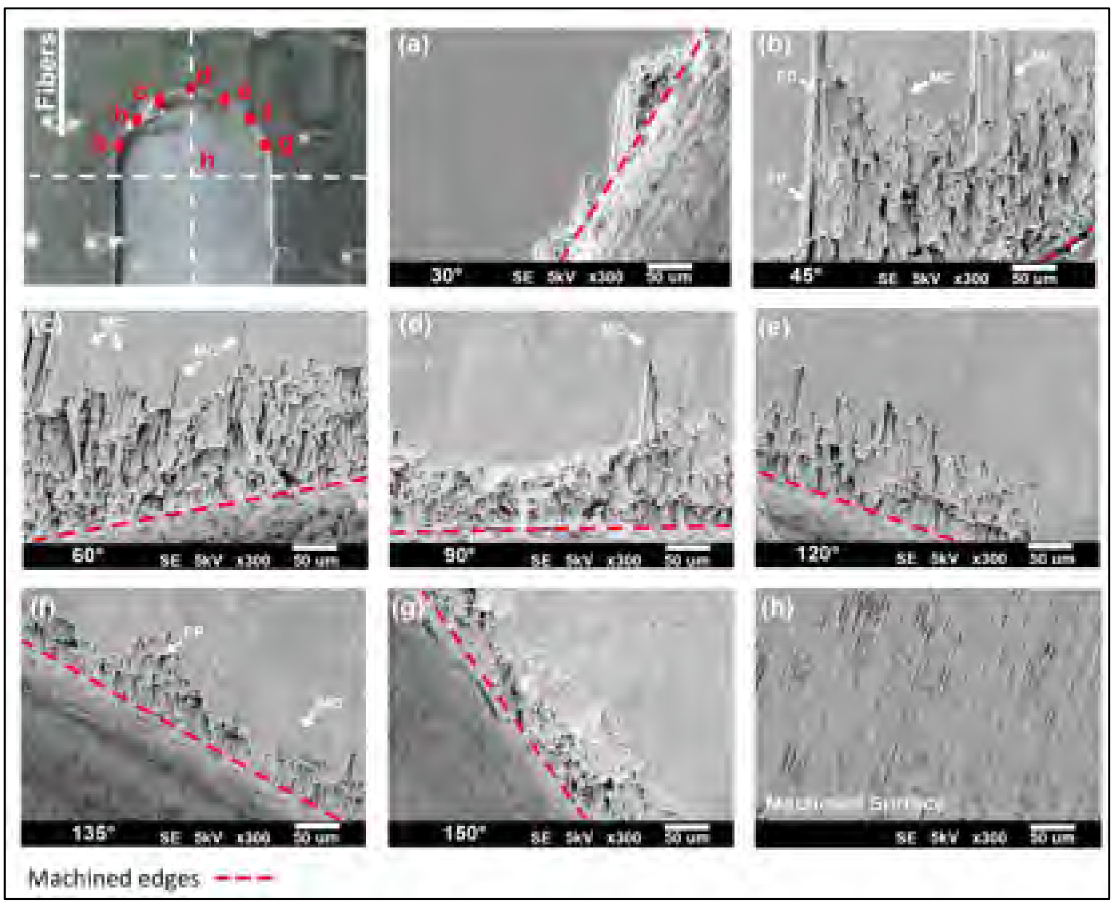


Figure 5-9 Machining damage at different tool rotation angles: fiber pullout (FP), fiber/matrix de-cohesion (F.D), Matrix Cracking (MC), magnification x300

Figure 5-9 illustrates the SEM photographs of the machined surface and edges for different tool rotation angles and for the 0° machining direction in same magnification (300x). As can be seen, the larger damaged zones on the machined edges are observed at tool rotation angles of 45° and 60° (Figure 5-9(b) and (c)), compared to other tool rotation angles (Figure 5-9 (a) and (d-e).

This is in agreement with Figure 5-5, where the modeling results show that the compressive damage failure mode affects a large zone of uncut materials for tool rotation angles of 45° and 60°. As described in the modeling results, matrix cracking failure affects a relatively large zone around the cutting area. This modeling prediction is confirmed by the presence of deep matrix cracking damage in SEM images. A SEM image of the machined surface is shown in Figure 5-9 (h). As can be seen, a good surface quality was produced with the cutting condition used in this research (250 m/min cutting speed, 0.063 mm/rev feed rate, 0.5 mm depth of cut).

## 5.6 Conclusion

In this work, the surface milling of unidirectional carbon fiber reinforced laminates was studied by comparing finite element analysis results with experimental results. The chip formation mechanism, machining damage and cutting forces were investigated with the proposed finite element model. Based on the results, the following conclusions are drawn:

- A 2D finite element model based on orthogonal cutting can successfully predict the cutting forces in a complex flat end milling process.

- The cutting forces do not have similar profiles for different machining directions (angle between the carbon fibers and feed direction), meaning that the cutting force profile depends on the fiber orientation.

- The extension of machining damage strongly depends on the fiber orientation. During milling in a 0° machining direction, for all tool rotation angles, the compressive damage in uncut materials extends in the direction of fibers. For 45 and 60° tool rotations, this failure mode affects a large zone of uncut materials, as was confirmed by micrographic images. The matrix cracking failure also affected a relatively large zone of uncut material below the tool for all tool rotation angles.

- The numerical predictions of machining damage around the cutting area, due to fiber compressive damage and matrix cracking, are confirmed by SEM images of the edges and surface of the machined zone.

### 5.7 Acknowledgments

This research was funded by the Consortium for Research and Innovation in Aerospace in Quebec (CRIAQ), and the Natural Sciences and Engineering Research Council of Canada (NSERC).

### 5.8 References

Arola, D, et M Ramulu. 1997. « Orthogonal cutting of fiber-reinforced composites: a finite element analysis ». *International Journal of Mechanical Sciences*, vol. 39, n° 5, p. 597-613.

Arola, D, MB Sultan et M Ramulu. 2002. « Finite element modeling of edge trimming fiber reinforced plastics ». Journal of Manufacturing Science and Engineering, vol. 124, n° 1, p. 32-41.

ASTM. 2008. *D 792–08. Standard test methods for density and specific gravity (relative density) of plastics by displacement*. West Conshohocken, PA

ASTM. 2009. *D6641/D6641M-09: Standard test method for compressive properties of polymer matrix composite materials using a combined loading compression (CLC) test fixture*. West Conshohocken, PA.

ASTM. 2012. *D5379/D5379M: Standard test method for shear properties of composite materials by the V-notched beam method*. West Conshohocken, PA

ASTM. 2014. *D3039/D3039M: Standard test method for tensile properties of polymer matrix composite materials*. West Conshohocken, PA

Calzada, Kevin A, Shiv G Kapoor, Richard E DeVor, Johnson Samuel et Anil K Srivastava. 2012. « Modeling and interpretation of fiber orientation-based failure mechanisms in machining of carbon fiber-reinforced polymer composites ». *Journal of Manufacturing Processes*, vol. 14, n° 2, p. 141-149.

Dandekar, Chinmaya R, et Yung C Shin. 2008. « Multiphase finite element modeling of machining unidirectional composites: prediction of debonding and fiber damage ». *Journal of Manufacturing Science and Engineering*, vol. 130, n° 5, p. 051016.

Dandekar, Chinmaya R, et Yung C Shin. 2012. « Modeling of machining of composite materials: a review ». *International Journal of Machine tools and manufacture*, vol. 57, p. 102-121.

Davim, J. Paulo. 2015. *Machinability of Fibre-Reinforced Plastics*, 4. Berlin: Walter de Gruyter GmbH & Co KG.

Dieter, George Ellwood, et David Bacon (9-10). 1986. *Mechanical metallurgy*, 3. McGraw-Hill New York.

Ghafarizadeh, Seyedbehzad, Jean-François Chatelain et Gilbert Lebrun. 2014. « Effect of cutting tool lead angle on machining forces and surface finish of CFRP laminates ». *Science and Engineering of Composite Materials*, DOI: 10.1515/secm-2013-0188.

Ghafarizadeh, Seyedbehzad, Gilbert Lebrun et Jean-François Chatelain. 2015. « Experimental investigation of the cutting temperature and surface quality during milling of unidirectional carbon fiber reinforced plastic ». *Journal of Composite Materials*, DOI: 0021998315587131.

Hashin, Zvi. 1980. « Failure criteria for unidirectional fiber composites ». *Journal of Applied Mechanics,* vol. 47, n° 2, p. 329-334.

Hashin, Zvi, et Assa Rotem. 1973. « A fatigue failure criterion for fiber reinforced materials ». *Journal of Composite Materials*, vol. 7, n° 4, p. 448-464.

Hibbitt, D, B Karlsson et P Sorensen. 2012. *Abaqus 6.12 Documentation and User Manual*. Dassault Systèmes Simulia Corp.

Lapczyk, Ireneusz, et Juan A Hurtado. 2007. « Progressive damage modeling in fiber-reinforced materials ». Composites Part A: *Applied Science and Manufacturing*, vol. 38, n° 11, p. 2333-2341.

Lasri, L, M Nouari et M El Mansori. 2009. « Modelling of chip separation in machining unidirectional FRP composites by stiffness degradation concept ». *Composites Science and Technology*, vol. 69, n° 5, p. 684-692.

Li, Chengfeng, Xinmin Lai, Hongtao Li et Jun Ni. 2007. « Modeling of three-dimensional cutting forces in micro-end-milling ». *Journal of Micromechanics and Microengineering*, vol. 17, n° 4, p. 671.

Mahdi, Mofid, et Liangchi Zhang. 2001. « A finite element model for the orthogonal cutting of fiber-reinforced composite materials ». *Journal of Materials Processing Technology*, vol. 113, no 1, p. 373-377.

Mkaddem, A., et M. El Mansori. 2009. « Finite element analysis when machining UGF-reinforced PMCs plates: Chip formation, crack propagation and induced-damage ». *Materials & Design*, vol. 30, n° 8, p. 3295-3302.

Mkaddem, Ali, Ibrahim Demirci et Mohamed El Mansori. 2008. « A micro–macro combined approach using FEM for modelling of machining of FRP composites: Cutting forces analysis ». *Composites Science and Technology*, vol. 68, n° 15, p. 3123-3127.

Nayak, D, N Bhatnagar et P Mahajan. 2005. « Machining studies of UD-FRP composites part 2: finite element analysis ». *Machining science and technology*, vol. 9, n° 4, p. 503-528.

Özel, Tuğrul, et Taylan Altan. 2000. « Process simulation using finite element method—prediction of cutting forces, tool stresses and temperatures in high-speed flat end milling ». *International Journal of Machine Tools and Manufacture*, vol. 40, n° 5, p. 713-738.

Ramesh, MV, KN Seetharamu, N Ganesan et MS Sivakumar. 1998. « Analysis of machining of FRPs using FEM ». *International Journal of Machine Tools and Manufacture*, vol. 38, n° 12, p. 1531-1549.

Ramulu, M, M Faridnia, JL Garbini et JE Jorgensen. 1991. « Machining of graphite/epoxy composite materials with polycrystalline diamond (PCD) tools ». *Journal of Engineering Materials and Technology*, vol. 113, n° 4, p. 430-436.

Rao, G Venu Gopala, Puneet Mahajan et Naresh Bhatnagar. 2007a. « Machining of UD-GFRP composites chip formation mechanism ». *Composites Science and Technology*, vol. 67, n° 11, p. 2271-2281.

Rao, G., P. Mahajan et N. Bhatnagar. 2007b. « Micro-mechanical modeling of machining of FRP composites–Cutting force analysis ». Composites Science and Technology, vol. 67, n° 3, p. 579-593.

Rentsch, R, O Pecat et E Brinksmeier. 2011. « Macro and micro process modeling of the cutting of carbon fiber reinforced plastics using FEM ». *Procedia Egineering*, vol. 10, p. 1823-1828.

Santiuste, C., X. Soldani et M.H. Miguélez. 2010. « Machining FEM model of long fiber composites for aeronautical components ». *Composite Structures*, vol. 92, n° 3, p. 691-698.

Soldani, Xavier, Carlos Santiuste, Ana Muñoz-Sánchez et MH Miguélez. 2011. « Influence of tool geometry and numerical parameters when modeling orthogonal cutting of LFRP composites ». *Composites Part A: Applied Science and Manufacturing*, vol. 42, n° 9, p. 1205-1216.

Wang, XM, et LC Zhang. 2003. « An experimental investigation into the orthogonal cutting of unidirectional fibre reinforced plastics ». *International Journal of Machine Tools and Manufacture*, vol. 43, n° 10, p. 1015-1022.

# CONCLUSIONS

In this work, the surface milling of carbon fiber reinforced plastic was studied by experimental and finite element modeling methods. In the experimental parts of this research, the milling experiments were carried out on unidirectional and multidirectional CFRP laminates in order to study the effects of cutting parameters, such as the fiber orientation, feed rate, cutting speed, and lead angle on the cutting force, cutting temperature, and surface quality. In the modeling part, the finite element analysis was used to study the cutting force, machining damage and chip formation for the CFRP milling operation. The major findings and contributions of this research are summarized below.

- Machining conditions has significant influence on the resultant surface roughness and damages/surface integrity in CFRP milling process. Generally, a better surface quality (in terms of lower surface roughness and surface damages) was achieved using lower feed rate (0.063), moderate cutting speed (250 m/min) and 0 degree tool lead angle. This better machining quality was obtained by smaller uncut chip thickness (in lower feed rate) and higher dynamic stability (lower forces in moderate cutting speed and 0 degree lead angle).

- The resultant cutting force in milling of unidirectional and multidirectional CFRP increases with the feed rate. The cutting forces do not vary linearly with the cutting speed. The effect of the cutting speed on cutting force is more significant for moderate cutting speed values.

- The cutting speed has a significant effect on the cutting force and cutting temperature. The cutting temperature increases linearly with the cutting speed for the studied cutting speeds range (200 to 375 m/min).
- The variation of cutting forces and cutting temperature over the fiber orientation follow the same trend. Maximum and minimum cutting forces and cutting temperatures values are achieved at fiber orientations of 90 and 0 degrees, respectively.

- The study of surface damages with SEM images showed that the best surface integrity are produced for the 0 and 90 degree fiber orientation angles and moderate cutting speeds (200 and 250 m/min).

- The developed numerical model provided a better understanding of the CFRP milling process. The model was validated by comparing its results with experimentally measured forces and SEM images of the machined surface. It was able to predict the cutting forces and machining damages, in good agreement with experiments.

- For all tool rotation angles during the milling process, the chip formation initiates ahead of the tool tip. At low tool rotation angles (30-60°), the fiber compressive failure and matrix crushing progressed in the fiber direction until completion of the chip formation. While in higher tool rotation angles (90° and more), the chip was formed by matrix crushing mode.

- The modeling results confirmed the brittle behaviour of CFRP materials. CFRPs undergo catastrophic failure with a negligible plastic deformation.

- The extension of machining damage strongly depends on the tool rotation angle (and as a result the fiber orientation). During milling in a 0° machining direction, for all tool rotation angles, the compressive damage in uncut materials extends in the direction of fibers. For 45° and 60° tool rotations, this failure mode affects a large zone of uncut materials. The matrix cracking failure also affected a relatively large zone of uncut material below the tool for all tool rotation angles.

- The machining direction (angle between the carbon fibers and feed direction) considerably influences the values and profile shape of cutting forces.

## RECOMMENDATIONS

Some directions for future research related to this study are proposed below.

1- The Finite element modeling is a good alternative method to investigate the effect of cutting conditions effects. Further modeling studies are required focusing on effects of cutting condition and tool geometry (rake, clearance and nose radius diameter) in CFRP milling process.

2- The proposed model in this research simulated the milling process with two flutes mill that has one tooth in contact with the workpiece. The model can be modified for the use of tools with more than two flutes by considering the trochoidal tool path and measuring the effective radial depth of cut for each edge. The cutting in each tooth can be modeled separately and the resultant cutting force for the tool can be calculated by adding the modeled force vectors for each tooth.

3- As shown in the experimental results, the tool run-out affects the cutting force profile. The effect of run-out hasn’t been considered in the model. The accuracy of the model in predicting the cutting forces and damages can be improved by considering the effect of the tool run-out on chip thickness.

4- Cutting temperature is an important factor in CFRP machining that affects the cutting forces through softening of the polymer matrix. The cutting temperature in CFRP was studied in this research. However, the material mechanical properties for the modeling process were measured at room temperature. More mechanical testing may be needed to find the material properties at higher temperatures. The effect of cutting temperature on cutting force can be included by adding the effect of temperature on composite’s mechanical properties in the proposed model

5- In the proposed model, the cutting mechanism was modeled based on quasi-static analysis. Thus, this model is not able to study the effect of cutting speed on cutting force. The experimental results showed that the cutting temperature increases linearly with cutting speed (section 4.4.1). Thus, the model can be modified to study the effect of the cutting speed by considering the effect of cutting temperature (as it is mentioned in recommendation 4).

**APPENDIX I**



Seyedbehzad Ghafarizadeh*, Jean-François Chatelain and Gilbert Lebrun

# Effect of cutting tool lead angle on machining forces and surface finish of CFRP laminates

**Abstract:** Machining is one of the most practical processes for finishing operations of composite components, allowing high-quality surface and controlled tolerances. The high-precision surface milling of carbon fiber-reinforced plastics (CFRP) is particularly applicable in the assembly of complex components requiring accurate mating surfaces as well as for surface repair or mold finishing. CFRP surface milling is a challenging operation because of the heterogeneity and anisotropy of these materials, which are the source of several types of damage, such as delamination, fiber pullout, and fiber fragmentation. To minimize the machining problems of CFRP milling and improve the surface quality, this research focuses on the effect of multiaxis machining parameters, such as the feed rate, cutting speed, and lead angle, on cutting forces and surface roughness. The results show that the surface roughness and cutting forces increase with the feed rate, whereas their variations are not uniform when changing the cutting speed. Generally, a lower surface roughness was achieved by using a lower cutting feed rate (0.063 mm/rev) and higher cutting speeds (250–500 m/min). It was also found that the cutting forces and surface roughness vary significantly and nonlinearly with the lead angle of the cutting tool with respect to the surface.

**Keywords:** carbon fiber-reinforced plastic; milling; surface machining; surface quality.

DOI 10.1515/secm-2013-0188
Received August 6, 2013; accepted December 16, 2014

***Corresponding author: Seyedbehzad Ghafarizadeh,** Mechanical Engineering Department, École de technologie supérieure, Université du Québec, 1100, rue Notre-Dame Ouest (corner of Peel Street), Montréal, Quebec, H3C 1K3 Canada,
e-mail: seyedbehzad.ghafarizadeh.1@ens.etsmtl.ca
**Jean-François Chatelain:** Mechanical Engineering Department, École de technologie supérieure, Université du Québec, 1100, rue Notre-Dame Ouest (corner of Peel Street), Montréal, Québec, H3C 1K3 Canada
**Gilbert Lebrun:** Mechanical Engineering Department, Université du Québec à Trois-Rivières (UQTR), 3351 Boul Des Forges, Trois-Rivières, Quebec, G9A 5H7 Canada

## 1 Introduction

In recent years, the use of carbon fiber-reinforced plastics (CFRP) has increased considerably, especially in aerospace industries. Nowadays, many aircraft parts are made of this composite material. For example, approximately 50% of the weight of the Boeing 787 aircraft is made of composite materials, such as carbon/epoxy and graphite/titanium [1]. CFRP composites are widely used for different parts of aircrafts, such as wing boxes, fuselages, ailerons, wings, spoilers, vertical stabilizers, traps, and struts [2]. CFRP materials present many advantages compared to other materials, including higher strength and stiffness, longer fatigue life, low density, and better corrosion and wear resistance. Because of a negative coefficient of thermal expansion along the axis of carbon fibers, carbon-reinforced composites can be patterned to minimize the thermal expansion over a wide range of temperatures. This is very important for aerospace structures [3].

CFRP components are usually produced to near net shape, but machining is often required to remove excess material and produce high-quality surfaces with controlled tolerances. In particular, drilling and trimming are extensively used to remove excessive material, to produce cutouts, or holes that are required for the product function, or to assemble components. The high-precision surface milling of CFRP is particularly useful for the assembly of complex components requiring accurate mating surfaces as well as for surface repair and mold finishing. CFRP surface milling is a challenging operation because of the heterogeneous and anisotropic nature of these composites that can cause some damages such as delamination, fiber pullout, fiber fragmentation, burring, fuzzing, or thermally affected matrix, which in turn may affect the surface finish and properties of the material [4, 5]. In addition, these composites are extremely abrasive; consequently, tool wear is one of the major problems encountered in CFRP machining. Poor cutting conditions produce increased specific cutting energies and higher tool temperatures, resulting in higher tool wear rates [6]. Choosing the appropriate conditions, such as feed rate, cutting speed, and lead angle, in the case of multiaxis machining is thus very important.

In recent years, many studies have been carried out to provide a better understanding regarding the effects of cutting conditions in CFRP machining on the quality of machined surfaces.

Davim and Reis [7] investigated the effects of milling parameters on surface roughness and machining damage; they concluded that surface roughness ($R_a$) increases with the feed rate and decreases with the cutting speed. It was also found that the feed rate presents the highest statistical and physical influence on surface roughness and delamination factor, respectively. In another study, El-Hofy et al. [8] investigated the effects of different slotting parameters, such as tool materials (WC & PCD) and the cutting environment (chilled air and dry) on the surface roughness and integrity, using 3D roughness parameters (arithmetical mean height $S_a$ and maximum peak to valley height $S_z$). According to the results of their research, the combination of low cutting speeds and high feed rates was recommended in view of improving surface roughness, with the feed rate being a significant factor. The effect of the feed rate on the surface roughness was also found to be significant from a study that was carried out by Chatelain et al. [9]. Sheikh-Ahmad et al. [10] carried out an experimental study aimed to determine the effects of cutting conditions on machining quality during the edge trimming of CFRP; they demonstrated that the surface roughness and average delamination depth increase with an increase in the feed rate and decrease with an increase in the spindle speed.

Cutting forces are among the important factors in machining, which influence the process stability, part quality, cutting temperature, and tool wearing condition [11]. Colligan and Ramulu [12] studied the edge trimming of graphite/epoxy with diamond abrasive cutters and demonstrated that cutting forces increase with the material removal rate $= V \times f \times d$, where $V$ is the cutting speed, $f$ is the feed rate, and $d$ is the depth of cut.

The experiments of Sreejith et al. [13] examining the face turning of fiber-reinforced plastics showed that the variations of cutting forces/specific cutting pressure is not uniform over the cutting speed and the moderate cutting speeds (200–300 m/min) are more suited for the machining of CFRP. Zhang [14] investigated the machining of long fiber-reinforced polymer matrix composites and found that cutting forces became greater when the depth of cut increases. Rusinek [15] studied the milling process of CFRP and concluded that the cutting force rises with an increase in the feed rate. Wang et al. [16] studied CFRP milling using a PCD tool and showed that good surface quality and low delamination could be achieved in high-speed milling of CFRP by using PCD tool. These authors found that cutting forces are an important factor for controlling surface roughness; they also observed that the surface roughness tends to increase with the cutting forces up to 250 N followed by a decrease when the cutting forces continue to rise from 250 to 400 N.

The lead angle is the rotation of the tool axis about the cross-feed axis [17] (Figure 1). This angle has a significant effect on process mechanics and dynamics, which have not been studied in CFRP milling until now. The study of the effect of the lead angle on metal milling has shown that the cutting geometry, mechanics, and dynamics vary drastically and nonlinearly with the lead angle [17].

Despite all researches that have been carried out to provide a better understanding of the machining of fiber-reinforced polymers, there are still many challenges with CFRP machining. This work presents some experiments that have been carried out on CFRP to study the optimum


Figure 1: Experimental setup for the machining of CFRP.

condition for the multiaxis milling of these materials and investigates the effects of different parameters such as the cutting speed, feed rate, and lead angle on the resulting cutting forces, surface quality, and machining damages.

## 2 Materials and methods

A set of experiments was carried out to provide a better understanding of the effects of machining parameters on surface quality and cutting forces. A high-performance carbon fiber epoxy prepreg having a 64% fiber volume content was used to produce stacks of 24 plies that were autoclave-cured to obtain composite plates with a final average thickness of approximately 3.5 mm. Quasi-isotropic laminates are an important class of composites and those that are most familiar to aerospace industries. With such laminates, the elastic properties are independent of orientation, and stiffness, compliance, and all engineering constants are almost identical in all directions [1, 18]. The symmetric stacking sequence $[90/-45/45/0/(\pm45)_2/0/-45/45/90]_s$ of the plies was such as to provide a laminate with in-plane quasi-isotropic properties (Figure 2). This layup is balanced and symmetric, and as a result, extension/bending coupling ($B_{ij}$) and shear coupling stiffnesses ($A_{ij}$) are zero; because of the fine ply distribution, the torsion coupling ($D_{ij}$) is relatively low ($i, j = x, y, s$; subscript $s$ denotes shear stress in the x-y plane and subscripts x and y denote normal strains in the x- and y-directions, respectively). Because of these characteristics, warpage and unexpected distortion are avoided and interlaminar stresses reduce [1].

The experiments were carried out using a Huron K2X8 five-axis CNC machine with a maximum spindle speed of 24,000 rpm under different cutting speeds, feed rates, and lead angles under dry cutting condition while keeping the axial depth of cut and radial depth of cut (or width of cut: distance between milling passes) constant and equal to 1.4 and 0.71 mm, respectively.

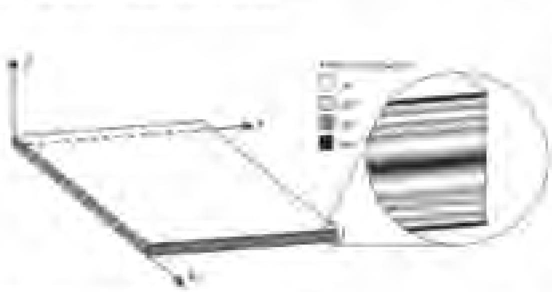

Figure 2: Layup of multidirectional CFRP.

The cutting mode was up-milling with a 3/8" diameter ball (LMT, ONSRUD, Waukegan, USA) end mill having two flutes with polycrystalline diamond (PCD) brazed inserts (Figure 3). Table 1 details the tool geometry.

Different cutting conditions were studied including the cutting speed (100–500 m/min), the feed rate (0.063–0.254 mm/rev), and the lead angle (-10° to +10°), as can be seen in Table 2. In this table, the cutting speed levels are calculated from the tool shank diameter. Each experimental run was repeated three times, with the same conditions, to evaluate the repeatability of the experiments. A Kistler 9255B (#3) three-axis dynamometer table (Kistler Group, Winterthur, Switzerland), connected to charge amplifiers, type Kistler 5010, was used for measuring the cutting forces during machining. The experimental setup is shown in Figure 1.

Commercially available dynamometers typically specify a bandwidth below the first natural frequency of the dynamometer structure [19]. The Kistler 9255B dynamometer table has a nominal natural frequency ($f_n$) equal to 2 kHz in x- and y-directions and 3.3 kHz in the z-direction [20]. Any machining operations reaching this range may lead to cutting force signals that are distorted because of the influence of the dynamic behavior of the dynamometer. Thus, the determination of the passing bandwidth is a very important step for an accurate force measurement during milling with high cutting speed. Zaghbani et al. [11] studied the dynamometer behavior of the Kistler 9255B (3#) dynamometer table with the same setup and calibration method as the ones used in the present study; they showed that the cutting force measurement setup has a passing bandwidth <1 kHz in the z-direction and 2 kHz in x- and y-directions. In the case of the z-direction (lower passing bandwidth), the highest tooth passing frequency should therefore not be higher than 1 kHz, which corresponds to a spindle speed of 450 Hz for a two-tooth cutter (27,000 rpm). In this study, all spindle speeds were lower than 27,000 rpm (800 m/min for a tool with 3/8" diameter), according to Table 2.

The roughness of the machined surfaces was measured using a Mitutoyo SJ400 contact profilometer (Mitutoyo Corporation, Tokyo, Japan) (Figure 4). Three readings were taken for each surface over an evaluation length of 12.5 mm, at regular intervals in a transverse direction to the cutting (feed direction), and their average was

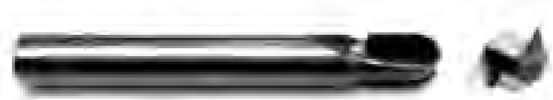

Figure 3: Two-flute PCD ball end mills.

**Table 1:** Description of tool geometries.

| Tool material | Number of flouts | Shank diameter | Flute length | Overall length | Helix angle | Rake angle | Overall length |
|---|---|---|---|---|---|---|---|
| PCD brazed inserts | 2" | 3/8" | 1/2" | 4" | 0 | 24° | 4" |

**Table 2:** Cutting parameters.

| Cutting speed (m/min) | Spindle speed (rpm) | Feed rate (mm/rev) | Lead angle (°) |
|---|---|---|---|
| 100 | 3341 | 0.063 | -10 |
| 175 | 5868 | 0.158 | -5 |
| 250 | 8354 | 0.254 | 0 |
| 375 | 12,531 | | 5 |
| 500 | 16,709 | | 10 |


**Figure 4:** Measuring of surface roughness.

**Table 3:** Values of resultant cutting force (Fc) and surface roughness ($R_a$) as a function of the cutting parameters (average of three times repetition).

| Test no. | Cutting speed (m/min) | Feed rate (mm/rev) | Lead angle (°) | Fc (N) | $R_a$ (μm) |
|---|---|---|---|---|---|
| 1 | 100 | 0.063 | 0 | 60.30 | 2.69 |
| 2 | 175 | 0.063 | 0 | 62.66 | 2.30 |
| 3 | 250 | 0.063 | 0 | 81.52 | 1.89 |
| 4 | 375 | 0.063 | 0 | 97.79 | 1.75 |
| 5 | 500 | 0.063 | 0 | 94.05 | 1.87 |
| 6 | 100 | 0.158 | 0 | 83.02 | 4.70 |
| 7 | 175 | 0.158 | 0 | 69.80 | 3.44 |
| 8 | 250 | 0.158 | 0 | 90.05 | 2.73 |
| 9 | 375 | 0.158 | 0 | 120.42 | 2.82 |
| 10 | 500 | 0.158 | 0 | 116.69 | 2.74 |
| 11 | 100 | 0.254 | 0 | 80.90 | 4.76 |
| 12 | 175 | 0.254 | 0 | 84.04 | 4.19 |
| 13 | 250 | 0.254 | 0 | 123.44 | 4.53 |
| 14 | 375 | 0.254 | 0 | 145.63 | 5.38 |
| 15 | 500 | 0.254 | 0 | 138.17 | 5.01 |
| 16 | 100 | 0.063 | -10 | 65.94 | 2.50 |
| 17 | 175 | 0.063 | -10 | 70.76 | 2.68 |
| 18 | 250 | 0.063 | -10 | 62.51 | 2.22 |
| 19 | 375 | 0.063 | -10 | 75.37 | 2.21 |
| 20 | 500 | 0.063 | -10 | 80.00 | 2.56 |
| 21 | 100 | 0.063 | -5 | 75.86 | 3.31 |
| 22 | 175 | 0.063 | -5 | 81.25 | 3.59 |
| 23 | 250 | 0.063 | -5 | 68.16 | 3.04 |
| 24 | 375 | 0.063 | -5 | 95.48 | 2.24 |
| 25 | 500 | 0.063 | -5 | 82.39 | 2.28 |
| 26 | 100 | 0.063 | 5 | 83.57 | 1.85 |
| 27 | 175 | 0.063 | 5 | 93.86 | 1.86 |
| 28 | 250 | 0.063 | 5 | 96.32 | 2.07 |
| 29 | 375 | 0.063 | 5 | 131.73 | 1.96 |
| 30 | 500 | 0.063 | 5 | 90.37 | 2.02 |
| 31 | 100 | 0.063 | 10 | 74.83 | 2.25 |
| 32 | 175 | 0.063 | 10 | 72.57 | 2.17 |
| 33 | 250 | 0.063 | 10 | 79.06 | 2.22 |
| 35 | 375 | 0.063 | 10 | 96.09 | 2.40 |
| 35 | 500 | 0.063 | 10 | 90.26 | 2.25 |

calculated. The measured values of $R_a$ (arithmetic average height) and $R_t$ (total height of the roughness profile) in different cutting conditions were compared to investigate the effect of cutting conditions on the surface quality. Table 3 indicates the average of measured resultant cutting forces and surface roughness for three times repetition of each condition.

The surfaces were also examined using a Keyence VHC-500F-type digital microscope (Keyence Corporation, Osaka, Japan) as well as Hitachi S-3600N electronic microscope (Hitachi Science Systems Ltd, Tokyo, Japan) [scanning electron microscopy (SEM)].

# 3 Results

## 3.1 Effects of feed rate and cutting speed on surface roughness

Surface morphology and integrity depend on the machining process and workpiece characteristics such as the cutting speed, the feed rate, the fiber type and volume content, the fiber orientation, and the matrix type [3].

Figures 5 and 6 show the effects of the feed rate and cutting speed on the average surface roughness ($R_a$) and total roughness ($R_t$), respectively. When comparing both figures, it is obvious that the variations of $R_t$ and $R_a$ with the cutting speed follow the same trends. All roughness results will therefore be discussed for $R_a$ values alone. As can be seen, $R_a$ increases with an increase in the feed rate. The dependence of the surface roughness on the cutting speed is more complex. However, it could generally be concluded that, for lower cutting speeds (100 and 175 m/min), the surface roughness decreases by increasing the cutting speed.

Increasing the cutting speed to more than 250 m/min does not have a significant effect on the surface roughness for lower feed rates (0.063 and 0.158 mm/rev). The minimum surface roughness values were achieved with a low feed rate (0.063 mm/rev) and higher cutting speed (250–500 m/min). For a higher feed rate (0.254 mm/rev), the roughness diagram has a minimum point at 175 m/min and a maximum point (point 2 in Figure 7) at 375 m/min cutting speed. Increasing the feed rate and cutting speed increases the cutting temperature [13], which can lead to the softening and burning of the matrix material [21]. Therefore, decreasing the surface roughness for higher feed rates (0.158 and 0.254 mm/rev) at a 500 m/min cutting speed might be explained by the adhering of the uncut fibers to the softened matrix under high cutting temperatures.

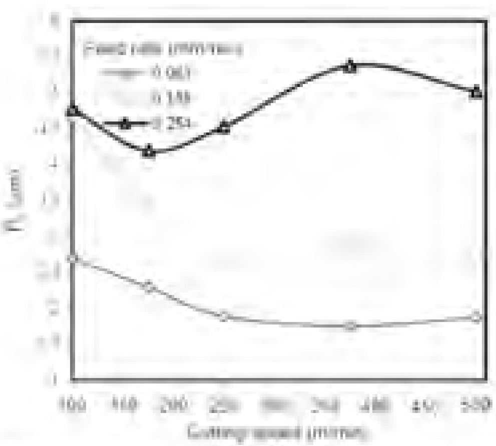

Figure 5: Effect of feed rate and cutting speed on the $R_a$, 0° lead angle.

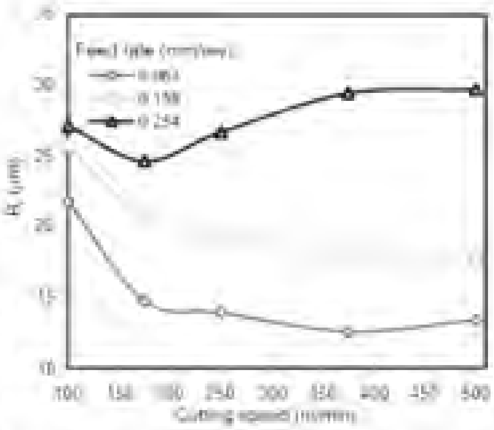

Figure 6: Effect of feed rate and cutting speed on the $R_t$, 0° lead angle.

## 3.2 Effects of feed rate and cutting speed on cutting force

According to the literature, cutting forces generally increase with an increase in the feed rate, but the dependence of cutting forces on the cutting speed is not uniform for different types of fiber-reinforced plastics [3]. Figure 7 illustrates the effect of the feed rate and cutting speed on the resultant cutting force in our experiments. It can be seen that the cutting force increases with an increase in the feed rate, and there is a greater influence on the cutting force for higher cutting speeds. The variation of cutting forces is not uniform over the cutting speed and can be studied in three cutting speed ranges, including (I) low cutting speeds (100–175 m/min), (II) moderate cutting speeds (175–375 m/min), and (III) high cutting speeds (375–500 m/min). In range I, the effect of cutting speed on resultant cutting force is not significant; in range II, the cutting force rises with the cutting speed; and in range III, the cutting force diminishes when the cutting speed increases. The nonuniform variation of the cutting force to cutting speed is consistent with other studies [3, 14, 21]. The rate of variation of the cutting forces with the cutting speed is related to cutting temperatures. At low cutting speeds, the cutting temperatures

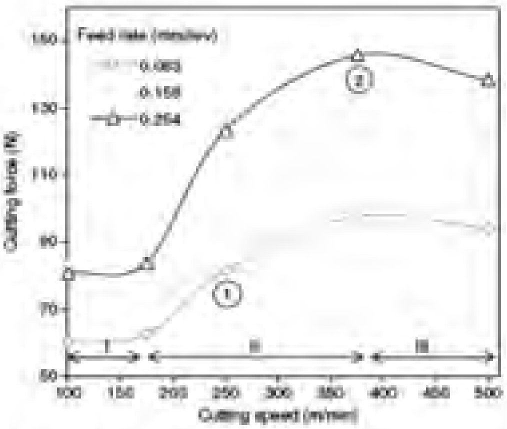


**Figure 7:** Effects of feed rate and cutting speed on the cutting force, 0° lead angle.

are not high enough to soften the polymer matrix, and dry friction predominates. The softening/degrading of the matrix in the cutting zone occurs at a critical speed and causes a reduction in cutting forces [3]. Figure 7 shows that this critical speed is probably reached in range III, where the cutting forces become almost independent of the cutting speed, and the minimum cutting force is achieved in this range.

Among the conditions resulting in lower roughness (feed rate 0.063 mm/rev and cutting speeds 250–500 m/min), point 1 in Figures 5 and 7 has the lowest cutting force, which produces greater process stability and part quality. Therefore, this condition is recommended for the surface machining of CFRP with this cutting tool. A comparison of the surface quality in point 1 with that in point 2 (the point with the highest surface roughness and cutting force) in Figure 8 shows that much damage occurs using a high feed rate.

## 3.3 Effects of lead angle on surface roughness and cutting force

The study of the effect of the lead angle on the surface roughness showed that it varies nonlinearly with the lead angle and that variation depends on the cutting speed. Figure 9 shows the effect of the lead angle on the surface roughness for different cutting speeds and a feed rate of 0.0635 mm/rev. The minimum $R_a$ is achieved for a lead angle of 5° for low cutting speeds (100 and 175 m/min) and 0° for higher cutting speeds (250–500 m/min). The diagram in Figure 9 illustrates that the variability in roughness curves is higher for negative lead angles. It is shown that the roughness curves for lower cutting speeds (100, 175, and 250 m/min) have high amplitudes compared to those for higher cutting speeds (375 and 500 m/min). In other words, the sensitivity of roughness to the lead angle is higher for the low cutting speeds.

Figure 10 shows the effect of the lead angle on the resultant cutting forces for different cutting speeds and a

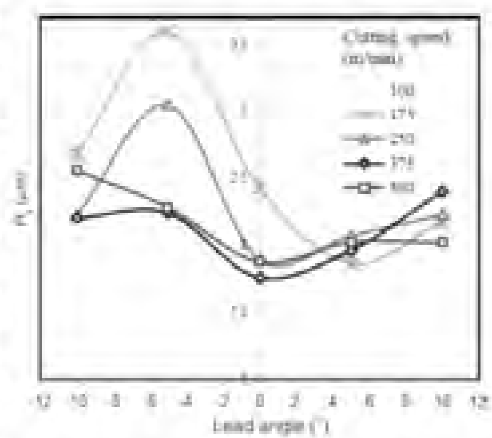


**Figure 9:** Effect of lead angle on the roughness $R_a$ for different cutting speeds (feed 0.0635 mm/rev).

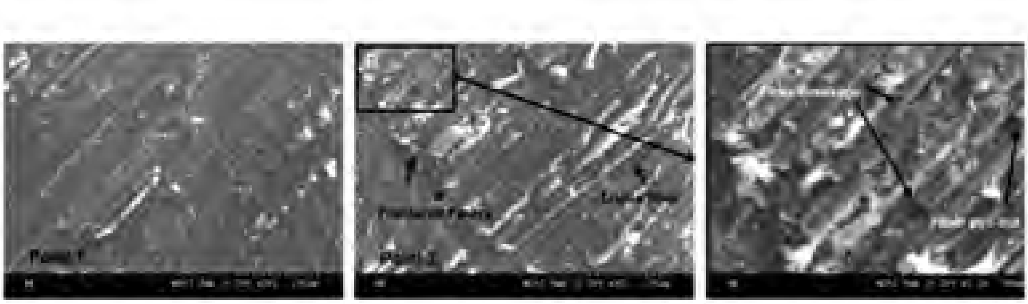


**Figure 8:** Effect of cutting speed on the quality of machined surface, lead angle 0°: (A) cutting speed 250 m/min and feed rate 0.063 mm/rev and (B) cutting speed 375 m/min and feed rate 0.254 mm/rev.

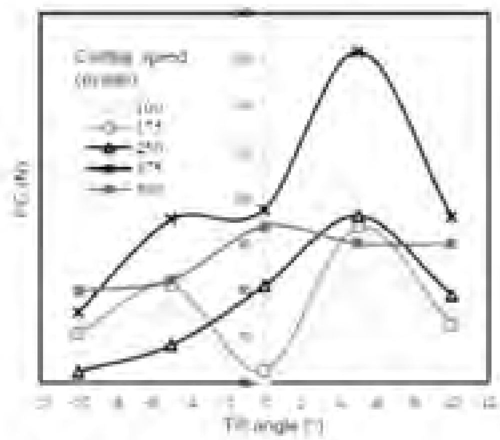


**Figure 10:** Effect of lead angle on the cutting force at cutting speed 250 m/min (feed 0.063 mm/rev).

feed rate of 0.063 mm/rev. As can be seen, the variation of the cutting force with the lead angle is not uniform for all cutting speeds. However, the minimum cutting forces were achieved at the lead angle 0° for low cutting speeds (100 and 175 m/min) and -10° for higher cutting speeds (250, 375, and 500 m/min). Figure 11 shows the SEM images of a machined surface with different lead angles. As can be seen, the best quality surface was achieved with a lead angle equal to 0° and -10°, where the roughness and cutting force are at minimum values, respectively. More damage, such as fiber breakage, fiber de-cohesion, and matrix damage, is observed in the case of 5° lead angle, whereas the roughness and cutting force have maximum values.

## 4 Conclusions

In this paper, surface milling experiments were carried out on carbon fiber-reinforced laminates to study the effects of cutting parameters on the cutting force and surface quality and to find the optimum conditions for this operation type using a PCD two-flute ball nose end mill. Based on the presented results, the following conclusions are drawn:

- The surface roughness increases with an increase in the feed rate.
- At lower cutting speeds (100 and 175 m/min), the surface roughness decreases with an increase in the

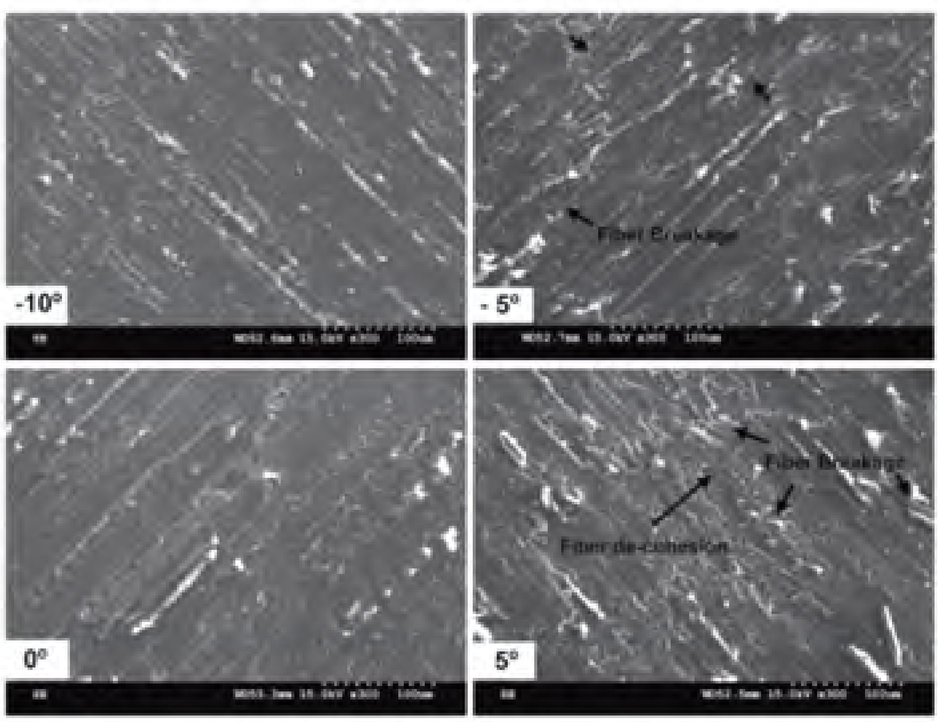


**Figure 11:** SEM images of machined surface with different lead angles (cutting speed 250 m/min and feed rate 0.063 mm/rev).

cutting speed, whereas increasing the cutting speed to more than 250 m/min has no significant effect on the surface roughness for lower feed rates (0.06) and 0.158 mm/rev).

- The cutting force increases with the feed rate, but the variation of cutting forces showed no consistent trend over the cutting speed range evaluated. However, the effect of the cutting speed on cutting force is more significant for moderate cutting speed values (175–375 m/min) while improving the cutting force.
- The variation of the cutting force and surface roughness with the lead angle is nonlinear, and the minimum values are found at the 250 m/min speed and 0.0635 mm/rev feed rate for lead angles equal to 0° and -10°, respectively. This latter value is unexpected because it is quite an unusual lead angle in multiaxis machining.
- Instability in the roughness diagram increases when using a negative lead angle. On the contrary, using a positive lead angle produces higher cutting forces.

**Acknowledgments:** This research was funded by the Consortium for Research and Innovation in Aerospace in Quebec (CRIAQ) and its partners the Natural Sciences and Engineering Research Council of Canada (NSERC), MITACS, Bombardier Aerospace, Avior Integrated Products, Delastek, and AV&R Vision & Robotics.

## References

[1] Daniel IM, Ishai O. *Engineering Mechanics of Composite Materials*, 2nd ed., Oxford University Press: New York, 2006.

[2] Gay D, Hoa SV. *Composite Materials*, 2nd ed., CRC Press: Boca Raton, 2007.

[3] Sheikh-Ahmad JY. *Machining of Polymer Composites*, Springer: New York, 2009.

[4] Ferreira JR, Coppini NL, Miranda GWA. *J. Mater. Process. Technol.* 1999, 92–93, 135–140.

[5] Wang XM, Zhang LC. *Int. J. Mach. Tools Manuf.* 2003, 43, 1015–1022.

[6] Boothroyd G, Knight WA. *Fundamentals of Machining and Machine Tools*, 3rd ed., CRC Press: New Delhi, 2006.

[7] Davim JP, Reis P. *J. Mater. Process. Technol.* 2005, 160, 160–167.

[8] El-Hofy MH, Soo SL, Aspinwall DK, Sim WM, Pearson D, Harden P. *Proc. Eng.* 2011, 19, 94–99.

[9] Chatelain JF, Zaghbani I, Monier J. *World Acad. Sci. Eng. Technol.* 2012, 68, 1204–1210.

[10] Sheikh-Ahmad J, Urban N, Cheraghi H. *J. Mater. Manuf. Processes* 2012, 27, 802–808.

[11] Zaghbani I, Chatelain JF, Songmene V, Berube S, Atarsia A. *J. Compos. Mater.* 2012, 46, 1955–1971.

[12] Colligan K, Ramulu M. *ASME Publ. PED* 1999, 121, 648–655.

[13] Sreejith PS, Krishnamurthy R, Malhotra SK, Narayanasamy K. *J. Mater. Process. Technol.* 2000, 104, 53–58.

[14] Zhang LC. *J. Mater. Process. Technol.* 2009, 209, 4548–4552.

[15] Rusinek R. *Int. J. Non-Linear Mech.* 2010, 45, 458–462.

[16] Wang YG, Yan XP, Chen XG, Sun CY, Liu G. *Adv. Mater. Res.* 2011, 215, 14–18.

[17] Ozturk E, Tunc LT, Budak E. *Int. J. Mach. Tools Manuf.* 2009, 49, 1053–1062.

[18] Soden PD, Hinton MJ, Kaddour AS. *Compos. Sci. Technol.* 1998, 58, 1011–1022.

[19] Burton D, Duncan S, Ziegert JC, Schmitz TL. *19th Annu. Meet. Am. Soc. Precision Eng. (ASPE 2004)* 2004, pp. 221–224.

[20] Kistler Group, *Cutting Force Measuring Catalog*, Data sheet: 9255B_000-148, 2009.

[21] Hamedanianpour H, Chatelain JF. *2nd International Conference on Manufacturing Engineering and Process*, Vancouver, 2013.

## LIST OF REFERENCES


Arola, D, et M Ramulu. 1997. « Orthogonal cutting of fiber-reinforced composites: a finite element analysis ». *International journal of mechanical sciences,* vol. 39, n° 5, p. 597-613.

Arola, D, MB Sultan et M Ramulu. 2002. « Finite element modeling of edge trimming fiber reinforced plastics ». *Journal of manufacturing science and engineering,* vol. 124, n° 1, p. 32-41.

ASTM. 2008. *D 792–08. Standard test methods for density and specific gravity (relative density) of plastics by displacement*. West Conshohocken, PA

ASTM. 2009. *D6641/D6641M-09: Standard test method for compressive properties of polymer matrix composite materials using a combined loading compression (CLC) test fixture*. West Conshohocken, PA.

ASTM. 2012. *D5379/D5379M: Standard test method for shear properties of composite materials by the V-notched beam method*. West Conshohocken, PA

ASTM. 2014. *D3039/D3039M: Standard test method for tensile properties of polymer matrix composite materials*. West Conshohocken, PA

Boothroyd, G, et WA Knight. 2006. *Fundamentals of Machining and Machine Tools, CRC Publication*. ISBN 1-57444-659-2.

Burton, David, G Scott Duncan, John C Ziegert et Tony L Schmitz. 2004. « High frequency, low force dynamometer for micro-milling force measurement ». In *19th annual meeting on American Society for Precision Engineering (ASPE 2004)*. (University of Florida), p. 221–224.

Calzada, Kevin A. 2010. « Modeling and Interpretation of Fiber Orientation-Based Failure Mechanisms in Machining of Carbon Fiber-Reinforced Composites ». University of Illinois at Urbana-Champaign.

Calzada, Kevin A, Shiv G Kapoor, Richard E DeVor, Johnson Samuel et Anil K Srivastava. 2012. « Modeling and interpretation of fiber orientation-based failure mechanisms in machining of carbon fiber-reinforced polymer composites ». *Journal of Manufacturing Processes,* vol. 14, n° 2, p. 141-149.

Campbell, Flake C. 2010. *Structural composite materials*. ASM international.

Chardon, Grégory, Olga Klinkova, Joël Rech, Sylvain Drapier et Jean-Michel Bergheau. 2015. « Characterization of friction properties at the work material/cutting tool interface during the machining of randomly structured carbon fibers reinforced polymer with Poly Crystalline Diamond tool under dry conditions ». *Tribology International,* vol. 81, p. 300-308.

Chatelain, J. F., I. Zaghbani et J. Monier. 2011. « Effect of ply orientation on roughness parameters for the trimming process of CFRP laminate ». *Accepted in journal of composite materials*.

Chatelain, Jean François, Imed Zaghbani et Joseph Monier. 2012. « Effect of Ply Orientation on Roughness for the Trimming Process of CFRP Laminates ». *C. World Academy of Science, Engineering and Technology,* vol. 68, p. 1204-1210.

Chatelain, JF, et I. Zaghbani. 2011. « Effect of tool geometry special features on cutting forces of multilayered CFRP laminates ». In *4th recent advances in manufacturing engineering*. (Barcelona, Spain), p. 79-84. WAEAS Press.

Chen, Wen-Chou. 1997. « Some experimental investigations in the drilling of carbon fiber-reinforced plastic (CFRP) composite laminates ». *International Journal of Machine Tools and Manufacture,* vol. 37, n$^{o}$ 8, p. 1097-1108.

Cheng, Du-qing, Xue-tao Wang, Jian Zhu, Dong-hua Qiu, Xiu-wei Cheng et Qing-feng Guan. 2009. « Friction and wear behavior of carbon fiber reinforced brake materials ». *Frontiers of Materials Science in China,* vol. 3, n$^{o}$ 1, p. 56-60.

Colligan, K, et M Ramulu. 1999. « Edge trimming of graphite/epoxy with diamond abrasive cutters ». *Journal of Manufacturing Science and Engineering,* vol. 121, n$^{o}$ 4, p. 647-655.

Dandekar, Chinmaya R, et Yung C Shin. 2008. « Multiphase finite element modeling of machining unidirectional composites: prediction of debonding and fiber damage ». *Journal of Manufacturing Science and Engineering,* vol. 130, n$^{o}$ 5, p. 051016.

Dandekar, Chinmaya R, et Yung C Shin. 2012. « Modeling of machining of composite materials: a review ». *International Journal of Machine tools and manufacture,* vol. 57, p. 102-121.

Daniel, I.M., et O. Ishai. 2006. *Engineering mechanics of composite materials*, second edition. New York, USA: Oxford university press.

Davim, J. Paulo. 2015. *Machinability of Fibre-Reinforced Plastics*, 4. Berlin: Walter de Gruyter GmbH & Co KG.

Davim, J.P., et P. Reis. 2005. « Damage and dimensional precision on milling carbon fiber-reinforced plastics using design experiments ». *Journal of materials processing technology,* vol. 160, n$^{o}$ 2, p. 160-167.

Davim, J.P., P. Reis et C.C. António. 2004. « A study on milling of glass fiber reinforced plastics manufactured by hand-lay up using statistical analysis (ANOVA) ». *Composite structures,* vol. 64, n° 3, p. 493-500.

De Lacalle, LN Lopez, A Lamikiz, FJ Campa, A Fdz Valdivielso et I Etxeberria. 2009. « Desing and test of a multitooth tool for CFRP milling ». *Journal of composite materials*.

Dieter, George Ellwood, et David Bacon (9-10). 1986. *Mechanical metallurgy*, 3. McGraw-Hill New York.

El-Hofy, MH, SL Soo, DK Aspinwall, WM Sim, D Pearson et P Harden. 2011. « Factors affecting workpiece surface integrity in slotting of CFRP ». *Procedia Engineering,* vol. 19, p. 94-99.

Farago, F.T., et M.A. Curtis. 1994. *Handbook of dimensional measurement*. Industrial Press Inc.

Ferreira, JR, NL Coppini et GWA Miranda. 1999. « Machining optimisation in carbon fibre reinforced composite materials ». *Journal of materials processing technology,* vol. 92, p. 135-140.

Gao, Chongyang, Jianzhang Xiao, Jiuhua Xu et Yinglin Ke. 2015. « Factor analysis of machining parameters of fiber-reinforced polymer composites based on finite element simulation with experimental investigation ». *The International Journal of Advanced Manufacturing Technology*, p. 1-13.

Gay, D, et SV Hoa. 2007. *Composite materials: design and applications*, 2nd. CRC Press.

Ghafarizadeh, Seyedbehzad, Jean-François Chatelain et Gilbert Lebrun. 2014. « Effect of cutting tool lead angle on machining forces and surface finish of CFRP laminates ». *Science and Engineering of Composite Materials*.

Ghafarizadeh, Seyedbehzad, Gilbert Lebrun et Jean-François Chatelain. 2015. « Experimental investigation of the cutting temperature and surface quality during milling of unidirectional carbon fiber reinforced plastic ». *Journal of Composite Materials*, p. 0021998315587131.

Girot, F, LN López de Lacalle, A Lamikiz, D Iliescu et ME Gutiérrez. 2009. « Machinability aspects of polymer matrix composites in machining composites materials ». *Wiley& Sons, New York (USA)*.

Gudimani, G. 2011. « Oblique machining of uni directional carbon fiber reinforced polymer composites ». Wichita state university.

Hamedanianpour, Hossein, et Jean François Chatelain. 2013. « Effect of Tool Wear on Quality of Carbon Fiber Reinforced Polymer Laminate during Edge Trimming ». In *Applied Mechanics and Materials*. Vol. 325, p. 34-39. Trans Tech Publ.

Hashin, Zvi. 1980. « Failure criteria for unidirectional fiber composites ». *Journal of applied mechanics,* vol. 47, n° 2, p. 329-334.

Hashin, Zvi, et Assa Rotem. 1973. « A fatigue failure criterion for fiber reinforced materials ». *Journal of composite materials,* vol. 7, n° 4, p. 448-464.

Hibbitt, D, B Karlsson et P Sorensen. 2012. *Abaqus 6.12 Documentation and User Manual*. Dassault Systèmes Simulia Corp.

Isbilir, Ozden, et Elaheh Ghassemieh. 2012. « Finite element analysis of drilling of carbon fibre reinforced composites ». *Applied Composite Materials,* vol. 19, n° 3-4, p. 637-656.

Kafyeke, Fassi. 2010. « Aviation Leadership for the Environment ». In *2nd UTIAS-MITACS International Workshop on Aviation and Climate Change*. (Toronto ), sous la dir. de Aerospace, Bombardier.

Kalla, Devi, Jamal Sheikh-Ahmad et Janet Twomey. 2010. « Prediction of cutting forces in helical end milling fiber reinforced polymers ». *International Journal of Machine Tools and Manufacture,* vol. 50, n° 10, p. 882-891.

Karpat, Yiğit, Onur Bahtiyar et Burak Değer. 2012. « Mechanistic force modeling for milling of unidirectional carbon fiber reinforced polymer laminates ». *International Journal of Machine Tools and Manufacture,* vol. 56, p. 79-93.

Kistler-Group. 2009. *Cutting Force Measuring Catalog, Data sheet: 9255B_000-148*. Switzerland: Kistler Group.

Kollár, László P, et George S Springer. 2003. *Mechanics of composite structures*. Cambridge University Press.

Kukureka, SN, CJ Hooke, M Rao, P Liao et YK Chen. 1999. « The effect of fibre reinforcement on the friction and wear of polyamide 66 under dry rolling–sliding contact ». *Tribology International,* vol. 32, n° 2, p. 107-116.

Lapczyk, Ireneusz, et Juan A Hurtado. 2007. « Progressive damage modeling in fiber-reinforced materials ». *Composites Part A: Applied Science and Manufacturing,* vol. 38, n° 11, p. 2333-2341.

Lasri, L, M Nouari et M El Mansori. 2009. « Modelling of chip separation in machining unidirectional FRP composites by stiffness degradation concept ». *Composites Science and Technology,* vol. 69, n° 5, p. 684-692.

Li, Chengfeng, Xinmin Lai, Hongtao Li et Jun Ni. 2007. « Modeling of three-dimensional cutting forces in micro-end-milling ». *Journal of Micromechanics and Microengineering,* vol. 17, n° 4, p. 671.

Li, Kuan-Ming, Chia Wang et Wei-Ying Chu. 2013. « An improved remote sensing technique for estimating tool–chip interface temperatures in turning ». *Journal of Materials Processing Technology,* vol. 213, n° 10, p. 1772-1781.

Liu, Jie, Guang Chen, Chunhui Ji, Xuda Qin, Hao Li et Chengzu Ren. 2014. « An investigation of workpiece temperature variation of helical milling for carbon fiber reinforced plastics (CFRP) ». *International Journal of Machine Tools and Manufacture,* vol. 86, p. 89-103.

Mahdi, Mofid, et Liangchi Zhang. 2001a. « An adaptive three-dimensional finite element algorithm for the orthogonal cutting of composite materials ». *Journal of Materials Processing Technology,* vol. 113, n° 1, p. 368-372.

Mahdi, Mofid, et Liangchi Zhang. 2001b. « A finite element model for the orthogonal cutting of fiber-reinforced composite materials ». *Journal of Materials Processing Technology,* vol. 113, n° 1, p. 373-377.

Marsh, George. 2011. « Bombardier throws down the gauntlet with CSeries airliner ». *Reinforced Plastics,* vol. 55, n° 6, p. 22-26.

Merino-Pérez, JL, R Royer, S Ayvar-Soberanis, E Merson et A Hodzic. 2015. « On the temperatures developed in CFRP drilling using uncoated WC-Co tools Part I: Workpiece constituents, cutting speed and heat dissipation ». *Composite Structures,* vol. 123, p. 161-168.

Miranzo, P, MI Osendi, E Garcia, AJS Fernandes, VA Silva, FM Costa et RF Silva. 2002. « Thermal conductivity enhancement in cutting tools by chemical vapor deposition diamond coating ». *Diamond and related materials,* vol. 11, n° 3, p. 703-707.

Mkaddem, A., et M. El Mansori. 2009. « Finite element analysis when machining UGF-reinforced PMCs plates: Chip formation, crack propagation and induced-damage ». *Materials & Design,* vol. 30, n° 8, p. 3295-3302.

Mkaddem, Ali, Ibrahim Demirci et Mohamed El Mansori. 2008. « A micro–macro combined approach using FEM for modelling of machining of FRP composites: Cutting forces analysis ». *Composites Science and Technology,* vol. 68, n° 15, p. 3123-3127.

Muhammad Nuruzzaman, Dewan, Mohammad Asaduzzaman Chowdhury et Mohammad Lutfar Rahaman. 2011. « Effect of duration of rubbing and normal load on friction coefficient for polymer and composite materials ». *Industrial Lubrication and Tribology,* vol. 63, n° 5, p. 320-326.

Nak-Ho, Sung, et Nam P Suh. 1979. « Effect of fiber orientation on friction and wear of fiber reinforced polymeric composites ». *Wear,* vol. 53, n° 1, p. 129-141.

Nayak, D, N Bhatnagar et P Mahajan. 2005. « Machining studies of UD-FRP composites part 2: finite element analysis ». *Machining Science and Technology,* vol. 9, n° 4, p. 503-528.

Özel, Tuğrul, et Taylan Altan. 2000. « Process simulation using finite element method—prediction of cutting forces, tool stresses and temperatures in high-speed flat end milling ». *International Journal of Machine Tools and Manufacture,* vol. 40, n° 5, p. 713-738.

Ozturk, Erdem, L Taner Tunc et Erhan Budak. 2009. « Investigation of lead and tilt angle effects in 5-axis ball-end milling processes ». *International Journal of Machine Tools and Manufacture,* vol. 49, n° 14, p. 1053-1062.

Ramesh, MV, KN Seetharamu, N Ganesan et MS Sivakumar. 1998. « Analysis of machining of FRPs using FEM ». *International Journal of Machine Tools and Manufacture,* vol. 38, n° 12, p. 1531-1549.

Ramulu, M. 1997. « Machining and surface integrity of fibre-reinforced plastic composites ». *Sadhana,* vol. 22, n° 3, p. 449-472.

Ramulu, M, M Faridnia, JL Garbini et JE Jorgensen. 1991. « Machining of graphite/epoxy composite materials with polycrystalline diamond (PCD) tools ». *Journal of Engineering Materials and Technology,* vol. 113, n° 4, p. 430-436.

Rao, G, Puneet Mahajan et Naresh Bhatnagar. 2008. « Three-dimensional macro-mechanical finite element model for machining of unidirectional-fiber reinforced polymer composites ». *Materials Science and Engineering: A,* vol. 498, n° 1, p. 142-149.

Rao, G Venu Gopala, Puneet Mahajan et Naresh Bhatnagar. 2007a. « Machining of UD-GFRP composites chip formation mechanism ». *Composites science and technology,* vol. 67, n° 11, p. 2271-2281.

Rao, G., P. Mahajan et N. Bhatnagar. 2007b. « Micro-mechanical modeling of machining of FRP composites–Cutting force analysis ». *Composites science and technology,* vol. 67, n° 3, p. 579-593.

Rentsch, R, O Pecat et E Brinksmeier. 2011. « Macro and micro process modeling of the cutting of carbon fiber reinforced plastics using FEM ». *Procedia engineering,* vol. 10, p. 1823-1828.

Rusinek, Rafal. 2010. « Cutting process of composite materials: An experimental study ». *International Journal of Non-Linear Mechanics,* vol. 45, n° 4, p. 458-462.

Santiuste, C, M Rodríguez-Millán, E Giner et H Miguélez. 2014. « The influence of anisotropy in numerical modeling of orthogonal cutting of cortical bone ». *Composite Structures,* vol. 116, p. 423-431.

Santiuste, C., X. Soldani et M.H. Miguélez. 2010. « Machining FEM model of long fiber composites for aeronautical components ». *Composite structures,* vol. 92, n° 3, p. 691-698.

Schellekens, JCJ, et R De Borst. 1990. « The use of the Hoffman yield criterion in finite element analysis of anisotropic composites ». *Computers & Structures,* vol. 37, n° 6, p. 1087-1096.

Shalin, Radiĭ Evgen′evich. 2012. *Polymer matrix composites*, 4. Springer Science & Business Media.

Shaw, Milton Clayton. 2005. *Metal cutting principles*, 2. New York: Oxford university press

Sheikh-Ahmad, J.Y. 2008. *Machining of polymer composites*. Springer Verlag.

Sheikh-Ahmad, Jamal, Nebu Urban et Hossein Cheraghi. 2012. « Machining damage in edge trimming of CFRP ». *Materials and Manufacturing Processes,* vol. 27, n° 7, p. 802-808.

Soden, PD, MJ Hinton et AS Kaddour. 1998. « Lamina properties, lay-up configurations and loading conditions for a range of fibre-reinforced composite laminates ». *Composites Science and Technology,* vol. 58, n° 7, p. 1011-1022.

Soldani, Xavier, Carlos Santiuste, Ana Muñoz-Sánchez et MH Miguélez. 2011. « Influence of tool geometry and numerical parameters when modeling orthogonal cutting of LFRP composites ». *Composites Part A: Applied Science and Manufacturing,* vol. 42, n° 9, p. 1205-1216.

Sreejith, PS, R Krishnamurthy, SK Malhotra et K Narayanasamy. 2000. « Evaluation of PCD tool performance during machining of carbon/phenolic ablative composites ». *Journal of Materials Processing Technology,* vol. 104, n° 1, p. 53-58.

Stein, Erwin, René de Borst et Thomas JR Hughes. 2004. *Encyclopedia of computational mechanics*, 1. Wiley & Sons, Ltd.

Suresha, B, G Chandramohan, P Samapthkumaran, S Seetharamu et S Vynatheya. 2006. « Friction and wear characteristics of carbon-epoxy and glass-epoxy woven roving fiber composites ». *Journal of reinforced plastics and composites,* vol. 25, nº 7, p. 771-782.

Teti, R. 2002. « Machining of composite materials ». *CIRP Annals-Manufacturing Technology,* vol. 51, nº 2, p. 611-634.

Turner, J, RJ Scaife et HM El-Dessouky. 2015. « Effect of machining coolant on integrity of CFRP composites ». *Advanced Manufacturing: Polymer & Composites Science,* vol. 1, nº 1, p. 54-60.

Wang, DH, M Ramulu et D Arola. 1995. « Orthogonal cutting mechanisms of graphite/epoxy composite. Part I: unidirectional laminate ». *International Journal of Machine Tools and Manufacture,* vol. 35, nº 12, p. 1623-1638.

Wang, XM, et LC Zhang. 2003. « An experimental investigation into the orthogonal cutting of unidirectional fibre reinforced plastics ». *International journal of machine tools and manufacture,* vol. 43, nº 10, p. 1015-1022.

Wang, Yong Guo, Xiang Ping Yan, XG Chen, Chang Yu Sun et G Liu. 2011. « Cutting performance of carbon fiber reinforced plastics using PCD tool ». In *Advanced Materials Research*. Vol. 215, p. 14-18. Trans Tech Publ.

Weiert, K, et C Kempann. 2004. « Cutting temperature and their effects on machining behavior in drilling reinforced plastics composites ». *Advanced engineering materials,* vol. 6, p. 684-689.

Yashiro, Takeshi, Takayuki Ogawa et Hiroyuki Sasahara. 2013. « Temperature measurement of cutting tool and machined surface layer in milling of CFRP ». *International Journal of Machine Tools and Manufacture,* vol. 70, p. 63-69.

Zaghbani, Imed, Jean-François Chatelain, Victor Songmene, Sébastien Bérubé et Abdelatif Atarsia. 2012a. « A comprehensive analysis of cutting forces during routing of carbon fiber-reinforced polymer laminates ». *Journal of composite materials*, p. 0021998311428362.

Zaghbani, Imed, Jean–Francois Chatelain, Sebastien Berube, Victor Songmene et Justin Lance. 2012b. « Analysis and modelling of cutting forces during the trimming of unidirectional CFRP composite laminates ». *International Journal of Machining and Machinability of Materials,* vol. 12, nº 4, p. 337-357.

Zenia, S, L Ben Ayed, M Nouari et A Delamézière. 2015. « Numerical prediction of the chip formation process and induced damage during the machining of carbon/epoxy composites ». *International Journal of Mechanical Sciences,* vol. 90, p. 89-101.

Zhang, LC. 2009. « Cutting composites: A discussion on mechanics modelling ». *Journal of materials processing technology,* vol. 209, n° 9, p. 4548-4552.